(2)

# MOCVD Growth of GaN, AlN and AlGaN for UV Photodetector Applications

ONR contract #N00014-93-1-0235

Principal Investigator: Prof. Manijeh Razeghi



Staff: Dr. Manijeh Razeghi
Dr. Erwan Bigan
Dr. Hitoshi Ohsato

Students: Patrick Kung
Adam Saxler
Chien-Jen Sun

# SUMMARY


For the growth of III-V nitrides, three main problems hinder the production of device quality materials. They are large lattice mismatch between nitride films and substrates, high n-type background concentration and difficulty in p-type doping. In the past year, we focused on the first problem, the lattice mismatch. Different substrates and different orientations of the substrates have been used in order to find a suitable substrate for the nitride growth.

An atmospheric horizontal-type metalorganic chemical vapor deposition (MOCVD) reactor was used for the growth of aluminum nitride (AlN), gallium nitride (GaN) and ternary $Al_xGa_{1-x}N$. (0001), $(11\bar{2}0)$ and $(01\bar{1}2)$ sapphire ($Al_2O_3$), (100) and (111)Si and (0001)6H-SiC were used as substrates. The best GaN films obtained by our group, in term of crystallinity, were grown on (0001)$Al_2O_3$ with an AlN mediate layer. The full width at half maximum (FWHM) of the x-ray rocking curve was as narrow as 400 arcsecs. The results on the other crystal orientations or substrates were 600 arcsecs for $(11\bar{2}0)Al_2O_3$, 600 arcsecs for $(01\bar{1}2)Al_2O_3$ and 700 arcsecs for (0001)6H-SiC. Only orientated films can be obtained on (100) and (111)Si. For the growth of AlN, a FWHM of only 97.2 arcsecs was obtained on (0001)$Al_2O_3$ which is the lowest value ever reported to our knowledge. Again, the best ternary nitride films with about 10% of Al were deposited on (0001)$Al_2O_3$ with a GaN/AlN structure as a buffer layer. The FWHM of this ternary is about 600 arcsecs.

In addition to optimizing the growth conditions, the surface polarity and thermal stability of the films has also been studied. It was found that N-terminated GaN film had the most stable surface, followed by the nonpolar surface, and the Ga-terminated GaN film had the least stable surface.

Theoretical epitaxial relationship studies were proceeded in order to understand the growth mechanisms. It showed that the interface between (0001)GaN and (0001)$Al_2O_3$ was better than that of $(11\bar{2}0)$GaN and $(01\bar{1}2)Al_2O_3$. Using a crystallographic model "Extended Atomic Distance Mismatch" (EADM), we showed that a better crystalline quality GaN would be grown on $(01\bar{1}2)Al_2O_3$, while a better crystalline quality AlN would be grown on (0001)$Al_2O_3$. We also showed that Ga terminated films would be grown on Si-terminated SiC surface, while N terminated films on C-terminated SiC surface.

## Introduction

Recently, the prospect of realizing photonic devices working in the blue-UV region of the optical spectrum has led renewed interest in wide bandgap semiconductors. Indium, gallium and aluminum nitrides (InN, GaN, AlN), with direct bandgaps of 1.9eV, 3.4eV and 6.2eV respectively, have been studied as alternative materials to existing large bandgap II-VI semiconductors (SiC and ZnSe).[1-3] The potential to realize $Al_xGa_{1-x}N$ alloys, and to a lesser extent GaInN[4] which would yield a tunable bandgap from 1.9 to 6.2eV is also an important advantage of III-Nitrides.

The main objective of this study is to investigate the feasibility of UV photodetectors with GaN, AlN and $Al_xGa_{1-x}N$.

Up to now, the realization of these devices with III-Nitrides thin films has been hindered by the lack of an ideal substrate on which are grown the epilayers, a high n-type background carrier concentration resulting in difficulty to dope the materials p-type, and a high growth temperature.[1,2] Although sapphire ($Al_2O_3$) has a large misfit with both GaN and AlN, it is the most widely used substrate[1] because of its availability, stability at high temperature. Moreover its hexagonal crystal symmetry makes it suitable for the growth of III-Nitrides which are wurtzitic in their stable phase.[1]

When we were awarded the ONR contract in January 1993, we had just begun the growth of GaN. At that time, excellent GaN and AlN epilayers have been reported[5,6], semi-insulating and p-type GaN leading to the realization of blue light emitting diodes (LEDs) have also been achieved.[7,8]

## I. Experimental details

All our thin films were grown in a horizontal atmospheric pressure metalorganic chemical vapor deposition (MOCVD) reactor. We used a SiC coated graphite susceptor on the back of which a thermocouple monitors the growth temperature and provides feedback to the heating system. The latter was composed of two infrared quartz lamps, which limited our growth temperature to 1050°C. The source material flows were mixed just at the entrance of the reactor tube in order to reduce parasitic pre-reactions.

The starting materials for group III elements were trimethylgallium (TMGa) and trimethylaluminum (TMAl). The sources for nitrogen were ammonia ($NH_3$), tertiarybutylamine (TBA) and methylamine ($CH_3NH_2$).

We studied the growth of III-Nitrides on several substrates. These included the (0001) and $(01\bar{1}2)$ orientations of sapphire substrates ($Al_2O_3$), (100)

oriented silicon (Si) and (0001) oriented silicon carbide (6H-SiC). More recently, we started to use $(11\bar{2}0)Al_2O_3$ and (111)Si. The substrates were first degreased in organic solvents, then etched in acid solutions, rinsed in deionized water and dried with filtered nitrogen. They were placed side by side on the susceptor during each growth.

## II. Approach

We successively optimized the growth of GaN, AlN and $Al_xGa_{1-x}N$, and compared the results on each substrate.

The epilayer surface morphology and chemical composition were investigated by scanning electron microscopy and Auger electron spectroscopy. The crystalline quality of the films was determined by high resolution x-ray diffraction. The electrical properties were studied through Hall effect measurements. The optical characterizations included Fourier Transform Infrared transmission (FTIR), and UV transmission. We have also mounted a photoluminescence (PL) experiment with a UV laser.

For each substrate we used, we devised a theoretical model based on crystallography and the atomic configurations of both epilayers and substrates in order to understand the growth mechanisms.[9-11]

## III. Growth of gallium nitride

The optimization of the growth conditions for GaN showed the best epilayers, structural, electrical and optically speaking, were obtained with $NH_3$ as the N source, and at the highest growth temperature we could provide (1050°C). Our epilayers were 2.5 to 3µm thick, corresponding to a growth rate of about 1.2 to 2µm/hr.

The x-ray rocking curve FWHM was reduced from more than several thousand to near 60 arcsecs for GaN epilayers grown directly on the substrates. Recently, we have shown that with the growth a high quality AlN thin film prior to that of the GaN, the x-ray rocking curve FWHM can become as low as 400 arcsecs (Fig. 1). We were still far from the best value[12] , but our results have to be considered knowing we are using a system that limits the uniformity and homogeneity of our films (atmospheric pressure). We believe that the use of a low pressure system will allow us to improve the crystallinity of our epilayers.

Sapphire and silicon carbide substrates yielded the best films in terms of crystalline quality.

All our as-grown GaN epilayers were n-type. The typical room temperature carrier concentration and electron mobility of the films grown on sapphire were $n \approx 10^{-20} cm^{-3}$ and $\mu \approx 50 cm^2/Vs$ respectively.[13] Electrical measurements were difficult to realize due to the low uniformity of our layers. We believe the electrical properties can be enhanced by the use of low pressure growth.

We conducted a comparison between the GaN thin films grown directly on both (0001) and (0112) orientation of sapphire substrates.[13] The following epitaxial relationships were confirmed: (0001)GaN/(0001)$Al_2O_3$ and $(11\bar{2}0)$GaN/(0112)$Al_2O_3$. We showed that the layers grown on (0112)$Al_2O_3$ yielded a higher crystalline quality, a lower oxygen incorporation as detected through Auger electron spectroscopy (Fig. 2), higher electron mobilities and lower carrier concentrations (Fig. 3) than the epilayers grown on (0001)$Al_2O_3$. A lattice mismatch between $(11\bar{2}0)$GaN and (0112)$Al_2O_3$ lower than between (0001)GaN and (0001)$Al_2O_3$ could explain these results.

Photoluminescence experiments were performed at room temperature to determine the optical quality of our GaN epilayers. A typical spectrum is shown in figure 4. The FWHM was measured to be about 100meV.

We investigated the thermal stability of GaN epilayers.[14] Thermal stability is an important parameter in the realization of optoelectronic devices since thermal treatment may be required for technological steps such as dopant activation. In addition, these devices are expected to work at high power and high temperature. The studied films were grown directly on (0001), (0112) sapphire, and Si terminated $(0001)_{Si}$ silicon carbide substrates. The annealing temperatures were 900 and 1000°C, and the ambient gases were $N_2$ and $H_2$. Annealed under $N_2$ ambient, the films did not decomposed. Their crystallinity even improved, especially for the films grown on (0112)$Al_2O_3$, which was attributed to the desorption of hydrogen atoms incorporated in the films. For $H_2$ ambient, we showed that the epilayers grown on $(0001)_{Si}$ SiC were the most stable, followed by those grown on $(01\bar{1}2)Al_2O_3$, and the least stable ones were those grown on (0001)$Al_2O_3$. We interpreted these results in terms of difference in the epilayer surface polarity. The N terminated surface of GaN grown on $(0001)_{Si}$ SiC was more slowly attacked by hydrogen atoms than the non polar surface of GaN grown on (0112)$Al_2O_3$. The Ga terminated surface of GaN grown on (0001)$Al_2O_3$ yielded the fastest decomposition rate.

## IV. Aluminum nitride

Up to now, we have obtained our best results for the growth of AlN using $NH_3$ as the nitrogen source. The growth temperature was still limited to 1050°C. Our layers were about 1µm thick and the growth rate was about 0.5 µm/hr.

Our epilayers grown on $(0001)Al_2O_3$ yielded the lowest x-ray rocking curve FWHM (97 arcsecs) ever reported to our knowledge.[15] In contrast to the growth of GaN, the AlN layers grown on $(0001)Al_2O_3$ had a much higher crystalline quality than those grown on $(01\bar{1}2)Al_2O_3$ (Fig. 5).

Electrical measurements were not possible due to the high resistivity of our AlN epilayers.

FTIR experiments conducted on silicon substrates successfully detected AlN phonon modes. A typical spectrum is shown in figure 6. UV transmission measurements were also performed. They allowed us to determine the band edge of our AlN epilayers to be near 6.2eV (200nm), in accordance with reported values.[16] We also showed that the edge was much sharper for the samples grown on the (0001) orientation than on the $(01\bar{1}2)$ orientation of $Al_2O_3$ substrates (Fig. 7).

Photoluminescence experiments did not show any peak because the energy of our excitation laser (3.8eV corresponding to 325nm) was lower than the bandgap of AlN (6.2eV).

Thermal annealing was performed on AlN epilayers grown on both (0001) and $(01\bar{1}2)Al_2O_3$.[17] As for GaN , the annealings were conducted at 1000°C, under $N_2$ and $H_2$ ambient gases. In contrast with GaN, no decomposition occured on either sample, under either ambient gas. The crystalline quality investigated by x-ray diffraction was barely altered for each sample. We attributed this to reported high decomposition temperatures of AlN. However, UV transmission spectra improved in all cases, a sharper edge was obtained. We are currently interpreting these results.

## V. Ternary $Al_xGa_{1-x}N$

Ternary compounds $Al_xGa_{1-x}N$ were successfully grown for x from 0 to 0.6 by varying the gallium flow rate.[18] The growth was preceded by that of a high quality AlN layer, or GaN/AlN heterostructure. We obtained a high crystalline quality ternary grown on $(0001)Al_2O_3$ substrates with a x-ray rocking curve FWHM of about 10 minutes (Fig. 8). The films grown on the other substrates had much poorer crystallinity. It was shown the crystallinity deteriorated as the value of x was increased.

Electrical measurements were not reliable because of the poor uniformity resulting from the growth at atmospheric pressure.

Photoluminescence experiments were successfully conducted on all these epilayers, at 77K room temperature[18]. In particular, a photoluminescence peak was detected for the epilayers grown on (100)Si (Fig. 9), in spite of their low the crystalline quality. All the FWHM, for GaN as well as for $Al_xGa_{1-x}N$, were about 95 meV.

## VI. Theoretical growth models

The first crystallographic model we developed concerned the growth of wurtzite-type thin films lattice matched to both (0001) and (0112) orientations of sapphire substrates.[9] Through this model, we demonstrated that the layers grown on $(0001)Al_2O_3$ should present a better epilayer-substrate interface quality than those grown on $(0112)Al_2O_3$, although the latter have a lower lattice mismatch with $(0112)Al_2O_3$. We also showed that the GaN films grown on $(0001)Al_2O_3$ were Ga-terminated, while those grown on $(0112)Al_2O_3$ had a non polar surface, which means both Ga and N atoms are present.

Our second model[10] introduced a concept we called 'Extended Atomic Distance Mismatch' (EADM) which is the lattice mismatch between epilayer and substrate using a longer period than the lattice constants. With this concept, we explained our experimental results, that is (0001)GaN grown on $(0001)Al_2O_3$ had poorer crystallinity than $(11\bar{2}0)$GaN grown on $(01\bar{1}2)Al_2O_3$, whereas (0001)AlN grown on $(0001)Al_2O_3$ had better crystallinity than $(11\bar{2}0)$AlN grown on $(0112)Al_2O_3$.

Our third model[11] described the growth of GaN and AlN on different SiC substrates. The (0001) 6H-SiC and (111) 3C-SiC planes have the same atomic configurations, that is a hexagonal close packed arrangement of either Si or C atoms. Thus, we predicted a same growth mechanism for $(0001)_{Si}$ 6H-SiC and $(111)_{Si}$ 3C-SiC, and another mechanism for $(0001)_C$ 6H-SiC and $(111)_C$ 3C-SiC. According to our model, the nitride epilayers grown on Si-terminated substrates should be Ga-(or Al)-terminated, while they should be N-terminated if grown on C-terminated substrates. However, other groups interpreted their experimental results in the opposite way.[19] They found that N-terminated and Ga-(or Al)-terminated nitride layers were grown on Si-terminated and C-terminated substrates respectively.

## VII. Future work

A new horizontal MOCVD reactor, from AIXTRON, will soon be assembled in our group. It will allow us to realize the growths at low pressure. We will also be able to use in-situ plasma activation of source materials. With this new system, we expect further improvements in the crystalline, electrical and optical quality of our epilayers.

We will continue to investigate the growth on different substrates and determine which one yields the best epilayers. In particular, on the new substrates we started to use $(11\bar{2}0)Al_2O_3$ and (111)Si.

Doping with bis(cyclopentadienyl)magnesium will be attempted in order to get p-type AlN. Then, the realization of p-n junctions with wide bandgap III-Nitrides and that of UV photodetectors will be possible.

Through the crystallographic models developed, we expect to improve the epitaxial growth as well as the doping efficiency.

## REFERENCES


[1] S. Strite and H. Morkoç, J. Vac. Sci. Technol. B **10**(4), 1237 (1992).
[2] J.H. Edgar, J. Mater. Res. **7**(1), 235 (1992).
[3] M. Henini, Microelectronics Journal **23**, 500 (1992).
[4] T. Nagatomo, T. Kuboyama, H. Minamino, and O. Omoto, Jpn. J. Appl. Phys. **28**(8), L1334 (1989).
[5] J.N. Kuznia et al., R. Kaplan et al., J. Appl. Phys. **73**(9), 4700 (1993).
[6] M.A. Khan et al., M.M. Millan and W.J. Choyke, Appl. Phys. Lett. **61**(21), 2539 (1992).
[7] N. Koide et al., M. Hashimoto, H. Amano et al., J. Cryst. Growth **115**, 639 (1991).
[8] I. Akasaki, H. Amano, M. Kito, and K. Hiramatsu, J. of Lumin. **48&49**, 666 (1991).
[9] P. Kung, C.J. Sun, A. Saxler, H. Ohsato, and M. Razeghi, accepted by J. Appl. Phys.
[10] C.J. Sun, P. Kung, A. Saxler, H. Ohsato, and M. Razeghi, accepted by J. Appl. Phys.
[11] in preparation.
[12] I. Akasaki et al., N. Koide et al., Physica B **185**, 428 (1993).
[13] C.J. Sun and M. Razeghi, Appl. Phys. Lett. **63**(7), 973 (1993).
[14] C.J. Sun, P. Kung, A. Saxler, H. Ohsato, E. Bigan, and M. Razeghi, submitted to J. Appl. Phys.
[15] A. Saxler, P. Kung, C.J. Sun, E. Bigan, and M. Razeghi, Appl. Phys. Lett. **64**(3), 17 January 1994.
[16] W.M. Yim, E.J. Stofko, P.J. Zanzucchi, J.I. Pankove, M. Ettenberg, and S.L. Gilbert, J. Appl. Phys. **44**, 292 (1973).
[17] P. Kung, A. Saxler, K. Haritos, C.J. sun and M. Razeghi, unpublished.
[18] C.J. Sun, P. Kung, A. Saxler, H. Ohsato and M. Razeghi, presented at the International Conference on Silicon Carbide and Related Materials, april 1994.
[19] T. Sasaki and T. Matsuoka, J. Appl. Phys. **64**(9), 4531 (1988).

## LIST OF FIGURES


Figure 1. X-ray rocking curve of GaN grown on $(0001)Al_2O_3$.

Figure 2. Auger electron spectra for (a) GaN grown on $(0001)Al_2O_3$ (b) GaN grown on $(01\bar{1}2)Al_2O_3$.

Figure 3. Room temperature carrier concentrations and electron mobilities of GaN grown on (0001) and $(01\bar{1}2)Al_2O_3$.

Figure 4. Room temperature photoluminescence spectrum of GaN grown on sapphire substrates.

Figure 5. X-ray rocking curve of (a) AlN grown on $(0001)Al_2O_3$ and (b) AlN AlN grown on $(01\bar{1}2)Al_2O_3$.

Figure 6. Fourier transform infrared spectrum of AlN grown on (100)Si.

Figure 7. UV transmission spectra of (a) AlN grown on $(0001)Al_2O_3$ and (b) AlN grown on $(01\bar{1}2)Al_2O_3$.

Figure 8. X-ray rocking curve of $Al_{0.13}Ga_{0.87}N$ grown on $(0001)Al_2O_3$.

Figure 9. Room temperature photoluminescence spectrum of GaN grown on (100)Si.

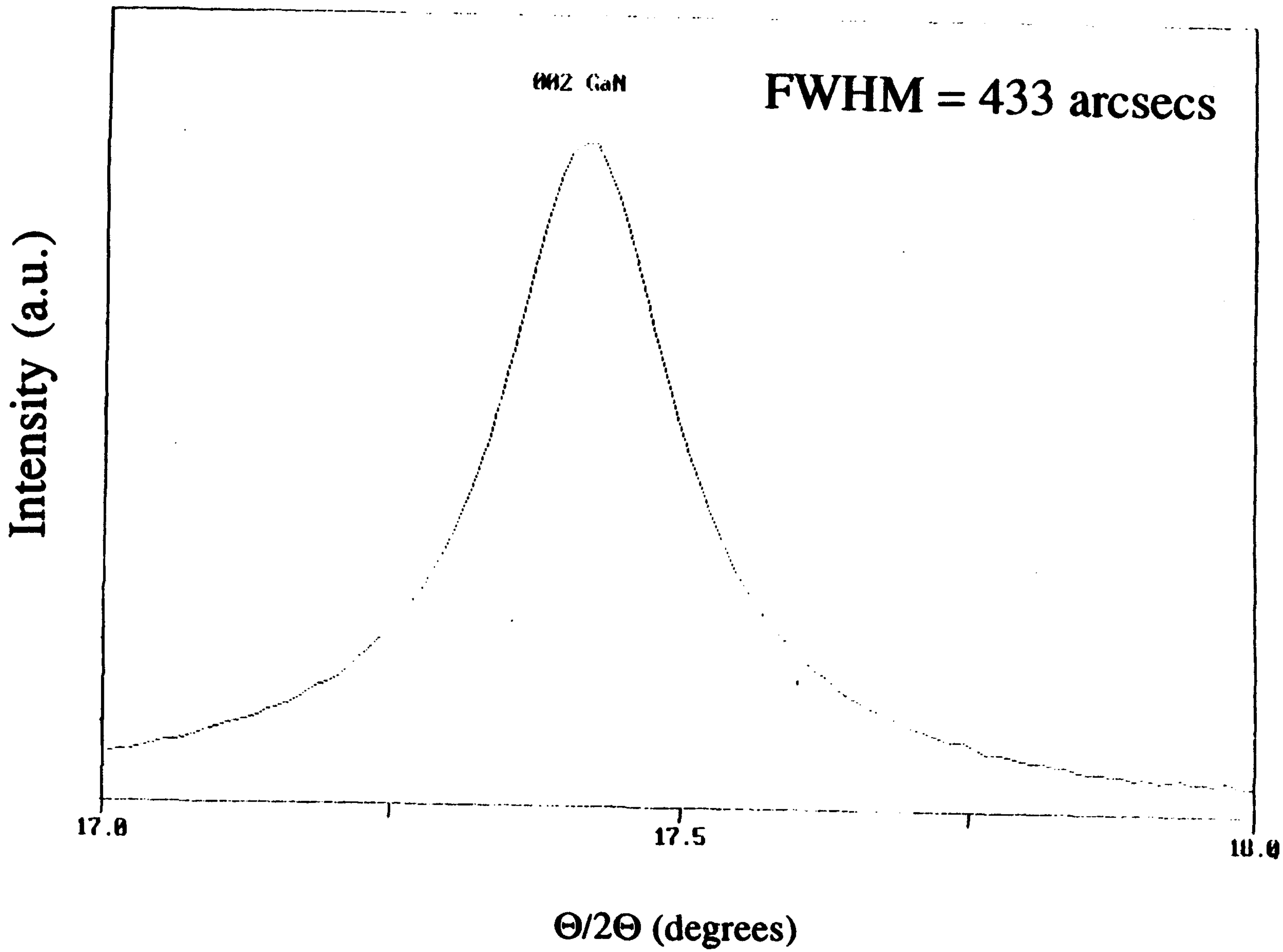

002 GaN
FWHM = 433 arcsecs
Intensity (a.u.)
17.0
17.5
18.0
Θ/2Θ (degrees)


**Figure 1**

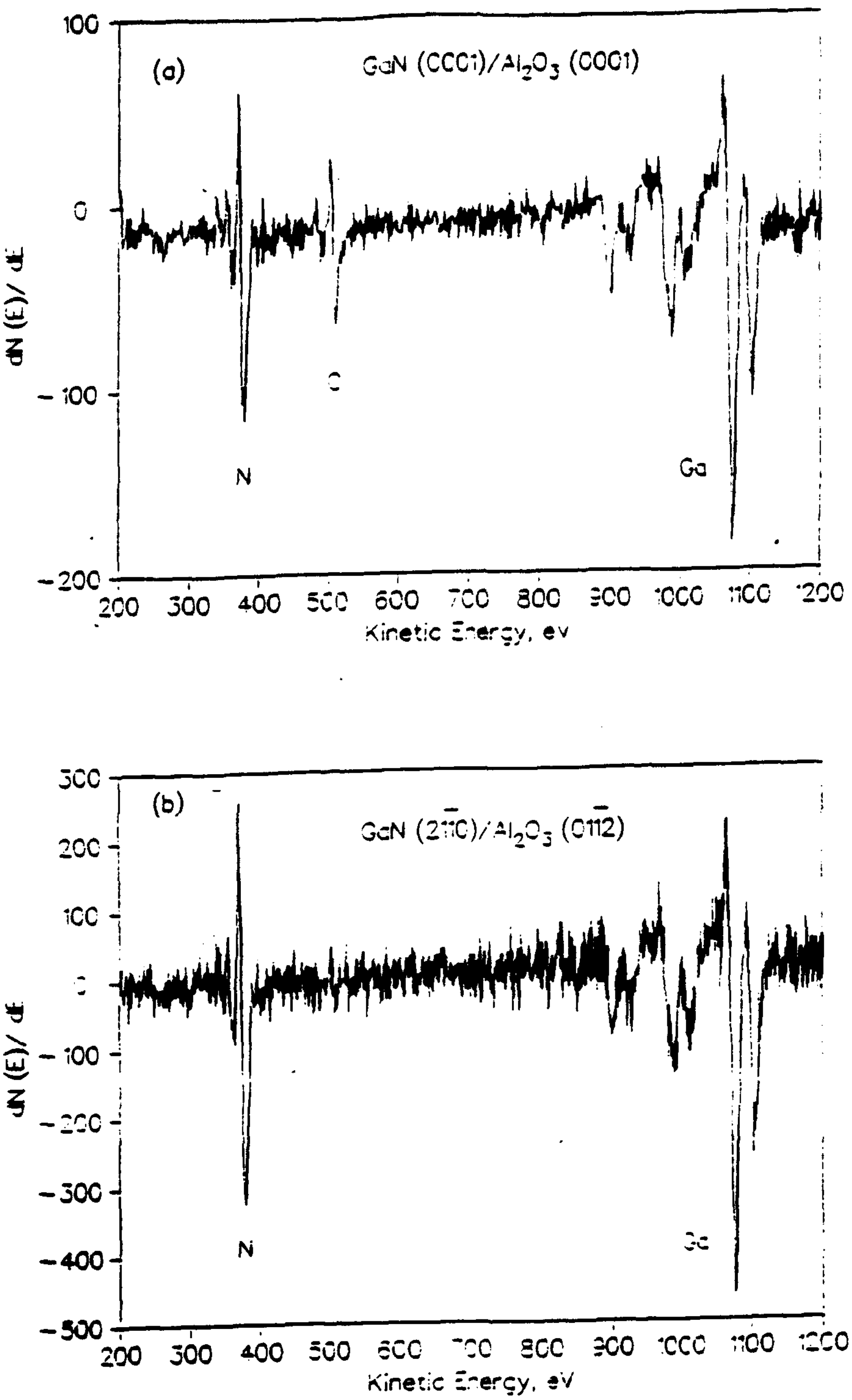
(a)
GaN (0001)/$Al_2O_3$ (0001)
100
0
-100
-200
dN (E)/ dE
N
O
Ga
200 300 400 500 600 700 800 900 1000 1100 1200
Kinetic Energy, ev
(b)
GaN ($2\bar{1}\bar{1}0$)/$Al_2O_3$ ($01\bar{1}2$)
300
200
100
0
-100
-200
-300
-400
-500
dN (E)/ dE
N
Ga
200 300 400 500 600 700 800 900 1000 1100 1200
Kinetic Energy, eV

# Figure 2

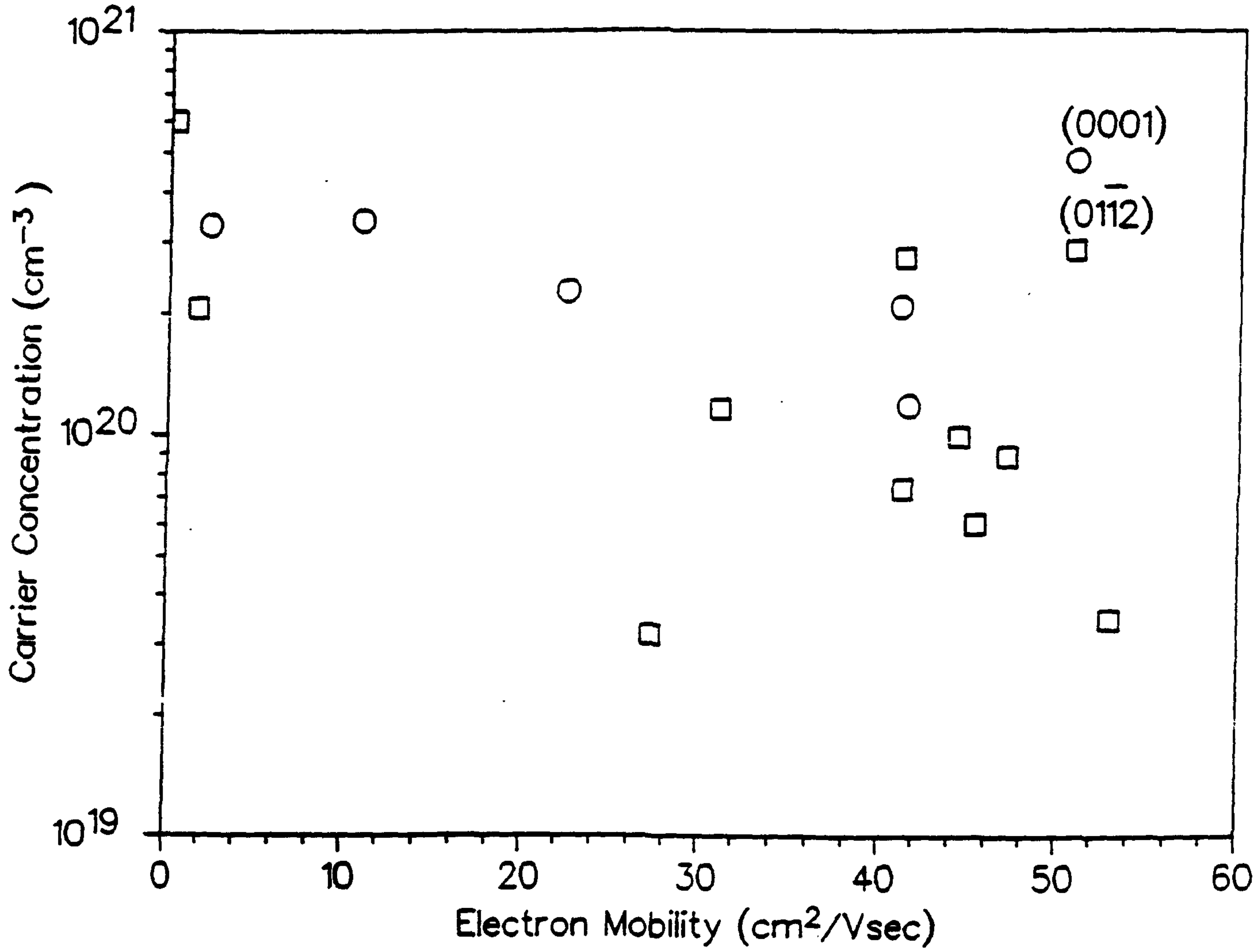
$10^{21}$
$10^{20}$
$10^{19}$
(0001)
$(01\bar{1}2)$
Carrier Concentration ($cm^{-3}$)
0
10
20
30
40
50
60
Electron Mobility ($cm^2$/Vsec)

# Figure 3

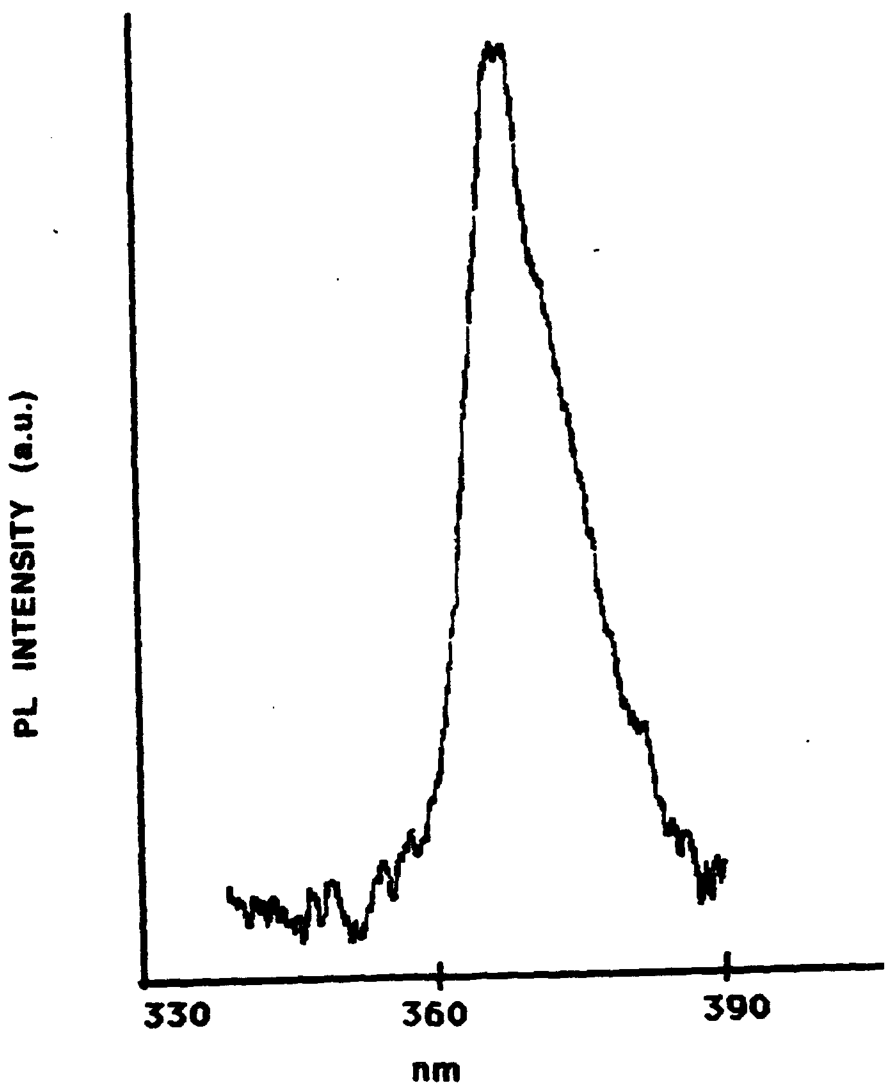


# Figure 4

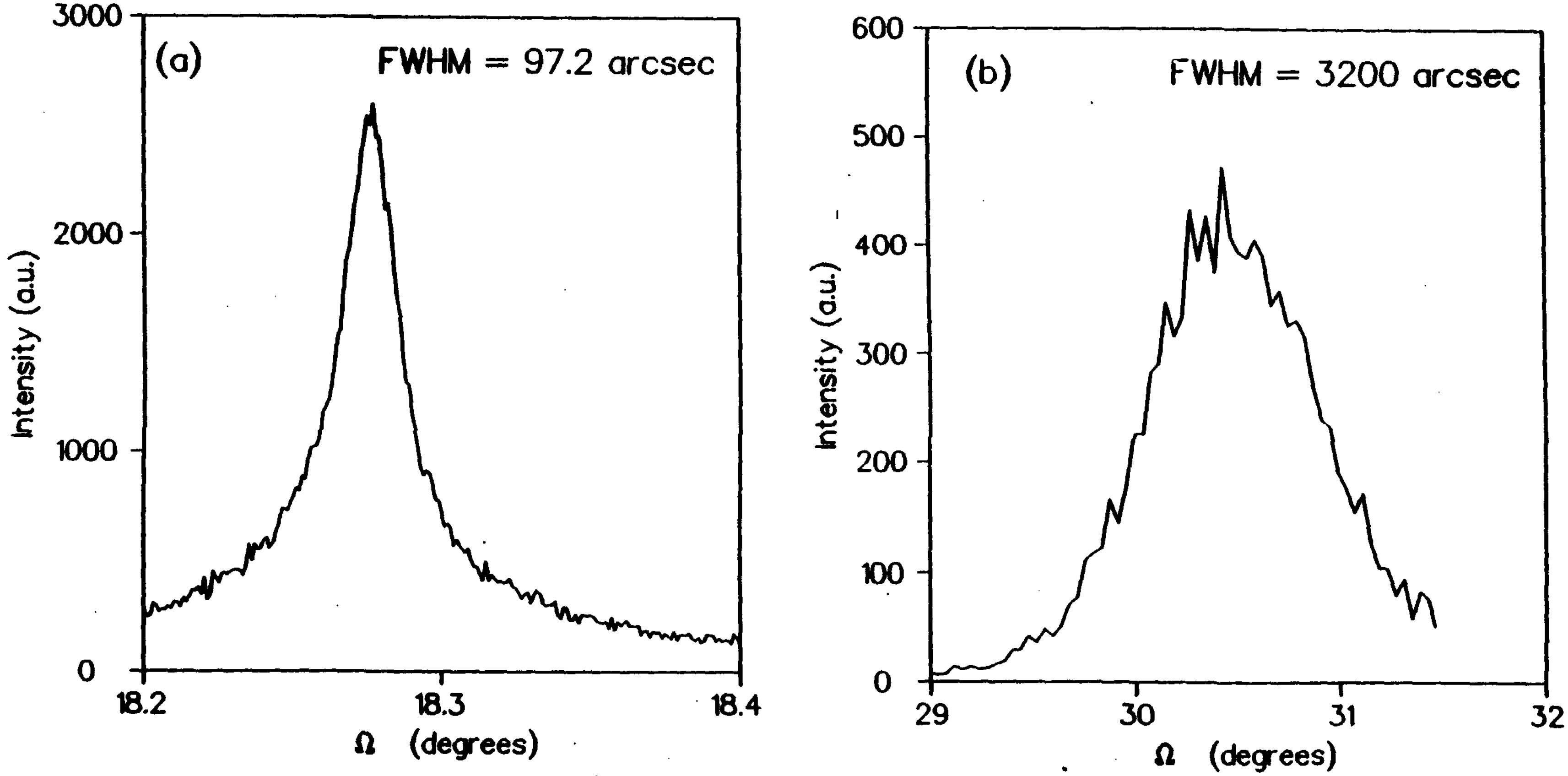
(a)
FWHM = 97.2 arcsec
3000
2000
1000
0
Intensity (a.u.)
18.2
18.3
18.4
Ω (degrees)
(b)
FWHM = 3200 arcsec
600
500
400
300
200
100
0
Intensity (a.u.)
29
30
31
32
Ω (degrees)

# Figure 5

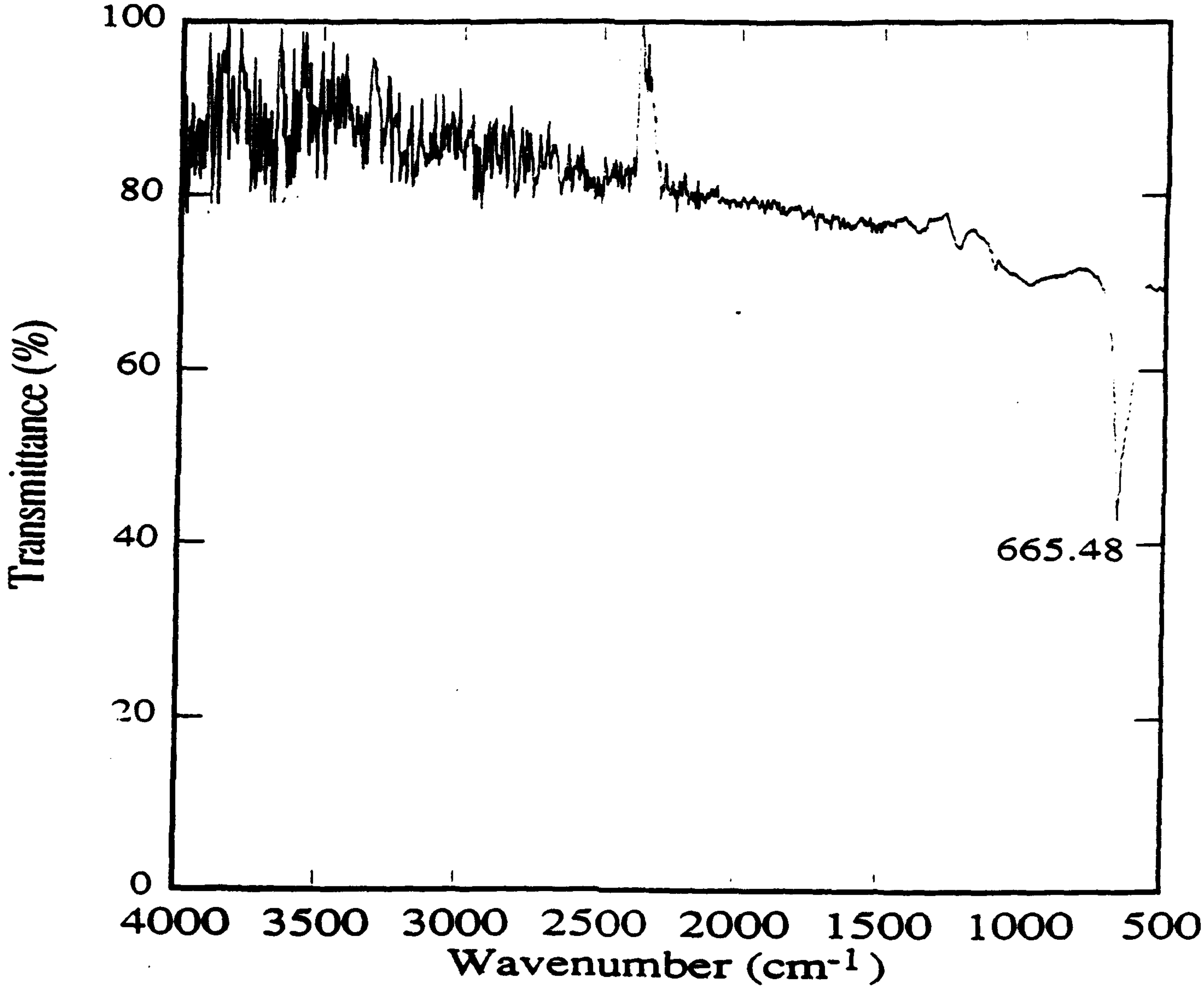

100
80
60
40
20
0
Transmittance (%)
665.48
4000
3500
3000
2500
2000
1500
1000
500
Wavenumber (cm-1)


# Figure 6

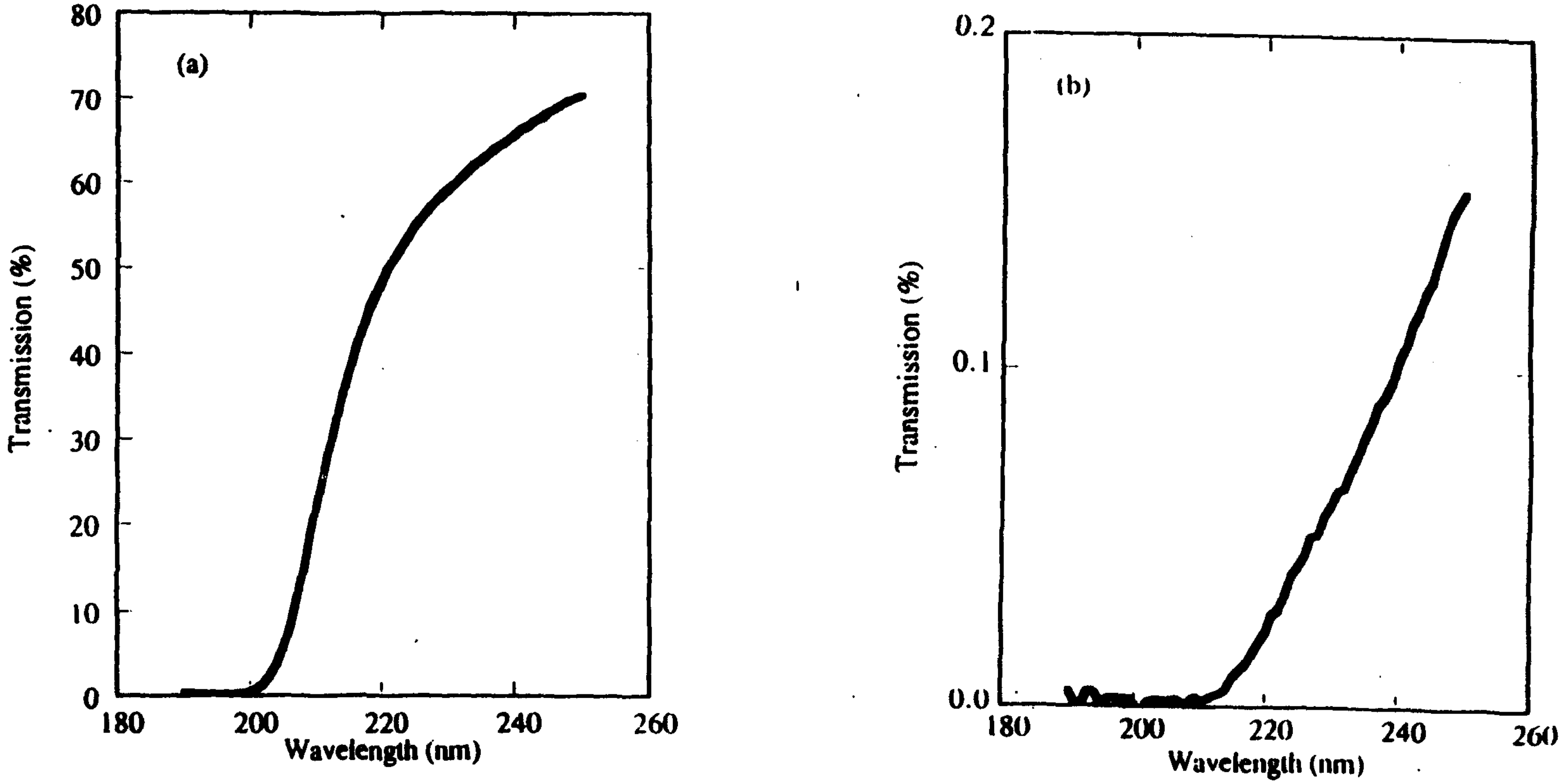
(a)
Transmission (%)
80
70
60
50
40
30
20
10
0
180
200
220
240
260
Wavelength (nm)
(b)
Transmission (%)
0.2
0.1
0.0
180
200
220
240
260
Wavelength (nm)

# Figure 7

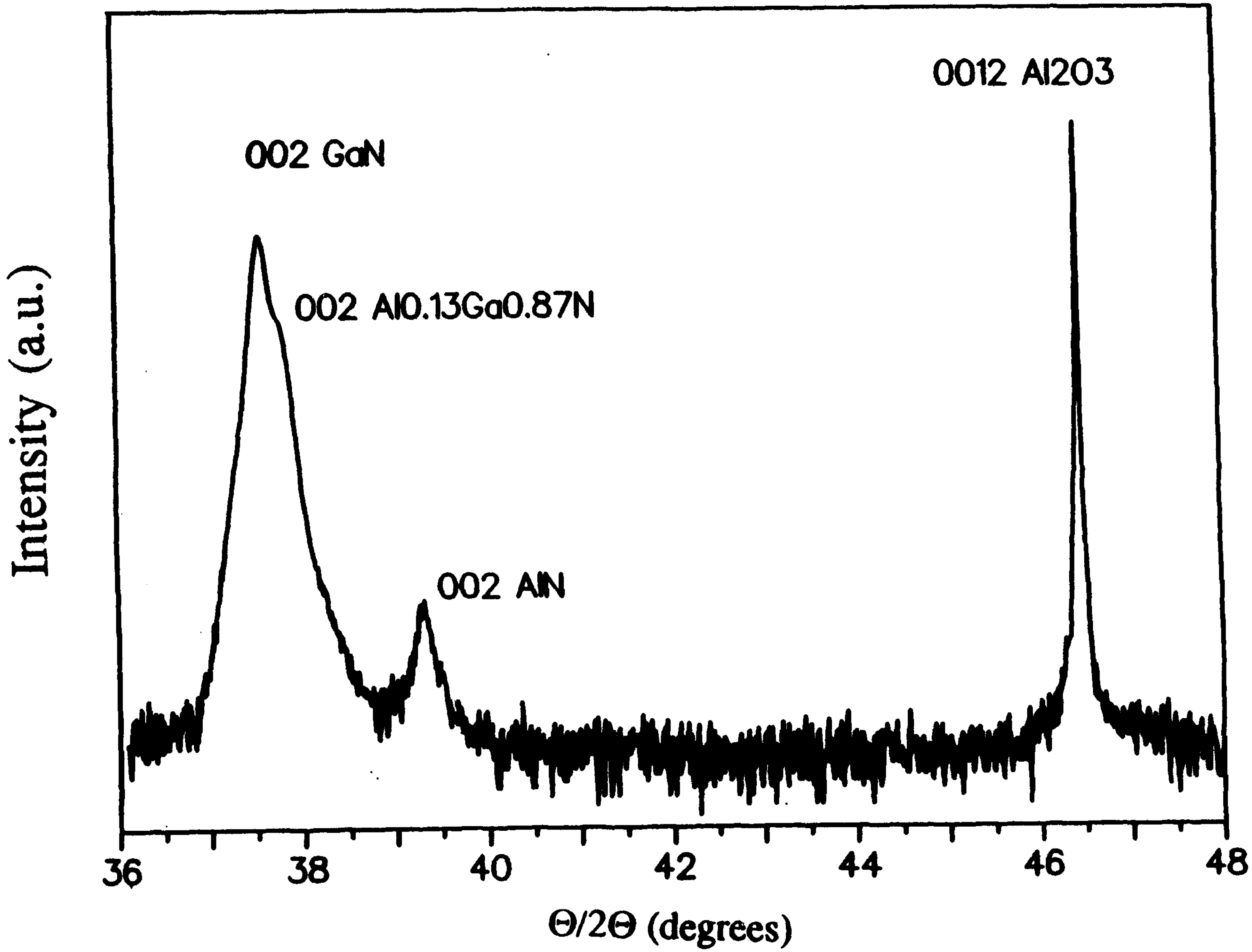
0012 Al2O3
002 GaN
002 Al0.13Ga0.87N
002 AlN
Intensity (a.u.)
36
38
40
42
44
46
48
Θ/2Θ (degrees)

**Figure 8**

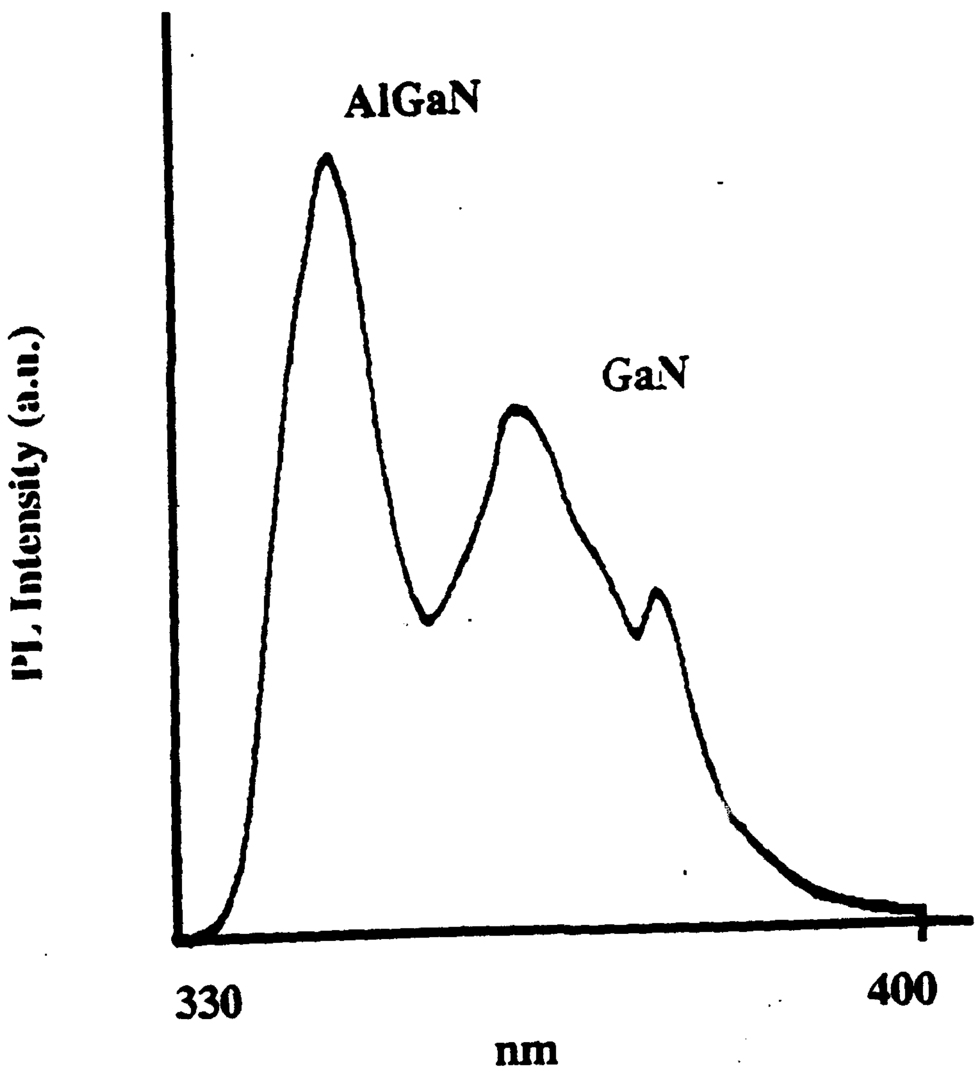


# Figure 9

# Crystallography of epitaxial growth of wurtzite-type thin films on sapphire substrates

P. Kung[a), C. J. Sun, A. Saxler, H. Ohsato[b), and M. Razeghi

*Center for Quantum Devices, Electrical Engineering and Computer Science Department*

*Northwestern University, Evanston, Illinois 60208*

In this paper, we present a crystallographic model to describe the epitaxial growth of wurtzite-type thin films such as gallium nitride (GaN) on different orientations of sapphire ($Al_2O_3$) substrates. Through this model, we demonstrate the thin films grown on (00•1)$Al_2O_3$ have a better epilayer-substrate interface quality than those grown on (01•2)$Al_2O_3$. We also show the epilayer grown on (00•1)$Al_2O_3$ are gallium-terminated, and both (00•1) and (01•2) surfaces of sapphire crystals are oxygen-terminated.

a) On leave from the Ecole Polytechnique. Palaiseau. France.

b) On leave from the Nagoya Institute of Technology. Gokiso-cho. Showa-ku. Nagoya 466. Japan.

## I. INTRODUCTION

Large-bandgap semiconductors, such as zinc selenide (ZnSe) and silicon carbide (SiC), and more recently gallium nitride (GaN), aluminum nitride (AlN) and Indium nitride (InN), have been widely studied for their ability to be used in optoelectronic devices working at short wavelengths (visible and UV).[1,2] The fabrication of such devices has been mainly limited by a high n-type background concentration and the lack of a lattice matched substrate. So far, sapphire ($\alpha$-$Al_2O_3$) substrates are the most commonly used, as they give the best crystalline quality. The GaN films grown on sapphire substrates crystallize in the wurtzite structure.

Manasevit *et al.*[3,4] have reported the growth of silicon (Si) thin films on (01•2)$Al_2O_3$. In particular, they showed the epitaxial relationship between (100)Si and (01•2)$Al_2O_3$. Experimental comparisons between the growth of III-V nitrides on the (00•1) and (01•2) orientations of sapphire have been performed, and the epitaxial relationships between GaN thin films and sapphire substrates have been established using electron diffraction and four-crystal x-ray diffraction methods.[5-8] It was shown that the (00•1) planes of GaN were parallel to the (00•1) planes of $Al_2O_3$ substrates, while the (11•0) planes of GaN were parallel to the (01•2) planes of $Al_2O_3$ substrates.

Sasaki and Zembutsu[6] showed the GaN epilayers grown on (00•1)$Al_2O_3$ had a smaller x-ray rocking curve full width at half maximum (FWHM) than the ones grown on (01•2)$Al_2O_3$, suggesting a superior crystallinity in the first case. More recently, Sun and Razeghi[8] obtained both better crystallinity and electrical results for the GaN thin films grown on the (01•2)$Al_2O_3$.

In this paper, we present a crystallographic model for the growth of an 'ideal' wurtzite-type crystal on both (00•1) and (01•2) oriented sapphire substrates, and compare this model with the experimental results. We call 'ideal' crystal an imaginary crystal that is lattice matched with both orientations of sapphire substrates used.

## II. GENERAL DESCRIPTION

Table I lists the crystallographic data for $Al_2O_3$ and GaN. Sapphire is composed of oxygen ($O^{2-}$) and aluminum ($Al^{3+}$) ions. The $O^{2-}$ form a hexagonal close packed (hcp) structure, while the $Al^{3+}$ occupy 2/3 of the octahedral sites (Fig. 1(a)). The ionic radii are: r($O^{2-}$) = 1.40Å, r($Al^{3+}$) = 0.51Å as determined by Ahrens.[9] Using hexagonal axes, with the origin at $\bar{3}c$, the ions are located at the positions and coordinates shown in Table I.

Gallium nitride has a wurtzite-type structure with nitrogen atoms forming a hcp structure and gallium atoms occupying 1/2 of the tetrahedral sites (Fig. 1(b)). The ionic radii for nitrogen and gallium are: r($N^{3-}$) = 1.71Å and r($Ga^{3+}$) = 0.62Å.[9] The positions and coordinates of all elements are given in Table I.

In this paper, we have chosen to use the Miller-Bravais notation, a four-digit notation for planes: (*hkil*) or (*hk•l*) with $i=-(h+k)$; and a three-digit notation for directions: [uvw] instead of [UVTW], the conversion being done as follows:[10]

$$U = (2u-v)/3 \qquad T = -(u+v)/3$$

$$V = (2v-u)/3 \qquad W = w$$

In order to have a lattice matched wurtzite-type epilayer on both (00•1) and (01•2) orientations of sapphire substrates, it is necessary to have the following lattice parameters for the epilayer:

$$a_{ideal} = \frac{a_{Al2O3}}{\sqrt{3}} = 2.747\text{Å}$$

$$c_{ideal} = \frac{\sqrt{3a^2_{Al2O3}+c^2_{Al2O3}}}{3} = 5.128\text{Å}$$

We will call 'ideal' such a wurtzite-structure crystal and develop our model with this ideal crystal.

## III. EPITAXIAL GROWTH

### A. Epitaxial relationship between (00•1)GaN and (00•1)$Al_2O_3$

Fig. 2(a) and 2(b) show the projections on the (00•1) planes for $Al_2O_3$ and GaN respectively. As we have mentioned before, these planes are parallel during the epitaxial growth. Generally, oxides like $Al_2O_3$ are ionic crystals in which small size cations $Al^{3+}$ with bigger valency attract the oxygen ions tightly. Thus, the surfaces of $Al_2O_3$ contain only oxygen ions. We will use the notation $(00{\bullet}1)_O$ $Al_2O_3$ for the surfaces in this orientation.

The relationships between the unit cells in (00•1)GaN epilayer and in (00•1) $Al_2O_3$ have been determined by several groups.[5,6,11] They showed there was a 30° rotation between the *a*-axes of GaN and $Al_2O_3$, as shown in Fig. 2(c). This configuration has also been confirmed by the precession x-ray diffraction experiments we have recently conducted, and which will be described in a subsequent publication.

As a result, the translational period for the $a'_1$ direction of GaN will be $a_{GaN}$, and the one for $Al_2O_3$ in the same direction will be $a_{Al2O3}/\sqrt{3}$. The lattice mismatch will then be:

$$\frac{a_{GaN} - \frac{a_{Al2O3}}{\sqrt{3}}}{\frac{a_{Al2O3}}{\sqrt{3}}} = 16.09\%$$

### B. Epitaxial growth of ideal (00•1) wurtzite-type thin films on (00•1)$Al_2O_3$

A model of epitaxial growth of (00•1) wurtzite-structure thin films on (00•1)$Al_2O_3$ substrates is now developed using the 'ideal' wurtzite-type crystal defined in section II. We shall use Ga and N to represent this imaginary crystal. The different steps in the growth model are shown in Fig. 3(a) to 3(d).

In the first step, gallium ions deposit among the oxygen ions of the sapphire substrate surface $(00\bullet1)_O$ $Al_2O_3$ represented in Fig. 3(a). More precisely, each $Ga^{3+}$ is stacked on a triangle of $O^{2-}$ (Fig. 3(b)), since this is the position that minimizes the electrostatic potential of the cation.

In the second step, nitrogen is deposited. We must consider two different cases. In the first case, the $N^{3-}$ ions form a triangle above each deposited $Ga^{3+}$, thus constituting an octahedron around the cation with the three $O^{2-}$ ions in $(00\bullet1)_O$ $Al_2O_3$ mentioned previously. In the second case, the $N^{3-}$ ions are positioned just above the deposited $Ga^{3+}$ ion, this time forming a tetrahedron around each cation with the three $O^{2-}$ ions of $(00\bullet1)_O$ $Al_2O_3$. The electrostatic valences around a nitrogen ion were calculated in both cases and gave a value of 3.75 for the first case, 3 for the second. According to Pauling's Second Rule (the Electrostatic Valency Principle)[12] the epitaxial growth is more likely to occur by the second mechanism, since the valence of a $N^{3-}$ ion is exactly 3. This is what has been illustrated in Fig. 3(c) for the second step. At this stage, the Ga-N bond is beginning to show a covalent aspect, with a tetrahedral configuration featuring a $sp^3$ hybrid orbital.

In the third step, Ga atoms are deposited among three N atoms to constitute a tetrahedron around each N and form the wurtzite-type structure of GaN thin films (Fig. 3(d)).

The $GaN_4$ tetrahedra in the epilayer are directed towards the top (away from the substrate). This has been illustrated in Fig. 1(b). The Ga-N bond in the *c*-axis direction is weaker than the sum of the three other Ga-N bonds in the tetrahedron. Thus, in the final stage of the growth, the film will be Ga terminated, since the first bond is likely to be cut.

We summarize the epitaxial relationships for the growth of (00•1)GaN thin film on (00•1)$Al_2O_3$ substrates in Table II.

### C. Epitaxial relationship between (11•0)GaN and (01•2)$Al_2O_3$

Fig. 4 shows the (01•2) plane of a sapphire crystal as well as some specific directions in the lattice. We can see the translational periods in the (01•2) planes are along the [100] (*a*-axis) and $[\bar{1}\bar{2}1]$ directions. The lattice periods in these directions are given in Table III. It can be easily calculated that the *c*-axis makes a 32° angle with the $[\bar{1}\bar{2}1]$ direction. Note that the (01•2) and (10•2) planes are not equivalent : the arrangement of $O^{2-}$ ions is the same in both planes, but that of the $Al^{3+}$ ions is different. The crystal symmetry confirms this description. Indeed, (10•2) planes are transformed into (01•2) planes by a rotation of 60° around the *c*-axis. Since $Al_2O_3$ is a trigonal system in which the c-axis is a 3-fold axis only, the two planes are not equivalent.

Fig. 5(a) represents the projection on the (01•2) plane for the sapphire crystal. The studies of the (01•2) planes of sapphire crystals conducted by Nolder and Cadoff[13] confirm our description of the atomic arrangements. We have colored the $Al^{3+}$ ions contained in a same atomic layer parallel to the (01•2) plane. It can be seen that the lattice they create is a centered square lattice, favorable to the growth of (100) silicon[13]. Fig. 5(b) shows a cross section by the $(2\bar{1}{\bullet}0)$ plane, which is perpendicular to the (01•2) plane (Fig. 4). The (01•2) planes are drawn horizontally in this cross section. We can see the remarkable property that each atomic layer parallel to the (01•2) plane only contains ions of the same kind ($O^{2-}$ or $Al^{3+}$).

Between two consecutive $O^{2-}$ layers, there are two possible configurations. In the first one, there is an $Al^{3+}$ layer that binds tightly the two $O^{2-}$ layers by attractive electrostatic forces. In the second case, there is no such atomic layer. As Fig. 5(b) shows it, there are 'sequences' of five atomic layers -(O-Al-O-Al-O)- bound tightly together, and the links between two of such 'sequences' are weaker. The (01•2) surface of the sapphire crystal can then be seen as a result of the cleavage between two 'sequences', as shown in Fig. 5(b). The $O^{2-}$ ions of the 'sequence' that has been removed by the cleavage to form the(01•2) surface are crosshatched in Fig. 5(a) and 5(b). As we can see in Fig 5(b), the (01•2) surface of the sapphire substrate will only contain $O^{2-}$ ions after cleavage.

These ions form strings on the (01•2) surface along the $[\bar{1}\bar{2}1]$ direction (Fig. 5(a)), and are periodic in the [100] direction with $a_{Al2O3}$ as the translation vector. The $O^{2-}$ ion layer just underneath has the same property, but the strings are shifted by half a translation vector (1/2 $a_{Al2O3}$) with respect to the first layer. This way, the $O^{2-}$ ions generate a ridge-like structure on the surface of the (01•2)$Al_2O_3$.

Fig. 6(a) and 6(b) represent projections on the (01•2) plane for $Al_2O_3$ and on the (11•0) plane for GaN with the translational symmetry directions. As determined by several groups[6,11], the relationships between translational symmetry directions, in this growth orientation, are listed in Table II. In Fig 6(c), we can see that the period of translation in the $[\bar{1}\bar{2}1]$ direction of $Al_2O_3$ is almost 3 times the period along the $c$-axis of GaN. The translational periods along these directions are listed in Table III. More precisely, the lattice mismatches are as follows:

for the direction [001]GaN $\parallel$ $[\bar{1}\bar{2}1]Al_2O_3$ : $\dfrac{3c_{GaN} - \left(\sqrt{3a^2_{Al2O3}+c^2_{Al2O3}}\right)}{\left(\sqrt{3a^2_{Al2O3}+c^2_{Al2O3}}\right)} = 1.11\%$

for the direction $[1\bar{1}0]$GaN $\parallel$ $[100]Al_2O_3$ : $\dfrac{a_{GaN} - \dfrac{a_{Al2O3}}{\sqrt{3}}}{\dfrac{a_{Al2O3}}{\sqrt{3}}} = 16.09\%$

The 1% lattice mismatch is much smaller along the [001] direction of GaN, parallel to the $[\bar{1}\bar{2}1]$ direction of $Al_2O_3$; than the 16% along the $[1\bar{1}0]$ direction of GaN, parallel to the [100] direction of $Al_2O_3$.

### D. Epitaxial growth of ideal (11•0) wurtzite-type thin films on (01•2)$Al_2O_3$

As in section **III. B**, we now use the 'ideal' wurtzite-type crystal to describe the growth model of (11•0) wurtzite-type thin films on (01•2) sapphire substrates. We will note Ga and N the atoms involved in this crystal.

As determined in the section above, the (01•2) surface of the sapphire substrate contains only $O^{2-}$, and the atomic layer just underneath contains only $Al^{3+}$. The presence of this cationic layer is the origin of electrostatic forces that prevent other cations from locating just above the surface $O^{2-}$ layer. This explains why, between $O^{2-}$ layers, there is not always an $Al^{3+}$ layer. Thus, it is not likely to have the deposition of cations ($Ga^{3+}$) first on the surface of the substrate.

In the first step, $N^{3-}$ ions occupy the sites vacated by the $O^{2-}$ ions (crosshatched in Fig. 5(a) and 5(b)), in the 'valleys' formed by the $O^{2-}$ ridges on the substrate surface. Just after, $Ga^{3+}$ ions bind with the $N^{3-}$ (Fig. 7(a) and 7(b)) to start constituting the atomic arrangement of the (11•0) planes of GaN (shown in Fig 7(c) and 7(d)). The $N^{3-}$ ions do not occupy all the vacated $O^{2-}$ sites, but only half of them because the whole pattern of Fig 7(c) cannot fit in a single 'valley'. In the second step, Ga and N atoms deposit in the hollow areas left after the first step, and combine with the previously deposited Ga and N atoms. In the third (Fig. 7(d)), and subsequent steps, another atomic pattern deposits in the same way.

The squares we have drawn on the figures illustrate that each step of the growth is always at the same vertical position (in the growth direction). We can thus see the relative disposition of the ions as the growth progresses if we stack the figures 7(a), (c) and (d).

We summarize the epitaxial relationships for the growth of (11•0)GaN thin film on (01•2)$Al_2O_3$ substrates in Table II.

## E. Discussion

For the 'ideal' wurtzite-type crystal grown on (00•1)$Al_2O_3$, the growth direction and the in plane-directions (Table II) are such that the hcp structure of the $O^{2-}$ in the sapphire substrate is continued by that of the N in GaN. The chemical bonds in the epilayer change gradually from their ionic nature at the interface to covalent in the wurtzite-type crystal. In the epitaxy of 'ideal'

wurtzite-type thin films on the (00•1) orientation of sapphire substrates, there is no defect at the interface.

For 'ideal' wurtzite-type crystals grown on (01•2)$Al_2O_3$, there is a discontinuity in the hcp stacking, which allows $N^{3-}$ to occupy only half the sites vacated by $O^{2-}$. This should increase the density of defects at the interface and lead to a lower crystal quality.

However, better experimental results have been obtained with GaN thin films grown on the (01•2) orientation of sapphire substrate[8]. This may prove that reducing the lattice mismatch between epilayer and substrate to 1% in the [001] direction of GaN (parallel to the $[\overline{1}\overline{2}1]$ direction of $Al_2O_3$), and a ridge-like structure that allows a progressive relaxation of the 16% mismatch in the $[1\overline{1}0]$ direction of GaN (parallel to the [100] direction of $Al_2O_3$), are key elements in growing high quality films.

## IV. SUMMARY

We have proposed a model describing the epitaxial growth of 'ideal' wurtzite-type thin films on both (00•1) and (01•2) orientations of sapphire substrates. Through this model, we have been able to deduce some information about the growth:

1. In the case of the 'ideal' wurtzite-type GaN thin films grown on (00•1)$Al_2O_3$ substrates, the hcp structure of the $O^{2-}$ ions in the sapphire is continued by that of the N atoms in the GaN, without any defect at the interface. In the case of the epitaxy of 'ideal' wurtzite-type GaN thin films on (01•2)$Al_2O_3$ substrates, the hcp structure of the $O^{2-}$ ions in the sapphire is not continued in the GaN epilayer, and some defects appear at the interface. As a result, the epilayer-substrate interface in the first case has a higher quality than in the second.

Better experimental results for the GaN epilayers grown on (01•2)$Al_2O_3$ can be explained by a lower lattice mismatch along one in-plane direction and a better relaxation of the mismatch along the other direction.

2. The GaN thin films grown on (00•1)$Al_2O_3$ substrates are Ga-terminated at the surface.

3. The surfaces of both (00•1) and (01•2) orientations of sapphire crystals are O-terminated.

## ACKNOWLEDGMENTS

The authors would like to thank Max Yoder of the Office of Naval Research for his interest and encouragement. This work is supported by the ONR contract through the contract No. N00014-93-1-0235.

We would like to thank Dr. T. Okuda and the Ministry of Education. Science and Culture of Japan for supporting the leave of H. Ohsato for one year: and Dr. H.-J. Drouhin and the Ecole Polytechnique in France for supporting P. Kung.

The authors would like to thank Dean J. Cohen for his permanent support and encouragement.

# REFERENCES


[1]M. Henini, Microelectronics Journal **23**, 500-506 (1992).

[2]S. Strite and H. Morkoç, J. Vac. Sci. Technol. B **10**(4), 1237 (1992).

[3]H.M. Manasevit, A. Miller, F.L. Morritz, and R. Nolder, Trans. Met. Soc. AIME **233**, 540 (1965).

[4]H.M. Manasevit, R.L. Nolder, and L.A. Mondy, Trans. Met. Soc. AIME **242**, 465 (1968).

[5]B.B. Kosicki and D. Kahng, J. Vac. Sci. Technol. **6**, 593 (1969).

[6]T. Sasaki and S. Zembutsu, J. Appl. Phys. **61**(7), 2533 (1987).

[7]R.C. Powell, N.-E. Lee, Y.-W. Kim, and J.E. Greene, J. Appl. Phys. **73**(1), 189 (1993).

[8]C. J. Sun and M. Razeghi, Appl. Phys. Lett. **63**(7), 973(1993).

[9]L.H. Ahrens, Geochim. Cosmochim. Acta **2**, 155 (1952).

[10]L.H. Schwartz, and J.B. Cohen, *Diffraction from Materials* (Springer-Verlag, New York, 1987), p. 14.

[11]H.M. Manasevit, F.M. Erdmann, and W.I. Simpson, J. Electrochem. Soc. **118**, 1864 (1971).

[12]R.C. Evans, *An Introduction to Crystal Chemistry* (Cambridge University, 1964), pp. 180-181.

[13]R. Nolder and I. Cadoff, Trans. Met. Soc. AIME **233**, 549 (1965).

[14]K.H. Hellwege and A.M. Hellwege, Eds, *Numerical Data and Functional Relationships in Science and Technology*, New Series, Group III, Vol. 17 (Springer-Verlag, New York, 1982).

TABLE I. Crystal data.

| | | $Al_2O_3$ | | GaN |
|---|---|---|---|---|
| Structure type | | corundum | | wurtzite |
| Crystal system | | trigonal | | hexagonal |
| Space group | | $R\bar{3}c$ (No. 167) | | $P6_3mc$ (No. 186) |
| Origin | | $\bar{3}c$ | | $3m1$ |
| Lattice parameters[a] | | $a_{Al2O3}$ = 4.758 Å | | $a_{GaN}$ = 3.189 Å |
| | | $c_{Al2O3}$ = 12.991 Å | | $c_{GaN}$ = 5.185 Å |
| Z[b] | | 6 | | 2 |
| Coordination | $O^{2-}$: | positions: 18e | $N^{3-}$: | positions: 2b |
| | | site symmetry: .2 | | site symmetry: $3m$. |
| | | (x,y,z) = (0.306 , 0 , 1/4) | | (x,y,z) = (0 , 0 , 0.375) |
| | $Al^{3+}$: | positions: 12c | $Ga^{3+}$: | positions: 2b |
| | | site symmetry: 3. | | site symmetry: $3m$. |
| | | (x,y,z) = (0 , 0 , 0.3520) | | (x,y,z) = (0 , 0 , 0) |

[a] Reference 14.
[b] Number of chemical formulae in a unit cell.

TABLE II. Epitaxial relationships for the growth of GaN crystal on (00•1) and (01•2)$Al_2O_3$.

| Growth direction relationship | | In-plane direction relationship | |
|---|---|---|---|
| **Epilayer** | **Substrate** | **Epilayer** | **Substrate** |
| (00•1)GaN | (00•1)$Al_2O_3$ | [100] (GaN) ‖ | $[1\bar{1}0]$ (Al2O3) |
| | | [010] (GaN) ‖ | [120] (Al2O3) |
| (11•0)GaN | (01•2)$Al_2O_3$ | $[1\bar{1}0]$ (GaN) ‖ | [100] (Al2O3) |
| | | [001] (GaN) ‖ | $[\overline{12}1]$ (Al2O3) |

TABLE III. In-plane translational periods for (11·0)GaN||(01·2)$Al_2O_3$.

| Directions in (11·0)GaN | | Directions in (01·2)$Al_2O_3$ | |
|---|---|---|---|
| $[\bar{1}10]$ (GaN) | $\sqrt{3}a_{GaN}$ | [100] (Al2O3) | $a_{Al2O3}$ |
| [001] (GaN) | $c_{GaN}$ | $[\overline{12}1]$ (Al2O3) | $\sqrt{3a^2_{Al2O3}+c^2_{Al2O3}}$ |

# FIGURE CAPTIONS

FIG. 1. Structures of sapphire and gallium nitride. (a): hcp structure of the $O^{2-}$ ions in $Al_2O_3$ with the $Al^{3+}$ ions occupying 2/3 of the octahedral sites. (b): hcp structure of the N atoms in GaN with the Ga atoms occupying 1/2 of the tetrahedral sites..

FIG. 2. Epitaxy of (00•1)GaN on (00•1)$Al_2O_3$. Projections on (00•1) planes (a): for $Al_2O_3$ and (b): for GaN. (c): Epitaxial relationship between the epilayer and the substrate.

FIG. 3. Epitaxial growth of ideal (00•1) wurtzite-type thin films (atoms labeled Ga and N) on (00•1)$Al_2O_3$. (a): $Al_2O_3$ substrate surface (00•1)O $Al_2O_3$. (b): 1st step, $Ga^{3+}$ ions deposit among the $O^{2-}$. (c): 2nd step, $N^{3-}$ combine with $Ga^{3+}$. (d): 3rd step, GaN thin film starts to grow.

FIG. 4. (01•2) plane of the sapphire crystal shown in an orthographic projection of the sapphire lattice.

FIG. 5. Projections of the sapphire crystal. (a): on (01•2) plane. (b): on ($\bar{2}$1•0) plane (cross section), the (01•2) planes are drawn horizontally. The crosshacthed $O^{2-}$ ions mark the location of the oxygen layer that would have been just above the (01•2) surface.

FIG. 6. Epitaxy of (11•0)GaN on (01•2)$Al_2O_3$. Projections (a): on (01•2) plane for $Al_2O_3$ and (b): on (11•0) plane for GaN. (c): Epitaxial relationship between the epilayer and the substrate.

FIg. 7. Epitaxial growth of ideal (11•0) wurtzite-type thin films (atoms labeled Ga and N) on (01•2)$Al_2O_3$. (a): 1st step, Ga and N deposit in the 'valleys' of the ridge-like structure of the (01•2)O $Al_2O_3$ surface: projection on (01•2) plane of $Al_2O_3$. (b): 1st step, projection on ($\bar{2}$1•0) plane of $Al_2O_3$ (cross section). (c): 2nd step. (d): 3rd step, GaN thin film growth.

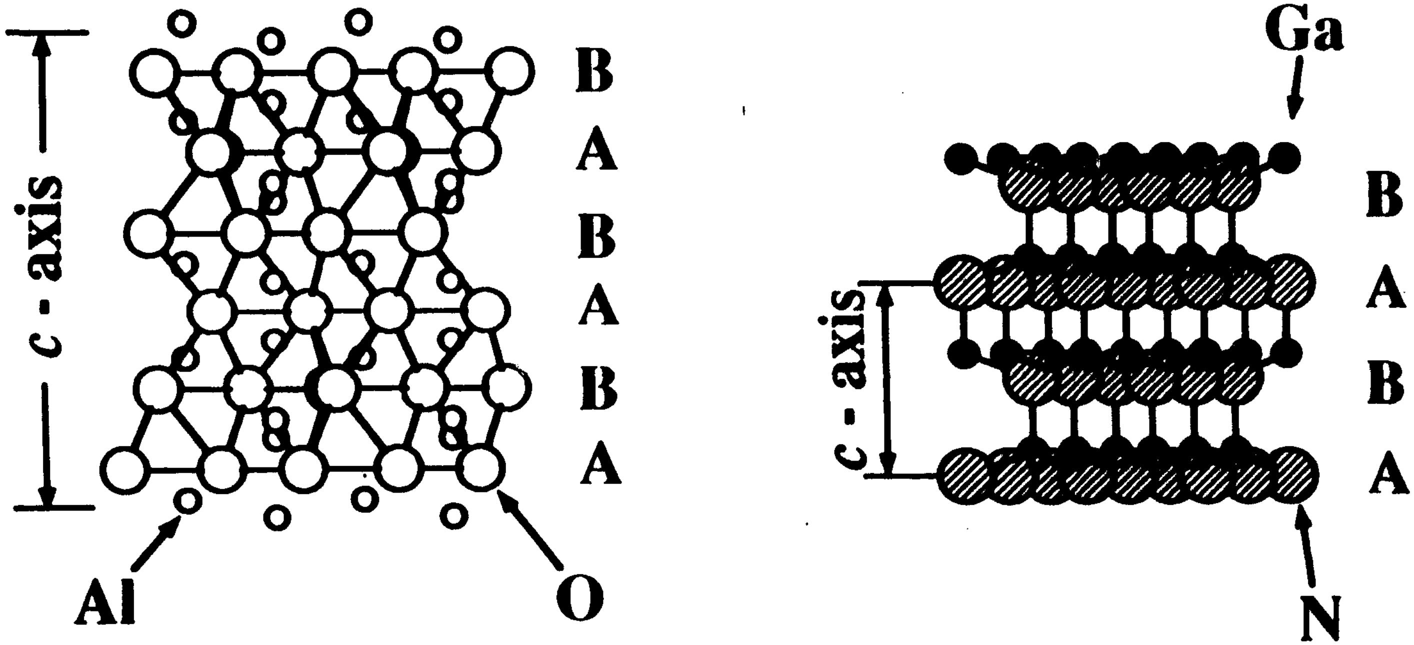


(a) (b)

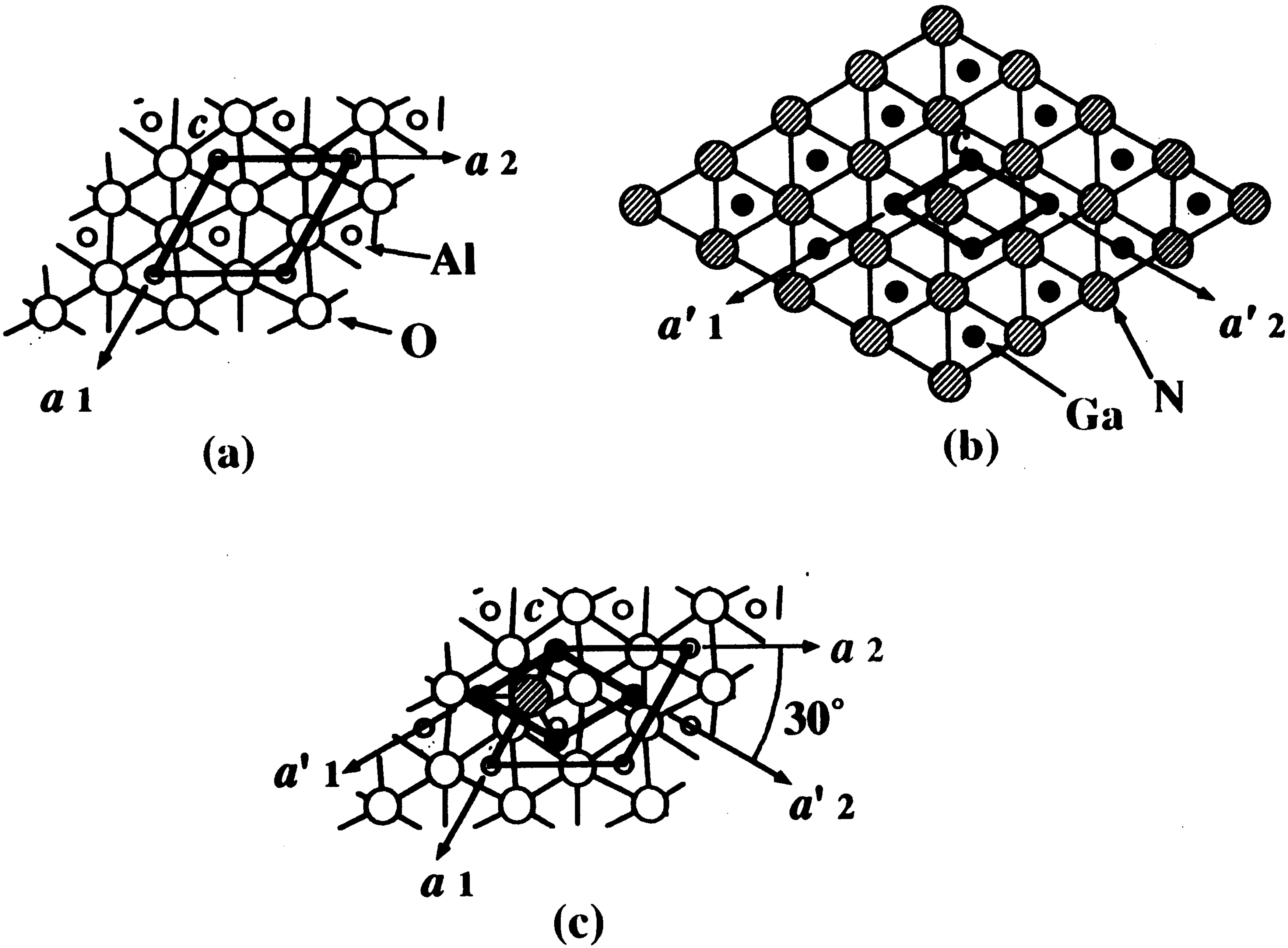

c
a 2
Al
O
a 1
(a)
c
a' 1
a' 2
Ga
N
(b)
c
a 2
30°
a' 1
a' 2
a 1
(c)

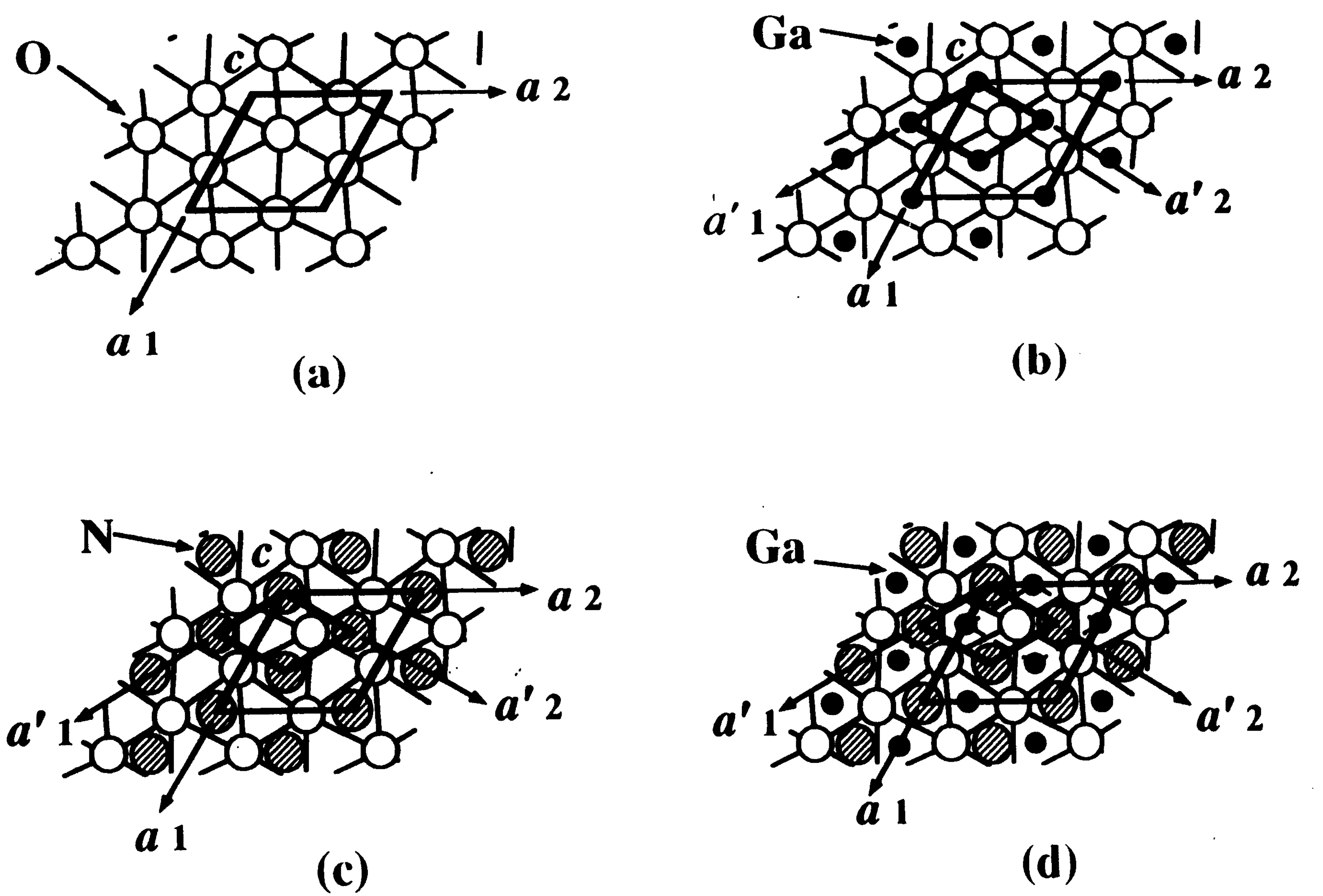
O
c
a 2
a 1
(a)
Ga
c
a 2
a' 1
a' 2
a 1
(b)
N
c
a 2
a' 2
a' 1
a 1
(c)
Ga
a 2
a' 1
a' 2
a 1
(d)

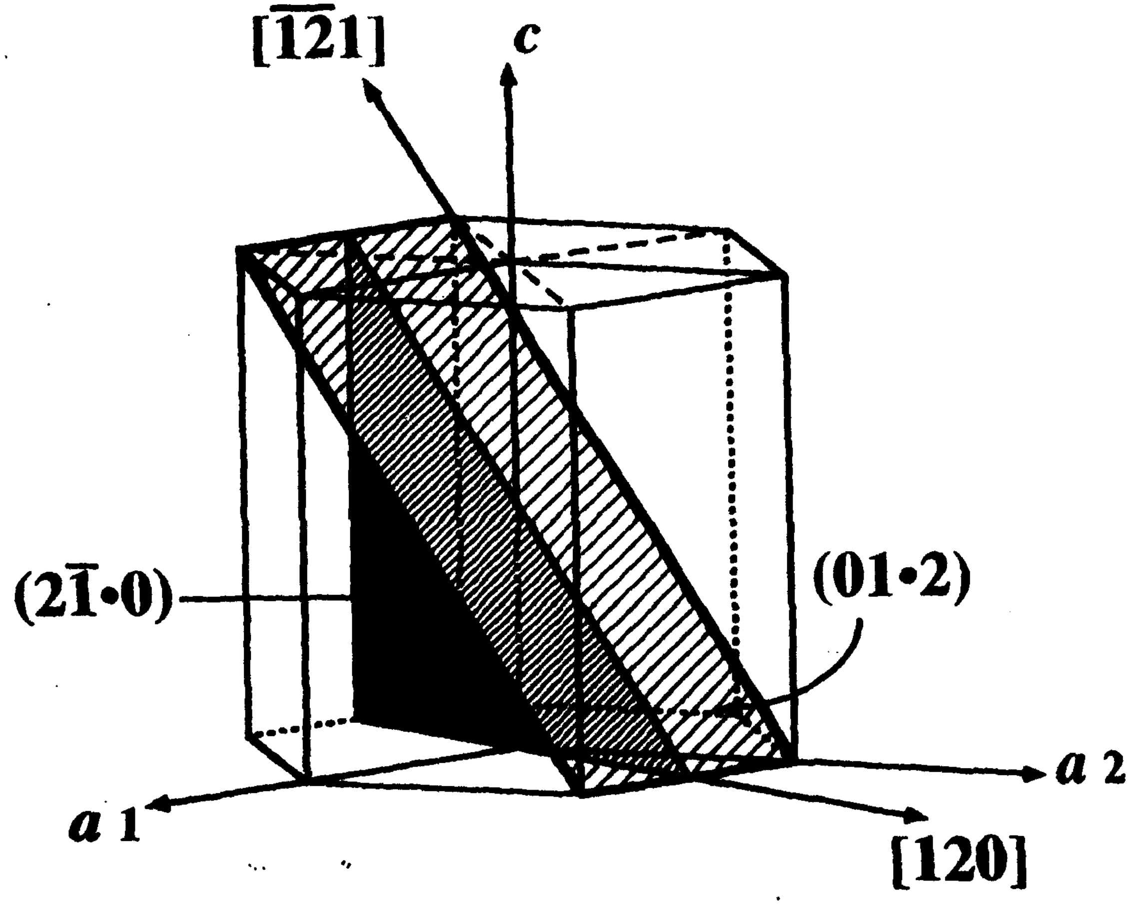

[$\bar{1}\bar{2}1$]
c
($2\bar{1}\cdot0$)
($01\cdot2$)
a 1
a 2
[120]

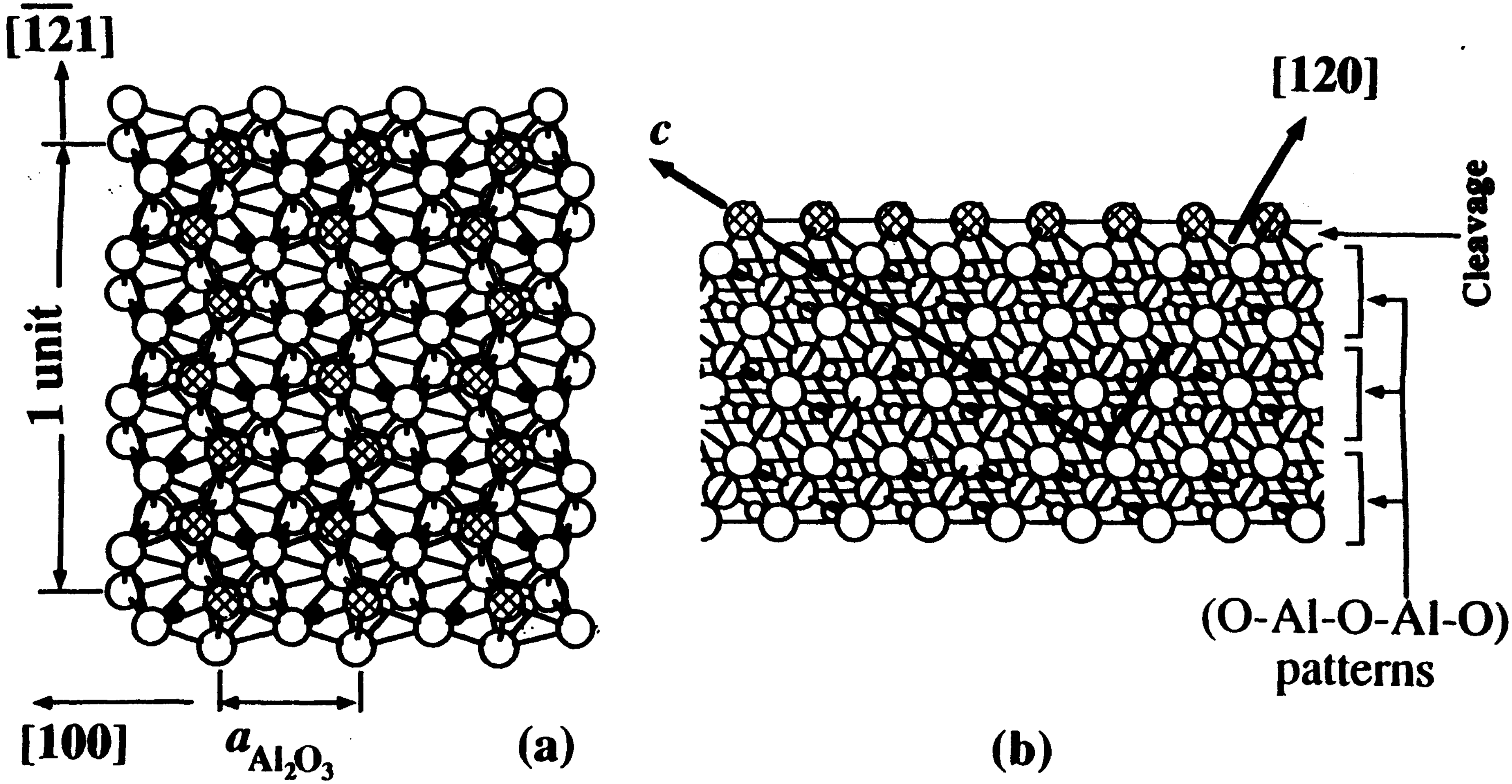

[$\overline{1}2\overline{1}$1]
1 unit
[100]
$a_{Al_2O_3}$
(a)
c
[120]
Cleavage
(O-Al-O-Al-O)
patterns
(b)

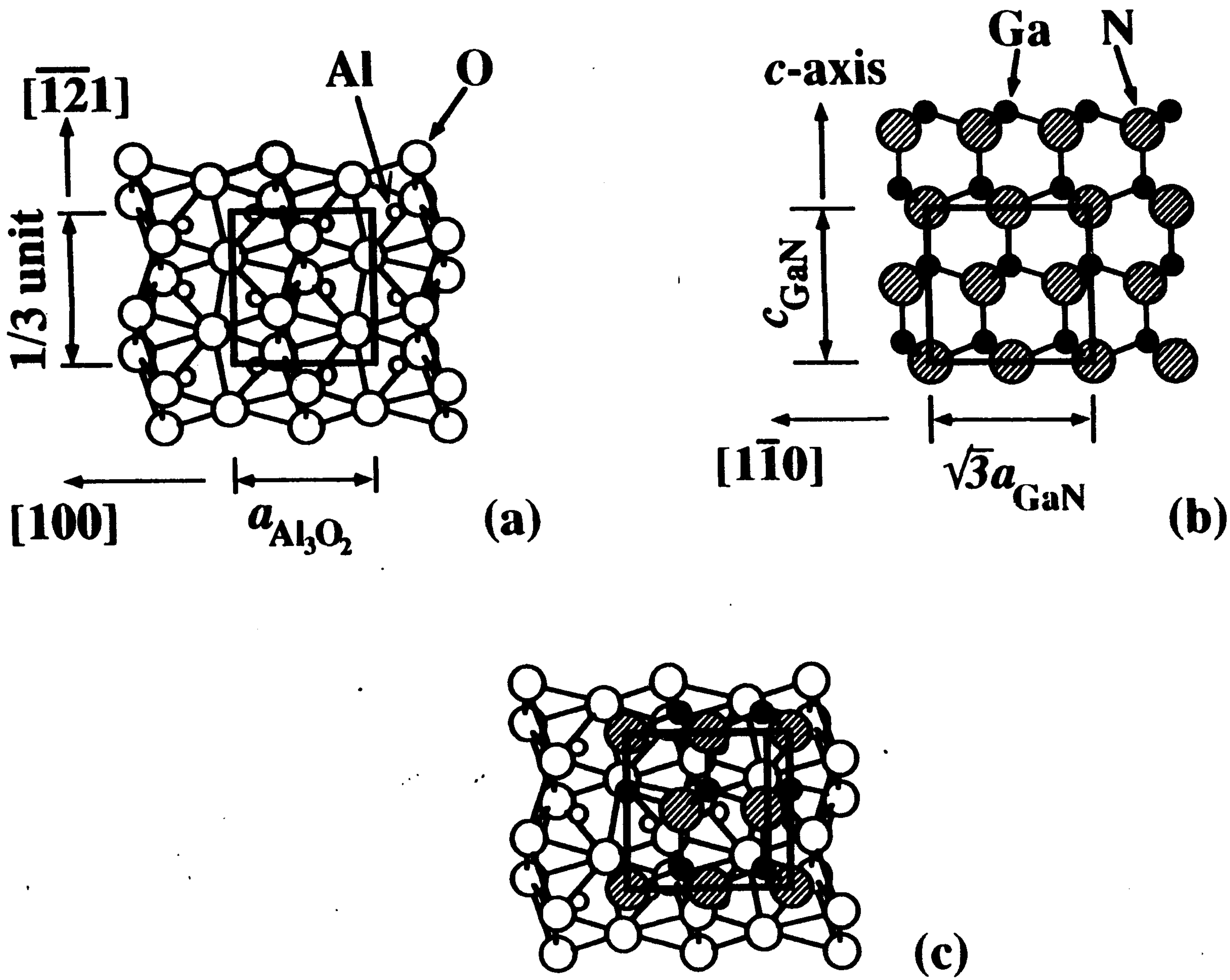

[$\bar{1}\bar{2}1$]
1/3 unit
Al
O
[100]
$a_{Al_3O_2}$
(a)
Ga
N
c-axis
$c_{GaN}$
[$1\bar{1}0$]
$\sqrt{3}a_{GaN}$
(b)
(c)

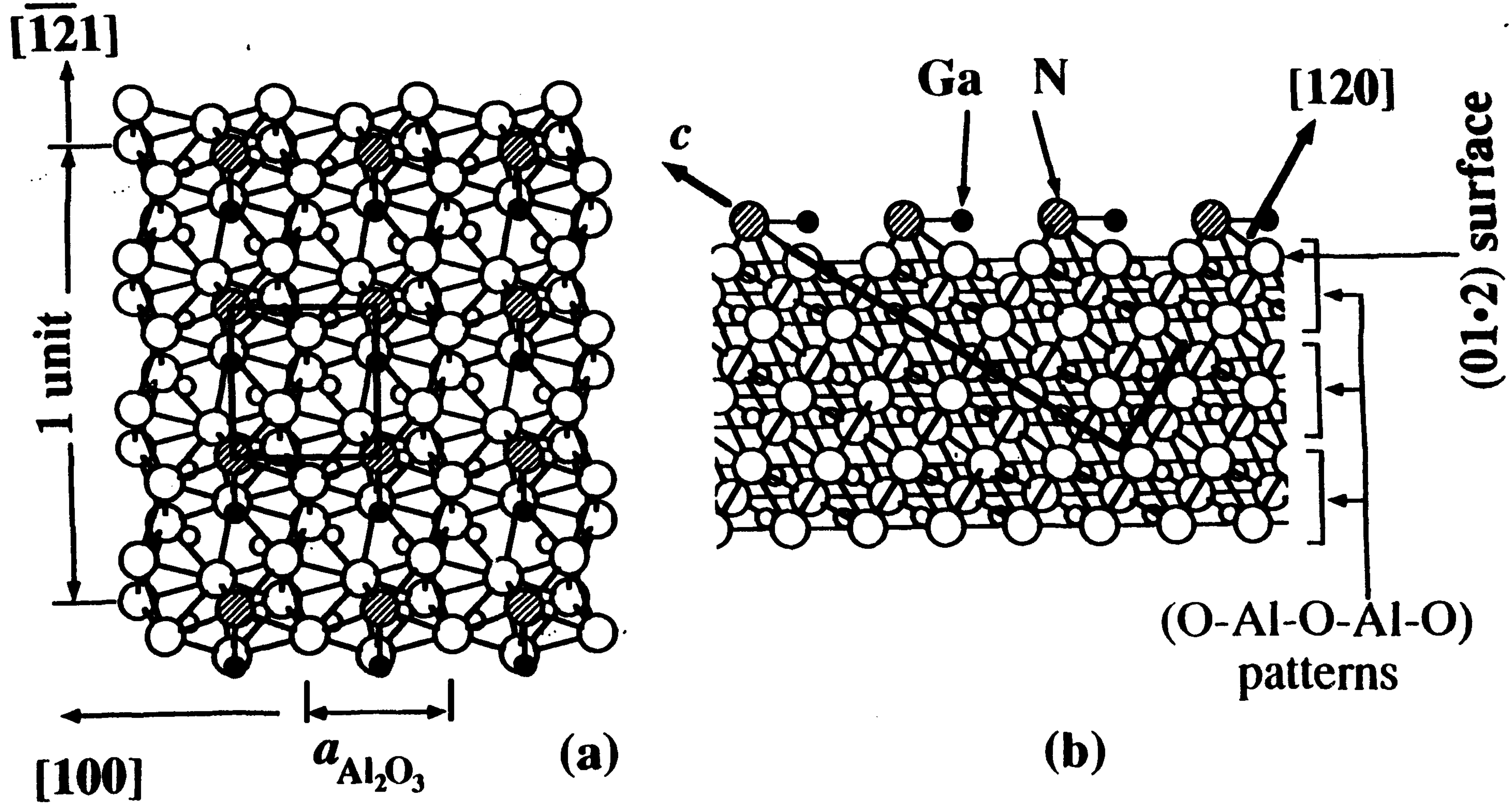

[$\bar{1}\bar{2}1$]
1 unit
[100]
$a_{Al_2O_3}$
(a)
c
Ga
N
[120]
(01•2) surface
(O-Al-O-Al-O)
patterns
(b)

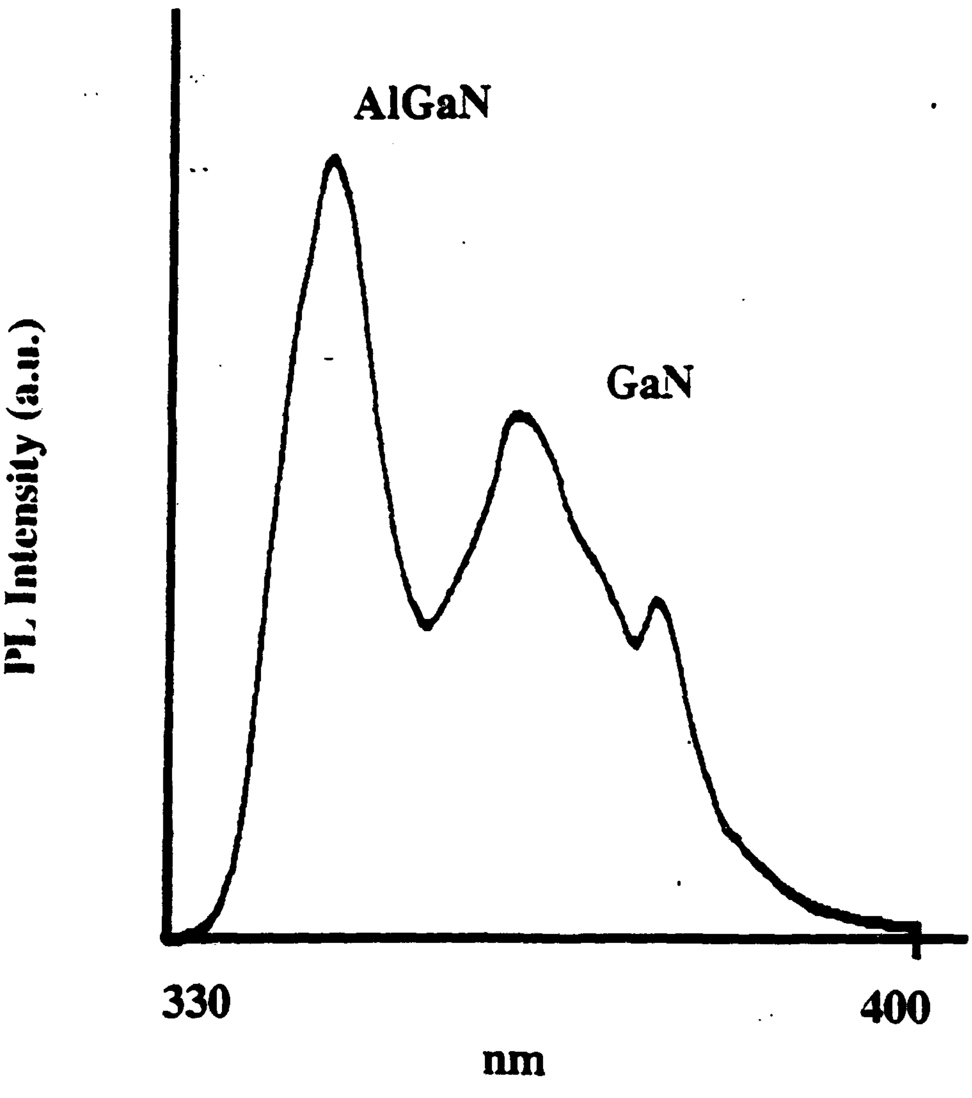

AlGaN
GaN
PL Intensity (a.u.)
330
400
nm

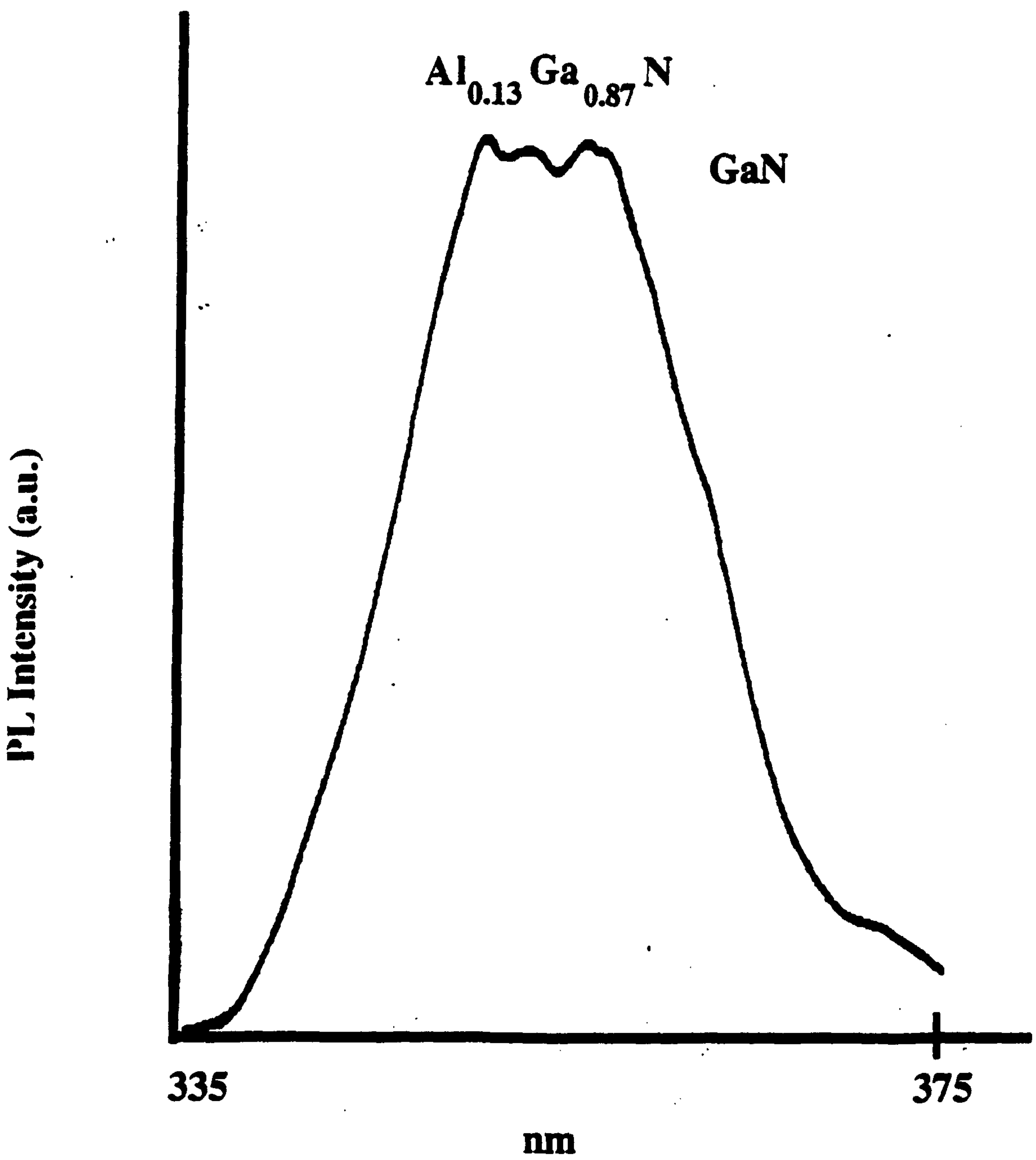

$Al_{0.13}Ga_{0.87}N$
GaN
PL Intensity (a.u.)
335
375
nm

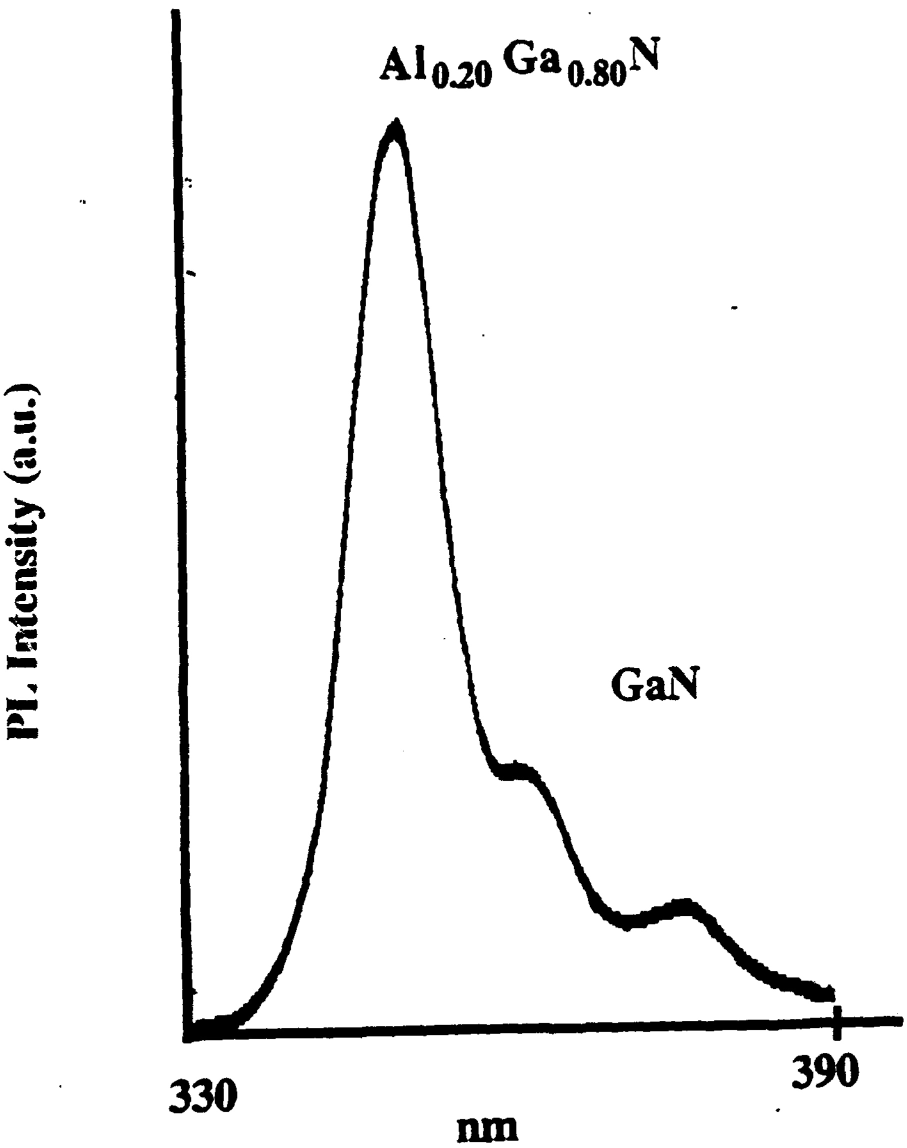

Al0.20 Ga0.80N
GaN
PL Intensity (a.u.)
330
390
nm

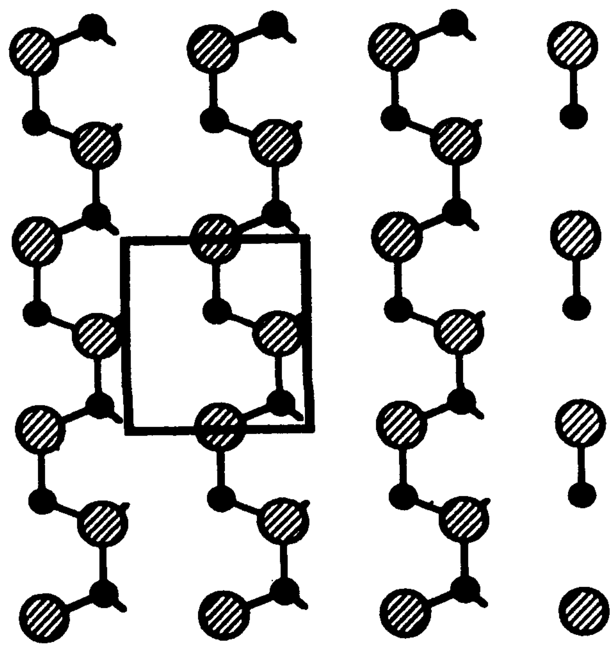
(c)

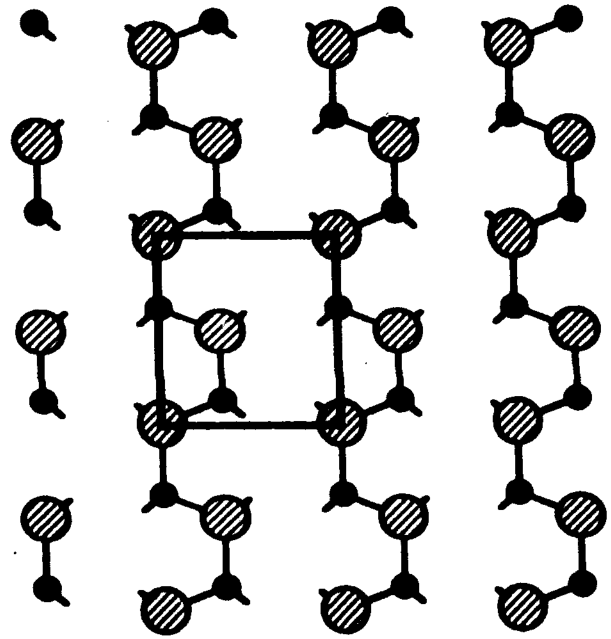
(d)

# A Crystallographic Model of (00•1) Aluminum Nitride Epitaxial Thin Film Growth on (00•1) Sapphire Substrate

C. J. Sun, P. Kung, A. Saxler, H. Ohsato and M. Razeghi

Center for Quantum Devices

Department of Electrical Engineering and Computer Science

Northwestern University, Evanston, Illinois 60208

High-quality thin aluminum nitride films were grown on different orientations of sapphire substrates by Metalorganic Chemical Vapor Deposition. (00•1) AlN thin film grown on (00•1) $Al_2O_3$ has better crystallinity than (11•0) AlN on (01•2) sapphire. Full width at half maximum of rocking curve is 97.2 arc seconds, which is the narrowest value to our knowledge. A crystallographic model between AlN thin films and sapphire substrates was proposed to explain the process of crystal growth. "Extended atomic distance mismatch" was introduced which is the mismatch of atomic distance for a longer period. It is shown that the mismatch is relaxed by edge-type dislocations. Extended atomic distance mismatch was used to interpret the results that (00·1) AlN has better crystallinity than (11•0) AlN, but (11•0) GaN has better crystallinity than (00•1) GaN.

## I. INTRODUCTION

Aluminum nitride (AlN) is one of the most promising wide-bandgap III-V semiconductors with GaN and InN for visible and ultra-violet (UV) optoelectronic devices. $Al_xGa_{1-x}N$[1] has a tunable direct band gap (6.28eV for x=1 to 3.39eV for x=0). The fabrication of such devices has been mainly limited by a high n-type background concentration and the lack of a lattice matched substrate. So far, sapphire substrates ($\alpha$-$Al_2O_3$) are the most commonly used as they give the best crystalline quality.[2]

The epitaxial relationship of 'ideal wurtzite-type' thin films without lattice mismatch on sapphire substrates has been reported.[3] Better quality thin films are expected to be on (00•1) $Al_2O_3$. In the case of (00•1) wurtzite-type thin films grown on (00•1) $Al_2O_3$, the hexagonal closed packing (hcp) of the $O^{2-}$ in the sapphire substrate is continuous with the hcp of N in GaN or AlN. For (11•0) oriented thin film grown on $(0\bar{1}\cdot2)$ sapphire, there is a discontinuity growth at the interface so as to make defects. Recently, Sun and Razeghi[4] reported that better quality of GaN films were found on (01•2) sapphire which is contrary to what is expected. In this work, we report the characterization of the AlN thin films and propose a new model of the epitaxial relationship between AlN thin films and sapphire substrates.

## II. GENERAL DESCRIPTION

### A. Crystal data

Table I lists the crystallographic data for $Al_2O_3$, AlN and GaN. The $O^{2-}$ ions of sapphire form a hcp structure and $Al^{3+}$ ions occupy 2/3 of the octahedral sites in the hcp. AlN and GaN have a wurtzite-type structure with nitrogen atoms forming hcp, and aluminum and gallium atoms occupying all of the upward tetrahedral sites. In this paper, we use the Miller-Bravais notation (*hkil*) or (*hk*•*l*) for planes and a three-digit notation [*uvw*] for directions as mentioned in our previous paper[3].

## B. Epitaxial relationship between AlN and GaN thin films and sapphire substrates

Fig.1(a) shows the epitaxial relationship of (00•1) AlN on (00•1) $Al_2O_3$. The AlN unit cell is rotated by 30° around the *c* -axis with respect to that of $Al_2O_3$. The lattice mismatch between [100] direction of AlN and [$1\bar{1}0$] direction of sapphire, is 13.29%. In the same way, the lattice mismatch is calculated to be 16.09% for GaN.[4]

Fig.1(b) shows the epitaxial relationship of (11•0) AlN on (01•2) $Al_2O_3$. "Valley" and "ridge" like structures were formed on the oxygen-terminated $(01{\cdot}2)_o$ surface of sapphire. Lattice mismatch in the c-axis direction of AlN is different from that in the direction perpendicular to the c-axis. The former is -2.85%, and the latter is 13.29%. The two values for GaN are 1.11% and 16.09%, respectively[4].

## III. Experimental results

### A. Growth of AlN

AlN thin films were grown on sapphire and silicon substrates by horizontal atmospheric pressure metalorganic chemical vapor deposition (MOCVD) reactor. A dual infra-red lamp heating configuration was used to heat the graphite susceptor which was inclined at 15° with respect to horizontal. A thermocouple inserted into the susceptor monitored its temperature and provided feedback to the temperature controller. Trimethylaluminum (TMAl) and ammonia ($NH_3$) were used as Al and N source materials, respectively. Nitrogen ($N_2$) was used as the carrier gas. Growth temperature was varied from 900°C to 1050°C. TMAl bubbler temperature was kept at 25°C and carrier gas bubbling flow rates were 2.5-5 cc/min. The ammonia flow rate varied from 400 to 800 cc/min, while total gas flow remained constant at 1600 cc/min. (00•1), (01•2) sapphire and (100) Si were used as substrates. Sapphire substrates were etched by a hot solution of $H_3PO_4 : H_2SO_4 = 1:3$, rinsed in deionized water and blowed dry with filtered nitrogen. Si substrates were cleaned by dipping in hydrofluoric acid prior to growth,

rinsed and blowed dry. In order to reduce parasitic chemical reactions, TMAl and $NH_3$ were mixed at the entrance of the reactor chamber.

A high resolution X-ray diffractometer with a four crystal monochrometer (MPD 1880 /HP) were used to identify the crystallinity of the films.[5] Fourier transform infrared spectroscopy (FTIR) was used to find the phonon modes for Al-N bonds. Only films grown on Si substrates were used since sapphire crystals absorb radiation in the Al-N spectral region. UV transmission spectroscopy was used for measuring the absorption edge of the AlN films.

### B. Characterization of AlN

Both AlN films grown on (00•1) and (01•2) sapphire were identified with wurtzite-type structures by X-ray diffraction spectra. AlN thin film grown on (00•1) sapphire is (00•1) oriented and that on (01•2) $Al_2O_3$ is (11•0) oriented. The full width at half maximum (FWHM) of 00•2 diffraction line of (00•1) AlN thin film was 97.2 arc seconds which is the narrowest value reported to our knowledge. While for (11•0) AlN thin film, the FWHM of 11•0 diffraction line is 3200 arc seconds.

FTIR transmission spectra show a clear peak at 665 $cm^{-1}$, which corresponds to the transverse optical mode $TO_1$=665 $cm^{-1}$ of Al-N bond[6].

UV transmission spectra show that (00•1) AlN thin film on (00•1) sapphire has a sharp edge at about 197 nm wave length, confirming the presence of high quality AlN thin film. (11•0) AlN thin film grown on (01•2) sapphire shows a much less sharp edge at 213 nm wave length.

## IV. A Crystallographic Model of AlN thin films on sapphire substrates

### A. Epitaxial relationship between (00•1) AlN and (00•1) sapphire

We previously reported a model of epitaxial growth of thin films with an 'ideal' wurtzite-type crystal structure, grown on sapphire substrates[3]. In this paper, a model of epitaxial growth of wurtzite-type AlN single crystal is proposed including the formation

of dislocations, as shown in Fig. 2. The theoretical model presented in Fig. 2 is derived based on the crystallographic relationship described previously and crystallochemistry. Since the (00•1) surface of sapphire is oxygen terminated, Al atoms will be seated among three oxygen atoms, making the same structure of sapphire in the first step of AlN epitaxial growth. Lattice mismatch was met when N generated from $NH_3$ combined with Al ions to make a tetrahedron with the oxygen on the sapphire surface. The chemical bonds change gradually from their ionic nature to covalent nature: the bonding between Al ion and O ion of sapphire is ionic, and the Al atoms and N atoms make $sp^3$ hybrid orbital with covalent nature. Lattice mismatch can be calculated from the change of Al-Al atomic distances between AlN and $Al_2O_3$. The Al-Al distance in $[1\bar{1}0]$ direction of sapphire is 2.747Å, and that of AlN in [100] is 3.112Å. Thus lattice mismatch is 13.29%. 8:9 is the smallest nonreducible integral ratio for 2.747: 3.112. Therefore, nine times the Al-Al distance of $Al_2O_3$ is nearly equal to eight times that of AlN as shown in Fig. 2. Edge type dislocations are generated in every 8 N atoms during the strain layer growth. Strain layer will be relaxed, that is the Al-Al atomic distance will gradually change from 2.747 to 3.112Å, and single crystal of AlN growth begins. A new definition of lattice mismatch "Extended Atomic Distance Mismatch" (EADM) for large lattice mismatch epitaxial growth is as follows:

$$\text{EADM} = \frac{Id - I'd'}{I'd'}$$

where, I and $I'$ are integers, d and $d'$ are atomic distances of epilayer and substrate, respectively. I and $I'$ are determined in the following way: $d:d' \sim I:I'$, where $I:I'$ is the smallest nonreducible integral ratio for $d:d'$. The difference of I and I' is one which introduces a periodic edge-type dislocation. In the case of (00•1) AlN, the dislocations appear on a nonoccupied octahedron as shown in Fig. 2.

According to this definition, I and $I'$ are found to be 9 and 8 which has exactly the same relationship as derived from the growth model. So EADM is equal to 0.70%

between [1C0] of AlN and $[1\bar{1}0]$ of sapphire. In the same way, I:I$'$ is 6:5 as considering the periodic array of Ga atoms, and EADM is -3.27% for the case of GaN, which has a lattice mismatch of 16.09% as shown in Table II.

**B. Epitaxial relationship between (11•0) AlN and (01•2) sapphire**

Contrary to the hcp symmetry of (00•1) AlN and (00•1) sapphire, (11•0) AlN and (01•2) sapphire have rectangular symmetry. Two directions of lattice mismatch have to be considered. One is calculated from the $[1\bar{1}0]$ direction of AlN and the [100] of sapphire. The other is calculated from the [001] direction of AlN and the $[\bar{1}\bar{2}1]$ of sapphire. As N and O atoms have a very important role in the initial few growth steps, N-N and O-O atomic distances are used to explain lattice mismatch.

In the first direction, we consider the lattice mismatch between $[1\bar{1}0]$ of AlN and [100] of sapphire. The N-N atomic distance of the $[1\bar{1}0]$ of AlN is 5.390Å and the O-O atomic distance of the [100] direction of sapphire is 4.758Å, so lattice mismatch is 13.29%. On the surface of (01•2) sapphire as shown in Fig. 3, O atoms form the ridge and valley-like structure and N atoms with Al will grow at the valley-like sites between the ridges. N atoms are attracted by Al ions underneath the O surface and form the $Al(O_5,N)$ octahedron. As the electrical charge and radius of N and O are different, N could not occupy all the valley sites. In $[1\bar{1}0]$ direction of AlN, there are five valley sites (stable) and three ridge sites (unstable) for nitrogen atoms, for every eight N-N atomic distances. Five N atoms will fill the five valley sites, while no N atoms will fill the ridge sites in both A and B layers. As EADM is considered, I and I$'$ are given to be 9 and 8, and EADM is calculated to be 0.70%. Nine times of O-O distance of sapphire is about equal to eight times the N-N distance of AlN, yielding the same results as (00•1) AlN on (00•1) $Al_2O_3$.

In the second direction, we consider [001] AlN and $[\bar{1}\bar{2}1]$ sapphire. The N atoms are seated in ...ABABAB... structure with about two and two third times the N-N atomic

distance shift between A and B layers. The N-N distance of [001] AlN is 4.982Å and the O-O distance of $[\overline{1}\overline{2}1]$ sapphire is 5.128Å, so the lattice mismatch is -2.85%. As EADM is considered, I and I' are given thirty-five and thirty-six, respectively. This period length is about 179 Å which is too long to introduce only one dislocation, because other defects might appear in this period. The actually lowest mismatch limit to the applicability of EADM cannot be determined without further study. This limit should depend on the deformation potentials of the epilayer as well as on the nature and concentration of defects present in the epilayer. So EADM can no longer be applied for this case. In other words, I and I' are chosen to be 1, when small lattice mismatch is met.

### C. Comparison of AlN and GaN growth on two different sapphire orientations

Table II shows the results of EADM of AlN and GaN growth on $Al_2O_3$. For AlN growth, EADM in [100] direction (0.70%) is equivalent to that in $[1\overline{1}0]$ direction, while EADM in [001] direction is -2.85%. As EADM between (00•1) AlN and (00•1) $Al_2O_3$ is smaller than that between (11•0) AlN and (01•2) $Al_2O_3$, better crystallinity is observed on (00•1) sapphire substrate.

For GaN growth, EADM in [001] direction is 1.11%, which is smaller than that (-3.27%) in [100] direction. So, (11•0) GaN thin films grown on (01•2) sapphire were observed to have better crystallinity than that on (00•1) sapphire.

## V. Conclusions

First, high quality AlN thin films were obtained on sapphire substrates by MOCVD. We showed that (00•1) AlN thin film grown on (00•1) sapphire has better crystallinity than (11•0) AlN on (01•2) sapphire. FWHM of the rocking curve is 97.2 arc seconds and the absorption edge is at 197nm.

Second, a crystallographic model between AlN thin films and sapphire substrates was proposed to explain the process of crystal growth:

(a) A new definition of lattice mismatch for a longer period called "extended Atomic Distance Mismatch" or "EADM", has been introduced.

(b) The relaxation of strain layer growth is due to the creation of edge-type dislocations.

Third, better crystallinity has been observed on (00•1) AlN and (11•0) GaN. EADM (0.70%) for (00•1) AlN thin film on the (00•1) sapphire is smaller than that (-2.85%) for (11•0) AlN on (01•2) $Al_2O_3$. While EADM (-3.27%) for (00•1) GaN thin film on the (00•1) sapphire is larger than that (1.11%) for (11•0) GaN on (01•2) $Al_2O_3$.

It was found EADM used for large lattice mismatch epitaxial growth can accurately explain the different phenomena in nitride growth.

## ACKNOWLEDGMENTS

The authors would like to thank Max Yoder of the Office of Naval Research for his interest and encouragement. This work is supported by the ONR contract through the contract No.N00014-93-1-0235.

We would like to thank Prof. T.Okuda and the Ministry of Education, Science and Culture of Japan for supporting the leave of H. Ohsato for one year, and Dr. H. -J. Drouhin and the ECOLE Polytechnique in France for supporting P.Kung.

The authors would like to thank Dean Jerome Cohen for his permanent support and encouragement.

## REFERENCES


1) S. Strite and H. Morkoç, J. Vac. Sci. Technol. B **10**(4), 1237 (1992).

2) H.Amano, M.Kito, K.Hiramatsu and I. Akasaki: Jpn.J.Appl.Phys. **28**, L2112 (1989).

3) P. Kung, C. J. Sun, A. Saxler, H. Ohsato and M. Razeghi, to be published in J. Appl. Phys., (1993).

4) C.J. Sun and M. Razeghi, Appl. Phys. Lett. **63**(7),973 (1993).

5) X. He and M. Razeghi, Appl. Phys. Lett. **73**(7), 3284 (1993).

6) K.Seki, X. Xu, H. Okabe, J.M. Frye, and J.B. Halpern, Appl. Phys. Lett, **60**(18), 2234 (1992).

## FIGURE CAPTIONS

Fig.1. Epitaxial relationship between AlN thin films and sapphire substrates. (a) (00•1) AlN crystal structure on (00•1) sapphire crystal structure. *d* and *d'* are the Al-Al atomic distances of sapphire and AlN, respectively. The unit cells of sapphire and AlN are expressed by thick solid lines. (b) (11•0) AlN crystal structure on (01•2) sapphire crystal structure.

Fig.2. A crystallographic model of cross sectional plane of Fig. 1(a), EADM is shown between eight times of the Al-Al atomic distance of AlN and nine times of the Al-Al atomic distance of sapphire. Moreover. The strain layer growth of AlN is relaxed by the creation of edge-type dislocations.

Fig.3. A crystallographic model of the first step growth of (11•0) AlN on (01•2) sapphire. Oxygen atoms on (01•2) sapphire surface form ridges and valleys. N atoms are filled in the valley sites but not in the ridge sites. The former are expressed by solid circles, and the latter are expressed by *null circles*. EADM, between [1$\bar{1}$ 0] AlN and [100] sapphire, has the same value as in Fig.2.

**TABLES**

Table I. Crystal data of AlN and sapphire.

Table II. Lattice mismatches and Extended Atomic Distance Mismatches (EADM) of AlN and GaN on sapphire.

Table I. Crystal data of AlN and sapphire.

| | $Al_2O_3$ | | AlN | |
|---|---|---|---|---|
| Structures | corundum | | wurtzite | |
| Crystal systems | trigonal | | hexagonal | |
| Space groups | $R\bar{3}c$ (No.167) | | $P\,6_3mc$ | |
| Origins | $\bar{3}c$ | | $3m1$ | |
| Lattice parameters $a$ = | 4.758Å | | 3.112Å | |
| $c$ = | 12.991Å | | 4.982Å | |
| $Z$ | 6 | | 2 | |
| Atoms | $O^{2-}$ | $Al^{3+}$ | $N^{3+}$ | $Al^{3+}$ |
| Positions | 18e | 12c | 2b | 2b |
| Site symmetries | .2. | 3. | $3m.$ | $3m.$ |
| coordinates | 0.306, 0, 1/4 | 0, 0, 0.352 | 0, 0, 0.375 | 0, 0, 0 |

Table II. Lattice mismatches and extended atomic distance mismatches (EADM) of AlN and GaN on sapphire.

| Films on substrates | Directions | Lattice mismatches | EADM |
|---|---|---|---|
| (00•1)AlN//(00•1)$Al_2O_3$ | [100]AlN//[$1\bar{1}0$]$Al_2O_3$ | 13.29% | 0.70% |
| (11•0)AlN//(01•2)$Al_2O_3$ | [$1\bar{1}0$]AlN//[100]$Al_2O_3$ | 13.29% | 0.70% |
| | [001]AlN//[$\bar{1}\bar{2}1$]$Al_2O_3$ | -2.85% | -2.85% |
| (00•1)GaN//(00•1)$Al_2O_3$ | [100]GaN//[$1\bar{1}0$]$Al_2O_3$ | 16.09% | -3.27% |
| (11•0)GaN//(01•2)$Al_2O_3$ | [$1\bar{1}0$]GaN//[100]$Al_2O_3$ | 16.09% | -3.27% |
| | [001]GaN//[$\bar{1}\bar{2}1$]$Al_2O_3$ | 1.11% | 1.11% |

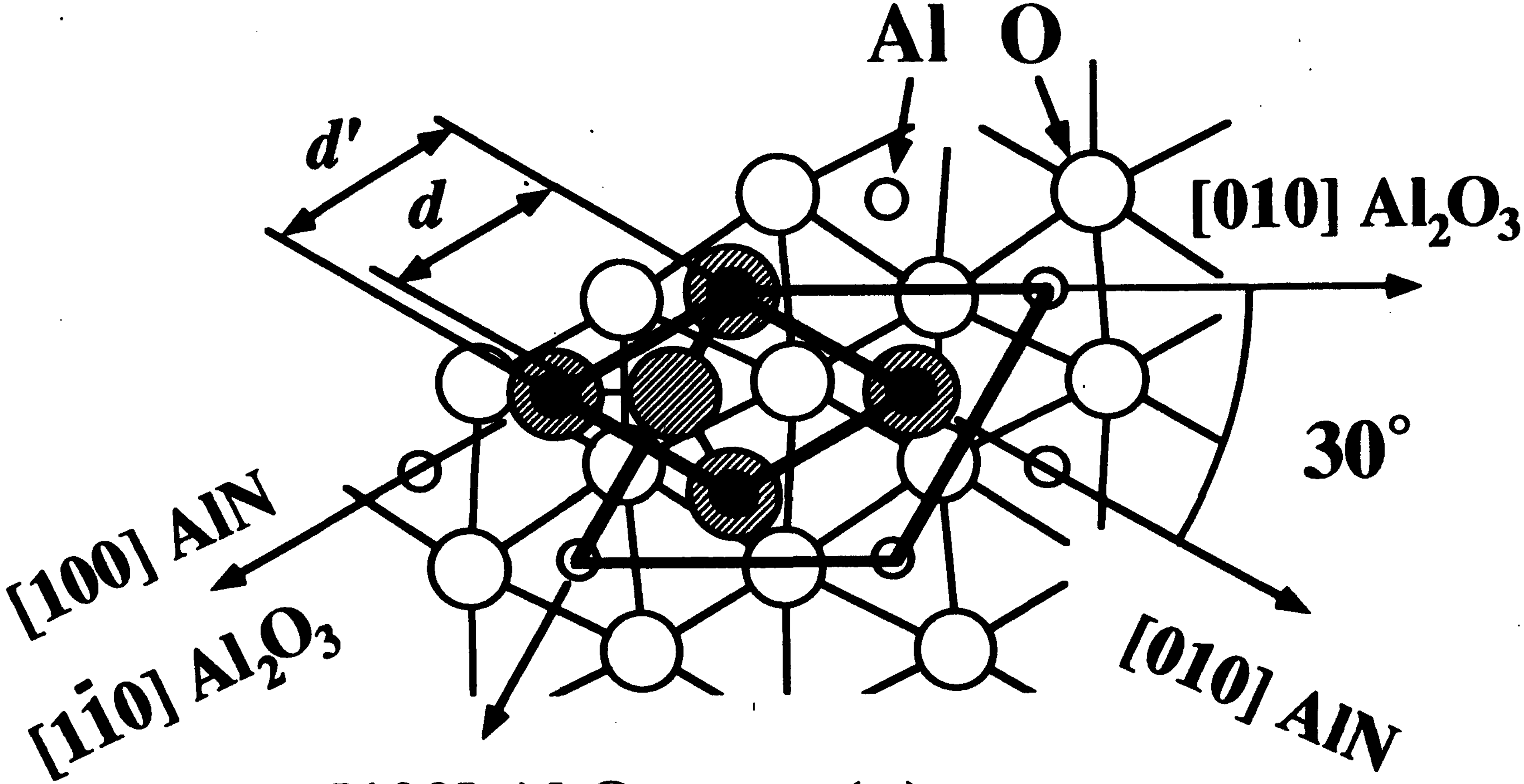


(a)

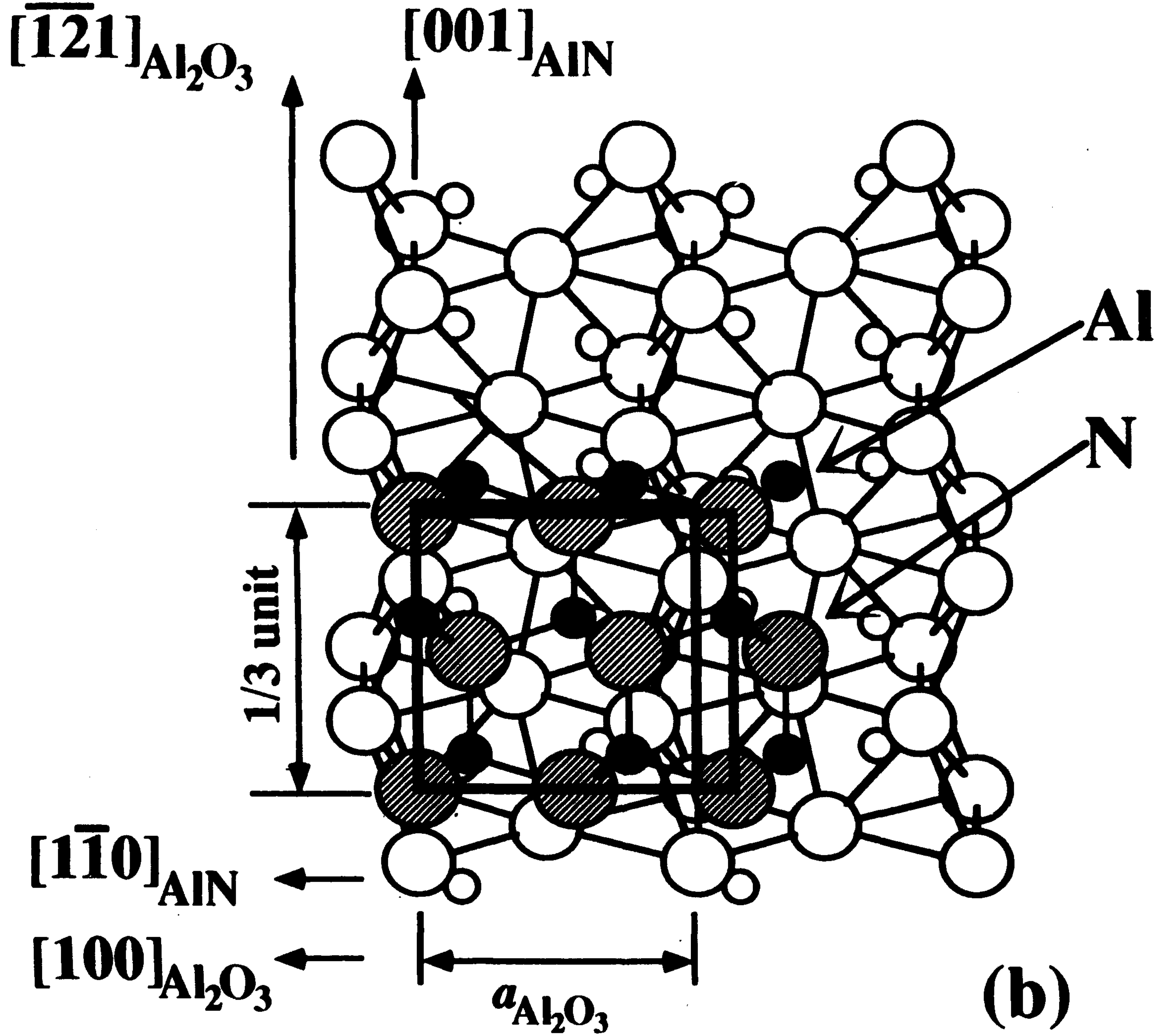

$[\bar{1}\bar{2}1]_{Al_2O_3}$
$[001]_{AlN}$
Al
N
1/3 unit
$[1\bar{1}0]_{AlN}$
$[100]_{Al_2O_3}$
$a_{Al_2O_3}$


(b)

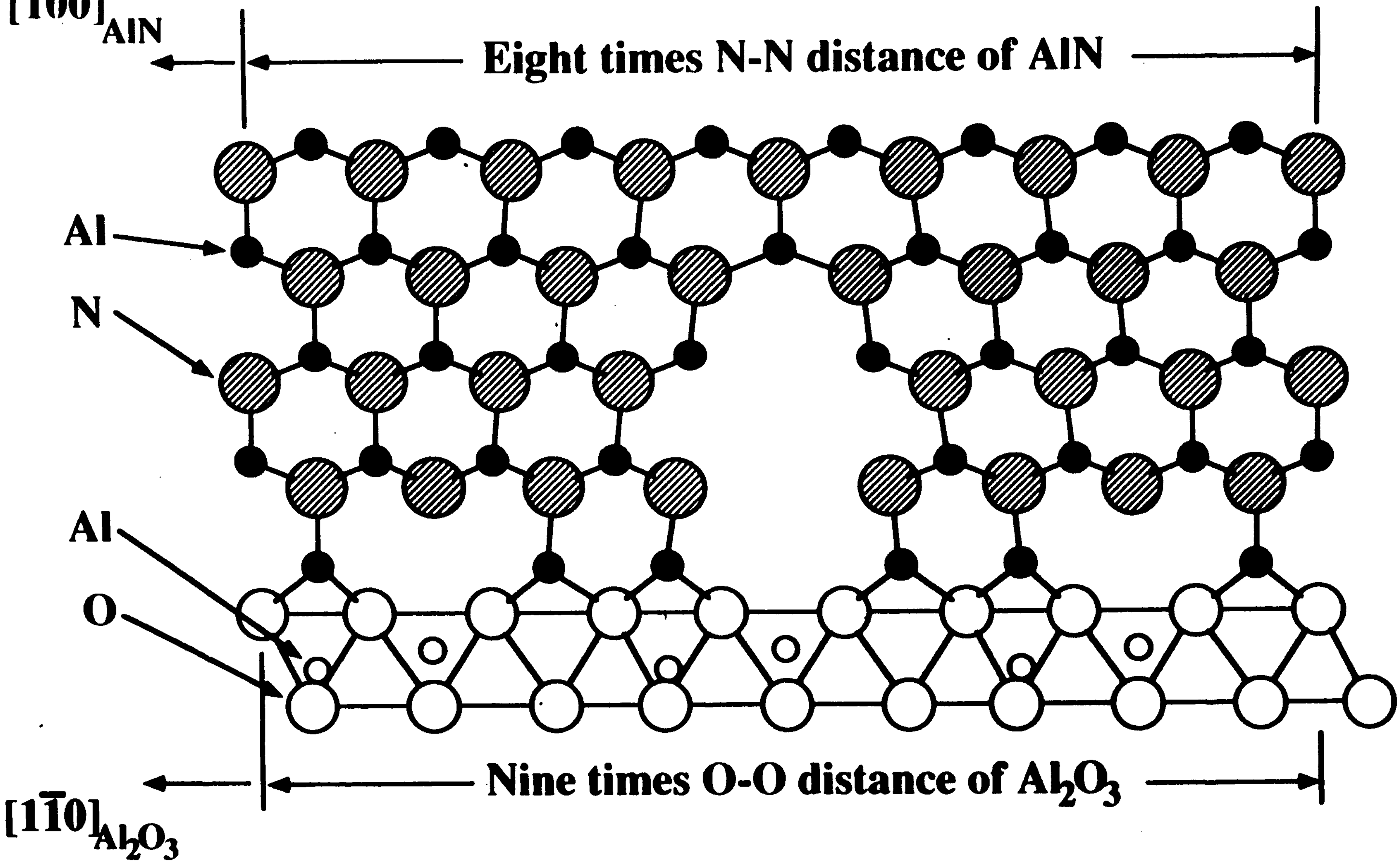

$[100]_{AlN}$
Eight times N-N distance of AlN
Al
N
Al
O
Nine times O-O distance of $Al_2O_3$
$[1\bar{1}0]_{Al_2O_3}$

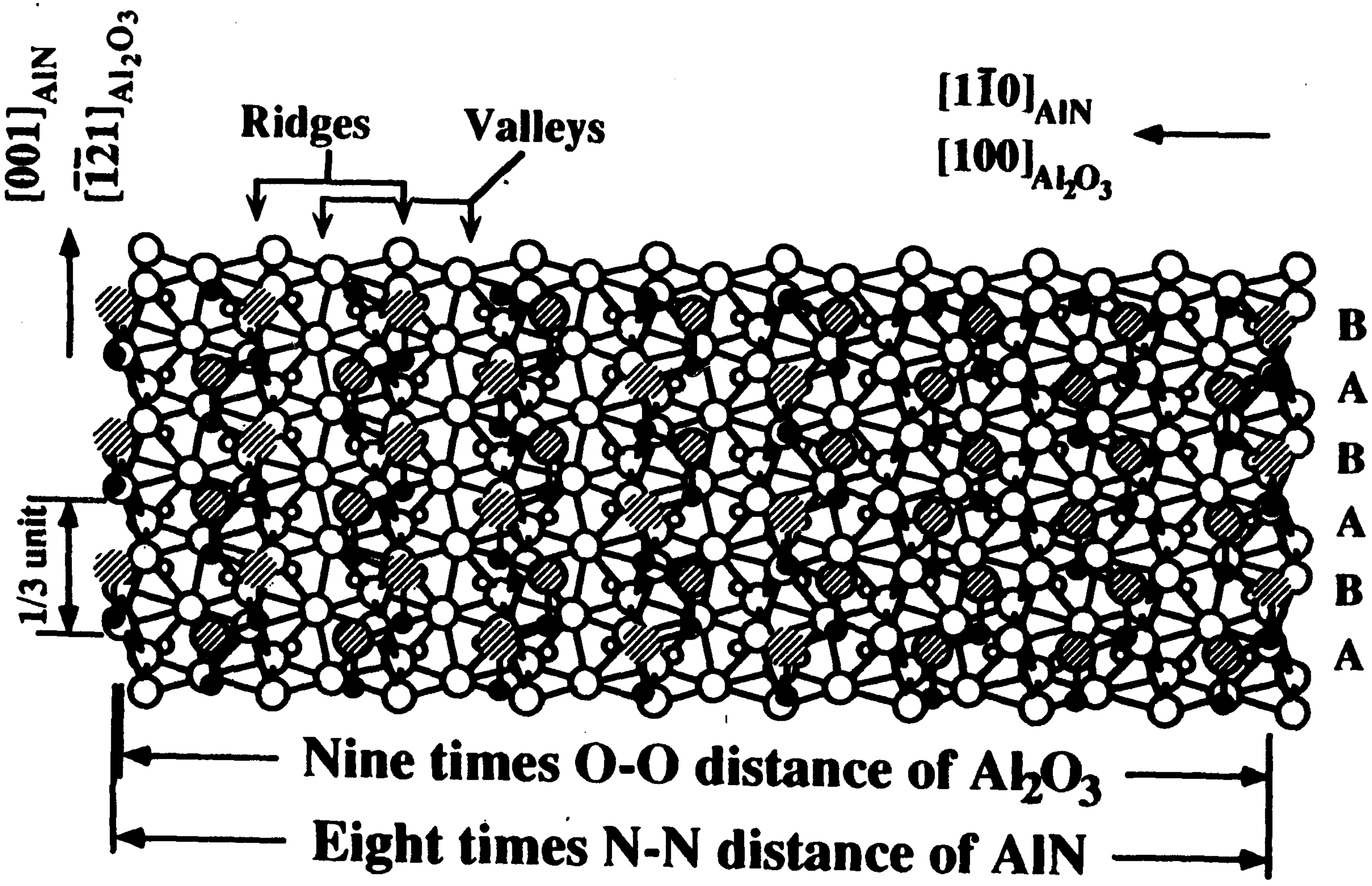

$[001]_{AlN}$
$[\bar{1}2\bar{1}]_{Al_2O_3}$
Ridges
Valleys
$[1\bar{1}0]_{AlN}$
$[100]_{Al_2O_3}$
1/3 unit
B
A
B
A
B
A
Nine times O-O distance of $Al_2O_3$
Eight times N-N distance of AlN

# Comparison of the physical properties of GaN thin films deposited on (0001) and (01$\bar{1}$2) sapphire substrates

Chien-Jen Sun and Manijeh Razeghi
*Center for Quantum Devices, Department of Electrical Engineering and Computer Science, Northwestern University, Evanston, Illinois 60208*

(Received 12 February 1993; accepted for publication 30 April 1993)

A direct comparison of the physical properties of GaN thin films is made as a function of the choice of substrate orientations. Gallium nitride single crystals were grown on (0001) and (01$\bar{1}$2) sapphire substrates by metalorganic chemical vapor deposition. Better crystallinity with fine ridgelike facets is obtained on the (01$\bar{1}$2) sapphire. Also lower carrier concentration and higher mobilities indicate both lower nitrogen vacancies and less oxygen incorporation on the (01$\bar{1}$2) sapphire. The results of this study show better physical properties of GaN thin films achieved on (01$\bar{1}$2) sapphire.

Gallium nitride (GaN) is one of the most promising wide-gap III-V semiconductors for optical devices in the region of blue to ultraviolet light, because it has a direct band gap of 3.39 eV and high external photoluminescence quantum efficiency. It has been very difficult to obtain high-quality GaN films because of the large lattice mismatch and the large difference in the thermal expansion coefficient between GaN and substrates.[1] Numerous substrate materials have been used for the deposition of GaN.[2] For lack of an ideal substrate, nearly all the GaN has been grown on sapphire substrates despite its poor structural and thermal match. In this study, a direct comparison is made of the structural, electrical, and optical properties of GaN thin films deposited on two sapphire substrate orientations of (0001) and (01$\bar{1}$2) under identical growth conditions.

A horizontal, atmospheric pressure metalorganic chemical vapor deposition (MOCVD) reactor was employed to deposit GaN. A dual IR lamp heating configuration was used to heat the graphite susceptor which was inclined at 15° with respect to horizontal. A thermocouple inserted into the susceptor monitored its temperature and provided feedback to the temperature controller. Trimethylgallium (TMG), and NH3 were used as Ga and N source materials, respectively. Hydrogen (H2) was used as the carrier gas. Carrier gas, metalorganic, and nitrogen sources were mixed just before entering the reactor, in order to reduce parasitic reactions of metalorganics (MO) with nitrogen source.

The total gas flow rate was maintained at 1.6 slm with 3–10 cc/min for TMG and 500–1100 cc/min for $NH_3$. The bubbler was kept at $-10$ °C for TMG. (0001) and (01$\bar{1}$2) sapphire were used as substrates. Sapphire substrates were etched by a hot solution of $H_3PO_4$:$H_2SO_4$ = 1:3 and then rinsed in deionized water and blown dry w ...tered nitrogen.

The growth of the GaN thin films was measured using a ball-polishing thickness measurement technique. The growth rate is about 1.2 μm/h. No variation in the growth rate was observed between the two different substrate orientations and over the growth temperature range of 900–1000 °C. The growth rate is proportional to the input TMG flux indicating the domination of mass transport process in this temperature region.

Figures 1(a) and 1(b) show the surface morphology of the GaN thin films deposited on (0001) and (01$\bar{1}$2) sapphire substrates through a scanning-electron microscope (SEM). The film on the (0001) sapphire shows the wurtzite symmetry with hexagonal pyramids, while the layer on the (01$\bar{1}$2) sapphire exhibits a more lateral growth mechanism as is evident from the more complete coalescence of the grains and the smoother surface morphology of the film.

The composition of the films was analyzed by Auger

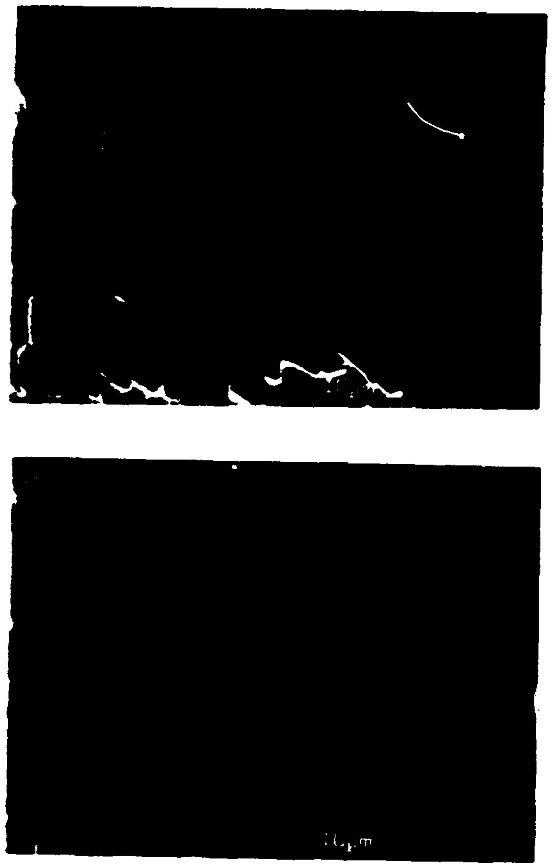

FIG. 1. SEM micrographs of GaN on (a) (0001) $Al_2O_3$ and (b) (01$\bar{1}$2) $Al_2O_3$.

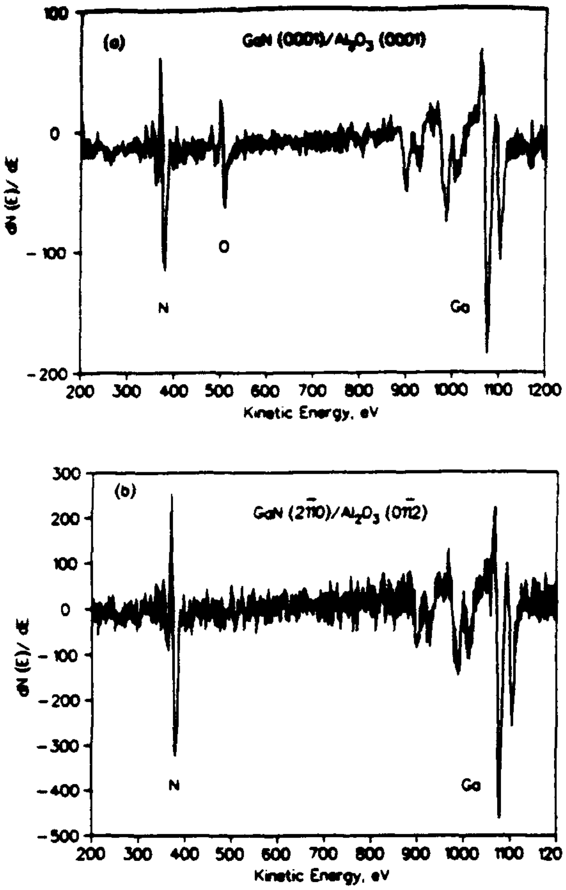


FIG. 2. Auger electron spectra of GaN thin films deposited on (a) (0001) $Al_2O_3$ and (b) $(01\bar{1}2)$ $Al_2O_3$ substrates.

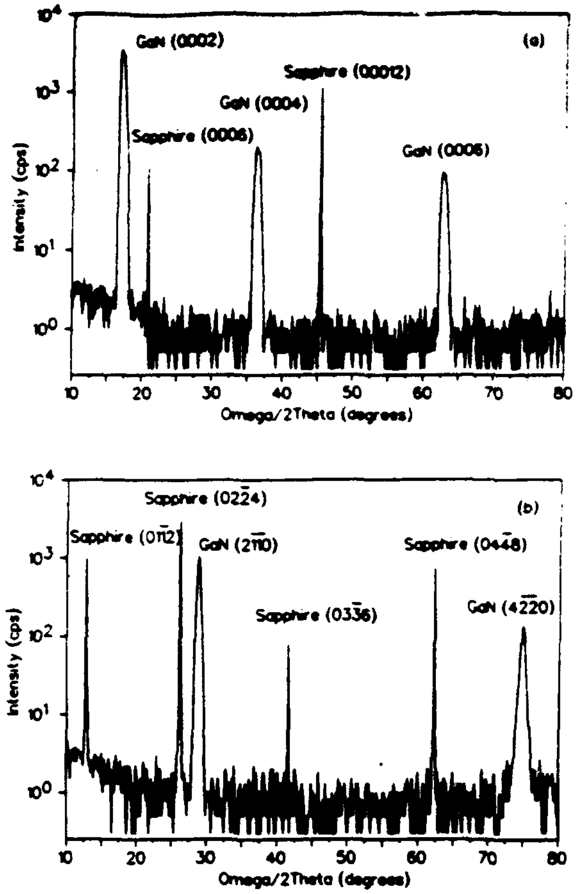


FIG. 3. X-ray diffraction spectra of GaN thin films deposited on (a) (0001) $Al_2O_3$ and (b) $(01\bar{1}2)$ $Al_2O_3$ substrates.

electron spectroscopy (AES). Figures 2(a) and 2(b) show the AES spectra for the samples produced at 1000 °C. The main elements present are Ga and N, the ratio of the Ga to N is close to unity. The Auger spectrum of the GaN thin film deposited on the $(01\bar{1}2)$ sapphire substrate did not exhibit the presence of other impurity species in detectable quantities. However, oxygen impurity species was detected on the (0001) sapphire sample. It is tentatively being attributed to differences in the initial growth mechanisms of the films on the different substrate orientation which may enhance the higher incorporation of residual impurity. A high resolution 5-crystal x-ray diffractometer using the Cu $K\alpha_1$ line was used to examine the crystalline quality of the GaN thin films. GaN single crystal growth on (0001) and $(01\bar{1}2)$ was achieved using MOCVD. It shows in Fig. 3 (0001) GaN is parallel to (0001) sapphire and $(2\bar{1}\bar{1}0)$GaN is parallel to $(01\bar{1}2)$ sapphire.[3–5] The results of x-ray rocking curve are shown in Fig. 4 as a function of film thickness. The x-ray rocking curve of the layer on the $(01\bar{1}2)$ sapphire is narrower than that of the layer on the (0001) sapphire. It may attribute to both the lower incorporation with the oxygen and the smaller lattice mismatch in the $(01\bar{1}2)$-sapphire-$(2\bar{1}\bar{1}0)$-GaN interface[4,5] than that in the (0001)-sapphire-(0001)-GaN interface.

The Hall electrical data of the films measured by Van der Pauw method at room temperature were shown in Fig. 5. The unintentionally doped GaN thin films were $n$-type conduction with carrier concentrations of $10^{19}$–$10^{20}$ $cm^{-3}$. The layers grown on $(01\bar{1}2)$ sapphire show lower carrier concentrations and higher mobilities. It suggests the better electrical properties on the $(01\bar{1}2)$ sapphire is attributed to both the less oxygen incorporation[6] and the lower nitrogen vacancies.[5] The further study of the electrical properties of GaN thin films was under investigation by using deep level transient spectroscopy method.

The 457.9 nm line of the argon laser was used for Raman scattering. GaN has hexagonal wurtzite structure

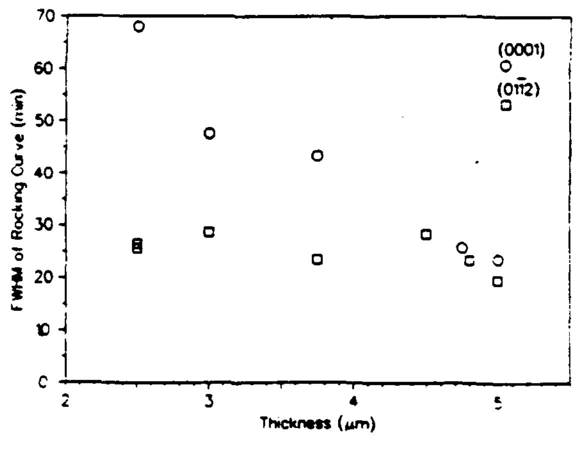


FIG. 4. FWHMs of x-ray rocking curves as a function of film thickness.

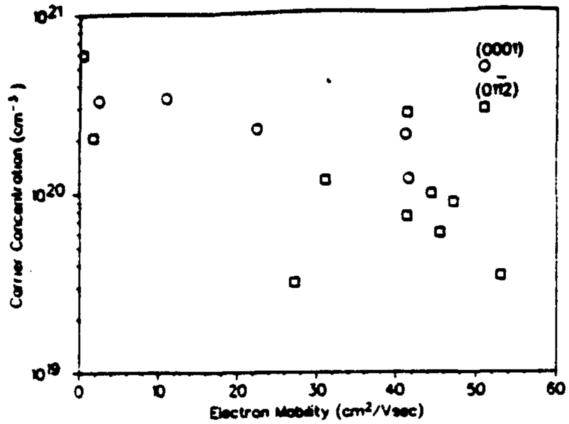


FIG. 5. Carrier concentrations and electron mobilities of GaN films.

with four atoms in the unit cell and belongs to the $C_{6v}$ space group. All spectra were recorded in the backscattering geometry and at room temperature. First-order Raman spectra of the two GaN thin films deposited at 1000 °C. On (0001) and (01$\bar{1}$2) sapphire are shown in Figs. 6(a) and 6(b), respectively. While the sapphire Raman scattering peaks are evident in the spectra of Fig. 6(a), the sapphire Raman peaks are not easily resolved in the corresponding spectra of the GaN thin films of Fig. 6(b). The line modes at 754, 647, and 579 cm$^{-1}$ correspond to the (01$\bar{1}$2) sapphire substrate alone, and the line modes at 754 and 579 cm$^{-1}$ correspond to the (0001) sapphire substrate. The GaN line modes at 570, 560, and 534 cm$^{-1}$ dominate the Raman spectra of the GaN thin films on both (0001) and (01$\bar{1}$2) sapphire orientations. These line modes closely correspond to the wurtzite symmetry phonon modes of GaN, labeled $A_1$ (LO), $E_1$ (TO), and $E_2$, respectively. The line modes observed in this study are in good agreement with those reported by Manchon *et al.*[7] and Burns *et al.*[8]

Single-crystal of GaN thin films was achieved on (0001) and (01$\bar{1}$2) sapphire substrate using MOCVD. Better surface morphology and the narrower of the x-ray rocking curve of GaN thin films on (01$\bar{1}$2) sapphire substrate were attributed to smaller lattice mismatch in the (01$\bar{1}$2)-sapphire-(2$\bar{1}\bar{1}$0)-GaN interface. Also the higher electrical quality of the GaN thin films on (01$\bar{1}$2) sapphire substrates indicates both less incorporation with the oxygen and lower N vacancy.

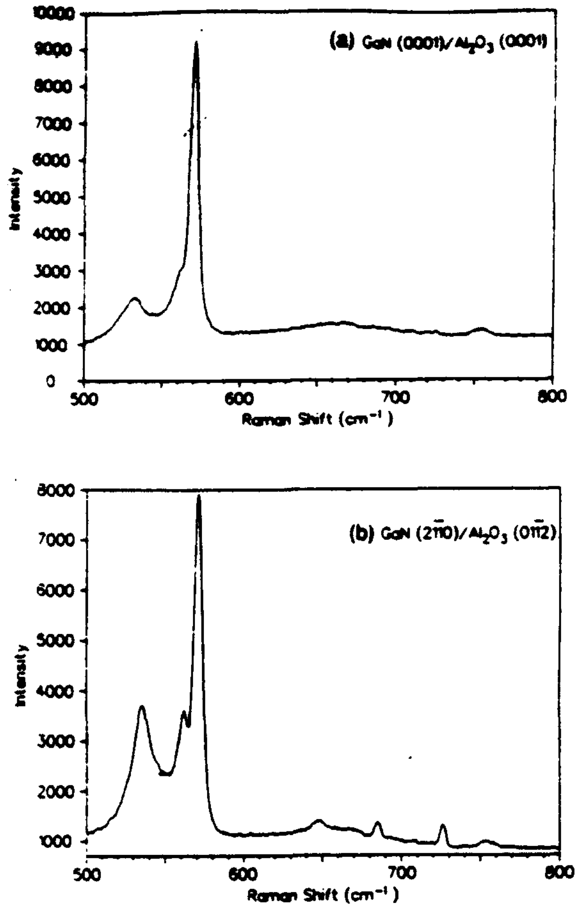


FIG. 6. Raman spectra of GaN thin films deposited on (a) (01$\bar{1}$2) $Al_2O_3$ and (b) (01$\bar{1}$2) $Al_2O_3$.


The authors gratefully acknowledge Max Yoder for his interest and encouragement. This work is supported by the ONR through Grant No. N00014-93-1-0235.



[1] I. Akasaki, H. Amano, Y. Koide, K. Hiramatsu, and N. Sawaki, J. Cryst. Growth 98, 209 (1989).
[2] J. H. Edgar, J. Mater. Res. 7, 235 (1992).
[3] M. Sano and M. Aoki, Jpn. J. Appl. Phys. 15, 1943 (1976).
[4] S. Yoshida, S. Misawa, and S. Gonda, Appl. Phys. Lett. 42, 427 (1983).
[5] T. Sasaki and S. Zembutsu, J. Appl. Phys. 61, 2533 (1987).
[6] B.-C. Chung and M. Gershenzon, J. Appl. Phys. 72, 651 (1992).
[7] D. D. Manchon, Jr., A. S. Barker, Jr., P. J. Dean, and R. B. Zetterstrom, Solid State Commun. 8, 1227 (1970).
[8] G. Burns, F. Dacol, J. C. Marinace, and B. A. Scott, Appl. Phys. Lett. 22, 356 (1973).

REF #16
Submitted to Journal of [illegible]

# Thermal stability of GaN thin films grown on (0001) $Al_2O_3$, $(01\bar{1}2)$ $Al_2O_3$ and $(0001)_{Si}$ 6H-SiC substrates


C. J. Sun, P. Kung, A. Saxler, H. Ohsato, E. Bigan, and M. Razeghi

Center for Quantum Devices, Department of Electrical Engineering and Computer Science, Northwestern University, Evanston, Illinois 60208

D. K. Gaskill

Laboratory for Advanced Material Synthesis, Naval Research Laboratory, Washington, DC 20375



Single-crystals of GaN were grown on (0001), $(01\bar{1}2)$ $Al_2O_3$ and $(0001)_{Si}$ 6H-SiC substrates using an atmospheric pressure Metalorganic Chemical Vapor Deposition reactor. We have studied the relationship between thermal stability of the GaN films and substrate's surface polarity. It appeared that N-terminated (0001) GaN surface grown on $(0001)_{Si}$ 6H-SiC has the most stable surface, followed by the nonpolar $(11\bar{2}0)$ GaN surface grown on $(01\bar{1}2)$ $Al_2O_3$, while Ga-terminated (0001) GaN surface grown on (0001) $Al_2O_3$ has the least stable surface. We explained this with the difference in the atomic configuration of each of these surfaces which induces a difference in their thermal decomposition.

GaN has been the most extensively studied III-V nitride, as it is a promising material for light emitters and detectors in the visible to ultraviolet region[1,2,3]. However, GaN films were reported to be unstable at high temperature under hydrogen ($H_2$) ambient.[4] This might prove detrimental to optoelectronic devices where thermal treatments can be required for technological steps such as dopant activation. In addition, these devices are expected to operate at high power and high temperature. However, the thermal decomposition mechanisms have not yet received a plausible explanation, and moreover, the reported experimental data have certain discrepancies.

GaN has been grown epitaxially on various substrates, mainly due to the lack of a suitable lattice-matched substrate.[5] Therefore, the most popular substrate used for the growth of the GaN is the (0001) plane of the $Al_2O_3$, which has a lattice mismatch of 14% with the epilayer[6]. Such a large mismatch induces a high density of defects which seriously degrades film quality. Alternative substrates having a closer lattice match such as $(01\bar{1}2)$ $Al_2O_3$ and both (0001) polar planes of the 6H-SiC have also been used, but to a lesser extent.[7,8] Along with the lattice match, the substrate's surface polarity has been studied in order to improve the growth of GaN. Sasaki et.al[8] reported that the substrate polarity has a strong influence on the surface morphology and the photoluminescence property of the GaN layer. It was shown that N-terminated GaN films grown on $(0001)_{Si}$ plane of the SiC have better surface and photoluminescence characteristics, when compared with Ga-terminated GaN films grown on $(0001)_C$ plane of SiC.

In our previous work[9], we showed that the physical properties of the GaN epilayer were enhanced when using the $(01\bar{1}2)$ $Al_2O_3$ instead of the (0001) $Al_2O_3$. In this paper, we discuss the thermal decomposition mechanism of single crystal GaN grown on (0001) and $(01\bar{1}2)$ $Al_2O_3$ and $(0001)_{Si}$ SiC substrates.

A horizontal type atmospheric pressure metalorganic chemical vapor deposition (MOCVD) reactor was employed to deposit GaN. A dual infra-red lamp heating configuration was used to heat the graphite susceptor which was inclined at 15° with respect to horizontal. A thermocouple inserted into the susceptor monitored its temperature and provided feedback to the temperature controller. Trimethylgallium (TMG), and ammonia ($NH_3$) were used as Ga and N source materials, respectively. Nitrogen ($N_2$) and $H_2$ were used as the ambient gases. Metalorganics (MO) sources and $NH_3$ were mixed just before entering the reactor, in order to reduce parasitic reactions between the MO and the N sources. $(0001)_{Si}$ 6H-SiC heavily N-doped Lely-grown wafers[10], (0001) $Al_2O_3$ and

$(01\bar{1}2)$ $Al_2O_3$ were used as substrates. Prior to the deposition, the $Al_2O_3$ substrates were etched by a hot solution of $H_3PO_4 : H_2SO_4 = 1:3$, then rinsed in deionized water and dried with filtered $N_2$. The SiC substrates were cleaned by dipping in hydrofluoric acid, rinsed and dried.

The growth temperature was varied from 900° C to 1050° C. The TMG bubbler temperature was kept at -10° C and the carrier gas bubbling flow rate was 2.5-5 cc/min. Ammonia flow rate varied from 550 to 1100 cc/min, while the total gas flow remained constant at 1600 cc/min. The films, deposited without any buffer layer, were 2.5-3 μm thick corresponding to a growth rate of 1.25-2.5 μm/h. The surface morphology of the GaN layers were observed using scanning electron microscopy (SEM). A high resolution 5-crystal x-ray diffractometer using the Cu $K\alpha_1$ line was used to obtain rocking curve data from which crystalline quality was inferred from the full width at half maximum (FWHM) of the lineshape. Finally, Hall measurements were performed at room temperature using the Van der Pauw method.

SEM observations showed that the GaN layers on $(0001)_{Si}$ SiC and on (0001) $Al_2O_3$ presented a hexagonal-shape and that the GaN layer grown on $(01\bar{1}2)$ $Al_2O_3$ appeared with a ridge-like facet[9]. Moreover, from x-ray spectra, the (0001) GaN was found parallel to the $(0001)_{Si}$ SiC and (0001) $Al_2O_3$ surfaces, and the $(11\bar{2}0)$ GaN, parallel to $(01\bar{1}2)$ $Al_2O_3$. FWHMs of the rocking curves of GaN films were about 20-30 min. Although the SiC substrates were heavily N-doped, they exhibited high resistivity which made Hall measurements possible. Electron concentration and Hall mobility were $1\times10^{20}$ $cm^{-3}$ and 20 $cm^2$/ Vsec for GaN / SiC samples, $2\times10^{19}$ $cm^{-3}$ and 60 $cm^2$/ Vsec for GaN / $(01\bar{1}2)$ $Al_2O_3$ samples, and, $7\times10^{19}$ $cm^{-3}$ and 40 $cm^2$/ Vsec for GaN / (0001) $Al_2O_3$ samples, respectively.

For this thermal stability study, as-grown GaN films were divided into two groups and annealed at two different temperatures (900° C and 1000° C) under $H_2$ and $N_2$ ambients. The first set of experiments was conducted on GaN / $(0001)_{Si}$ 6H-SiC and GaN / $(01\bar{1}2)$ $Al_2O_3$, and consisted of a 1 hour thermal annealing at 1000° C. The second set of experiments was conducted on films grown on (0001) and $(01\bar{1}2)$ $Al_2O_3$, and consisted of four consecutive cycles of 1 hour thermal annealing at 900° C.

The results obtained from the first set of experiments are as follows. Fig. 1 and 2 show the changes of surface morphology and x-ray spectra of GaN films before and after annealing under $H_2$-ambient at 1000° C for 1 hour, respectively. The GaN film grown on

$(01\bar{1}2)$ $Al_2O_3$ was totally decomposed leaving a residue in the form of Ga droplets and the $(11\bar{2}0)$ GaN diffraction peak disappeared. Surprisingly, no thermal decomposition was observed for the GaN film grown on $(0001)_{Si}$ SiC. Moreover, the x-ray spectra and Hall measurement of this latter film showed essentially no change in it's crystalline quality and electrical properties.

Similarly, the samples annealing under $N_2$-ambient at 1000° C for 1 hour produced no change in their crystalline quality and electrical properties. This is consistent with previous reports[4]. The results in $H_2$ ambient were very different. In the 1000° C thermal treatment, better thermal stability has been observed on the N-terminated (0001) surface. It is believed that surface polarity plays an important role in thermal decomposition, which will be addressed shortly.

The results obtained from the second set of experiments are as follows. Fig. 3 shows the surface morphology of GaN films after four cycles of 1 hour thermal annealing at 900° C under $N_2$-ambient and $H_2$-ambient. Under $N_2$-ambient, no change of surface morphology occured for both samples. However, the FWHM of rocking curve (Fig. 4) has been improved after annealing under $N_2$, especially for GaN / $(01\bar{1}2)$ $Al_2O_3$. Fig. 5 and 6 show the variation of electron concentration and Hall mobility after the annealing cycles. The variation of electron concentration and mobility is not pronounced for the films annealed under $N_2$ ambient. As we will explain latter, the improvement of the crystal quality can be due to the desorbing of atomic hydrogen in the hydrogen-passivated GaN films[11] which restores the crystallinity of the films. Remarkably, different results were obtained for films annealed under $H_2$. As shown in Fig. 3 (b,d), Ga metal droplets are present on the surface of the annealed samples. These droplets are probably produced by atomic hydrogen attack of the GaN films, as we will show in the following. Fig. 4 shows the effect of annealing under $H_2$ on the FWHM of rocking curve. The crystal quality was essentially unchanged under $H_2$-ambient, though severe change of the surface morphology was observed. This phenomenon might be explained by the nonuniformity of thermal decomposition of the surface. This thermal decomposition is confirmed by the variation of electron concentration and Hall mobility (see fig. 5 and 6). Electrical properties of (0001) GaN / (0001) $Al_2O_3$ became much worse than $(11\bar{2}0)$ GaN / $(01\bar{1}2)$ $Al_2O_3$ plane after annealing under $H_2$. This result is explained by a more severe decomposition of the (0001) GaN / (0001) $Al_2O_3$ surface compared to the $(11\bar{2}0)$ GaN / $(01\bar{1}2)$ $Al_2O_3$ surface.

Our interpretation of these results are as follows. The variation in thermal stability of GaN films grown on (0001), $(01\bar{1}2)$ $Al_2O_3$ and $(0001)_{Si}$ SiC under $H_2$ ambient is

attributed to the different surface polarities. As predicted by Sasaki and Matsuoka[8], the GaN epilayer grown on $(0001)_{Si}$ SiC is N-terminated, on (0001) $Al_2O_3$ is Ga-terminated and on $(01\bar{1}2)$ $Al_2O_3$ is nonpolar. The presence of Ga droplets, shows that the thermal decomposition process of the epilayer is based on the reduction of $Ga^{3+}$ ions by hydrogen ($GaN + \frac{3}{2}H_2 \rightarrow Ga + NH_3$). The thermal decomposition rate was the fastest on the (0001) Ga-terminated surface, followed by the nonpolar $(11\bar{2}0)$ surface, while the N-terminated (0001) surface had the slowest decomposition rate. On the N-terminated (0001) GaN surface, H atoms combine directly with N to form N-H (~ 3.9eV)[12] which is energetically more stable than Ga-H (< 2.8eV)[13]. Thus, the N-terminated (0001) GaN surface has the slowest thermal decomposition rate, and consequently, the best thermal stability. For the Ga-terminated (0001) and the nonpolar $(11\bar{2}0)$ GaN surfaces, H atoms combine first with Ga to form Ga-H covalent bonds and then move from Ga to N sites to form N-H bonds. Our explanation for the higher thermal stability of the nonpolar $(11\bar{2}0)$ GaN surface compared to the Ga-terminated surface consists of the following two points. First, half of the atoms on the nonpolar $(11\bar{2}0)$ surface are N atoms, which will combine with H to form N-H bonds, while Ga atoms on the Ga-terminated surface will form Ga-H bonds, which are less stable than N-H bonds. Second, after removing the Ga-terminated surface, only N atoms remain on the surface. However, this surface is different from the N-terminated surface, since only one Ga atom is bonded to one N atom in this case, instead of three Ga atoms bounded to one N atom in the normally N-terminated case, as shown in Fig. 7. Therefore, thermal decomposition is faster on the Ga-terminated surface than the nonpolar $(11\bar{2}0)$ surface.

In summary, single-crystal GaN films were grown by MOCVD on (0001) and $(01\bar{1}2)$ $Al_2O_3$ and $(0001)_{Si}$ SiC substrates. The variation in thermal stability of the films grown on different substrates should be attributed to surface polarity effects. Unlike the epilayers grown on sapphire substrates, GaN grown on $(0001)_{Si}$ SiC is thermally stable at temperatures as high as 1000° C under $H_2$-ambient gas. The crystallinity of $(11\bar{2}0)$ GaN grown on $(01\bar{1}2)$ $Al_2O_3$ has been improved after $N_2$ thermal annealing at 900° C, while thermal decomposition has been observed on the same samples under $H_2$-ambient. This is due to the desorbing and involvement of $H_2$. Hall measurement showed that electrical properties became worse after annealing under $H_2$-ambient. This is attributed to the reduction of $Ga^{3+}$ ions, which causes thermal decomposition. Based on the model, N-H (~ 3.9eV) is more stable than Ga-H (< 2.8eV), and it was found that N-terminated (0001) GaN surface has the slowest thermal decomposition rate, followed by nonpolar $(11\bar{2}0)$ surface, while Ga-terminated (0001) surface has the fastest thermal decomposition rate.

The authors would like to thank Mr. Max Yoder and Dean Jerome Cohen for their permanent support and encouragement. This work is supported by the ONR through Grant No. N00014-93-1-0235.

1. H. Amano, M. Kito, K. Hiramatsu, and I. Akasaki, Jpn. J. Appl. Phys. **28**, L2112 (1989).

2. S. Nakamura, T. Mukai, and M. Senoh, Jpn. J. Appl. Phys. **30**, L1998 (1991).

3. I. Akasaki and H. Amano, Optoelectron. Devices Technol. 7, 49 (1992).

4. Y. Morimoto, J. Electrochem. Soc., **121**, 1383 (1974).

5. S. Strite and H. Morkoc, J. Vac. Sci. Technol. B, **10**, 1237 (1992).

6. I. Akasaki, H. Amano, Y. Koide, K. Hiramatsu and N. Sawaki, J. Crystal Growth **98**, 209 (1989).

7. D. K. Wickenden, K. R. Faulkner, and R. W. Brander, J. Crystal Growth, **9**, 158 (1971).

8. T. Sasaki and T. Matsuoka, Appl. Phys. Lett. **64**, 4531 (1988).

9. C. J. Sun and M. Razeghi, Appl. Phys. Lett. **63**(7), 972 (1993).

10. A. Lely, Ber. Deut. Keram. Ges., **32**, 229 (1955).

11. S. Nakamura, N. Iwasa, M. Senoh and T. Mukai, Jpn. J. Appl. Phys. **31**, 1258 (1992).

12. M. Therald, Inorganic Chemistry, A Modern Introduction, John Wiley & Sons, New York, (1982).

13. K. Balasubramanian, Chem. Phys. Lett., **164**(2), 231 (1989).

Fig. 1 Surface morphology of GaN films with $H_2$ thermal annealing at 1000° C on $(01\bar{1}2)$ $Al_2O_3$ (a)before annealing, (b)after annealing, and on $(0001)_{Si}$ SiC (c)before annealing, (d)after annealing.

Fig. 2 X-ray spectra of GaN films with $H_2$ thermal annealing at 1000° C on $(01\bar{1}2)$ sapphire (a)before annealing, (b)after annealing, and on $(0001)_{Si}$ SiC (c)before annealing, (d)after annealing.

Fig. 3 Surface morphology of GaN films on $(01\bar{1}2)$ $Al_2O_3$ after four 1-hour consecutive thermal annealings at 900° C under (a) $N_2$ and (b) $H_2$ ambients, and on (0001) $Al_2O_3$ under (c) $N_2$ and (d) $H_2$ ambients.

Fig. 4 The variation of FWHM of the rocking curve for films annealed under $H_2$ and $N_2$.

Fig. 5 The variation of electron concentration for films annealed under $H_2$ and $N_2$.

Fig. 6 The variation of Hall mobility for films annealed under $H_2$ and $N_2$.

Fig. 7 Crystal structure of (a) Ga-terminated and (b) N-terminated (0001) GaN.

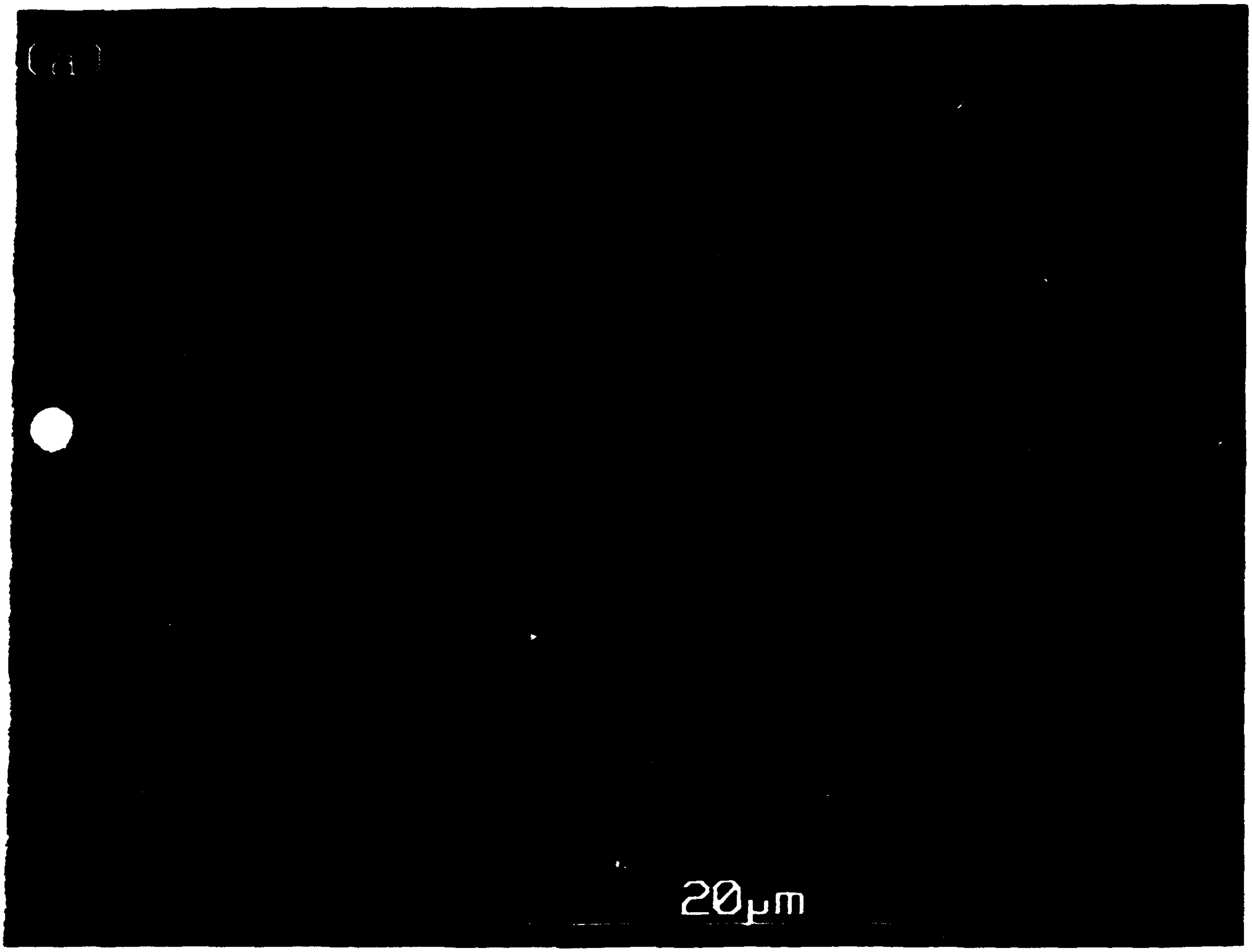
(a)
20μm


.0) GaN/ (01.2) Al2O3
2 μm


N terminated (00.1) GaN
20μm

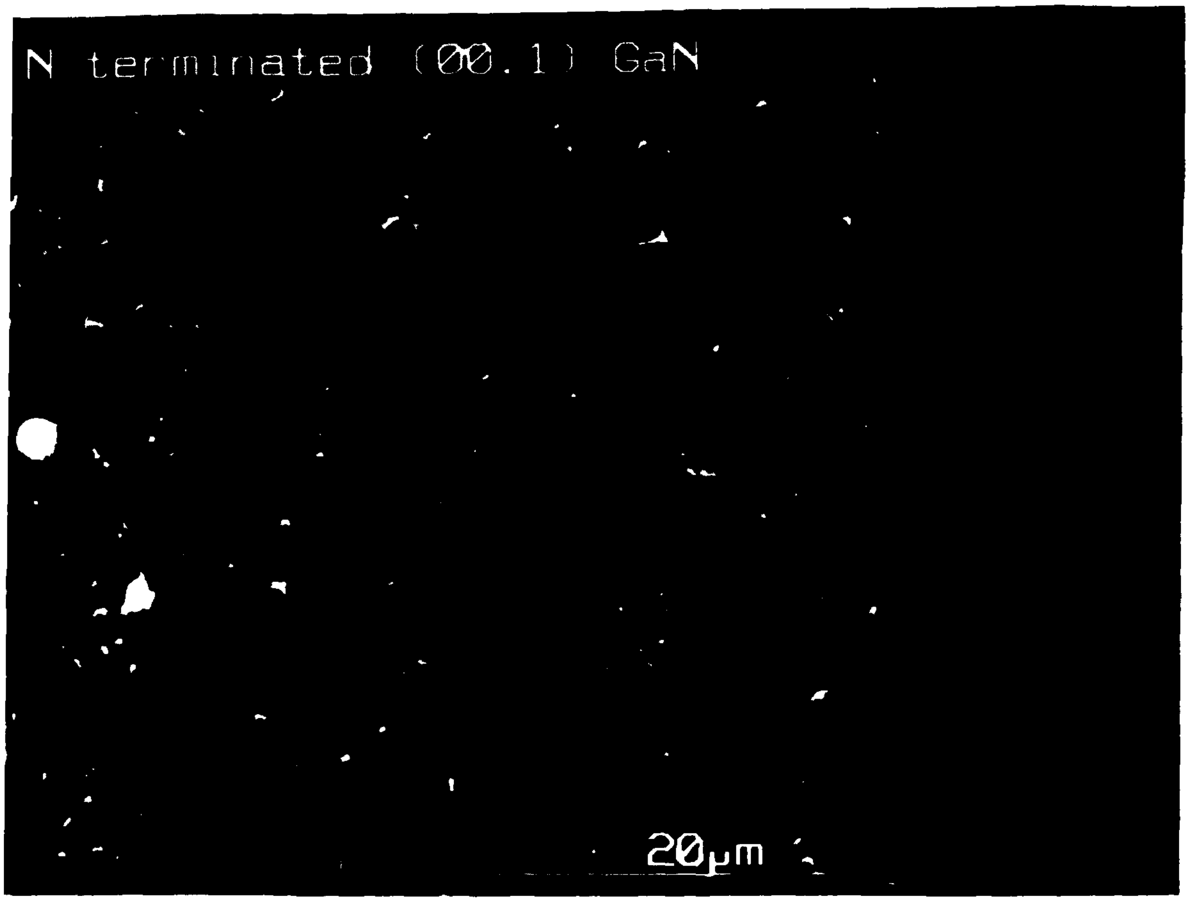




High quality aluminum nitride epitaxial layers grown on sapphire

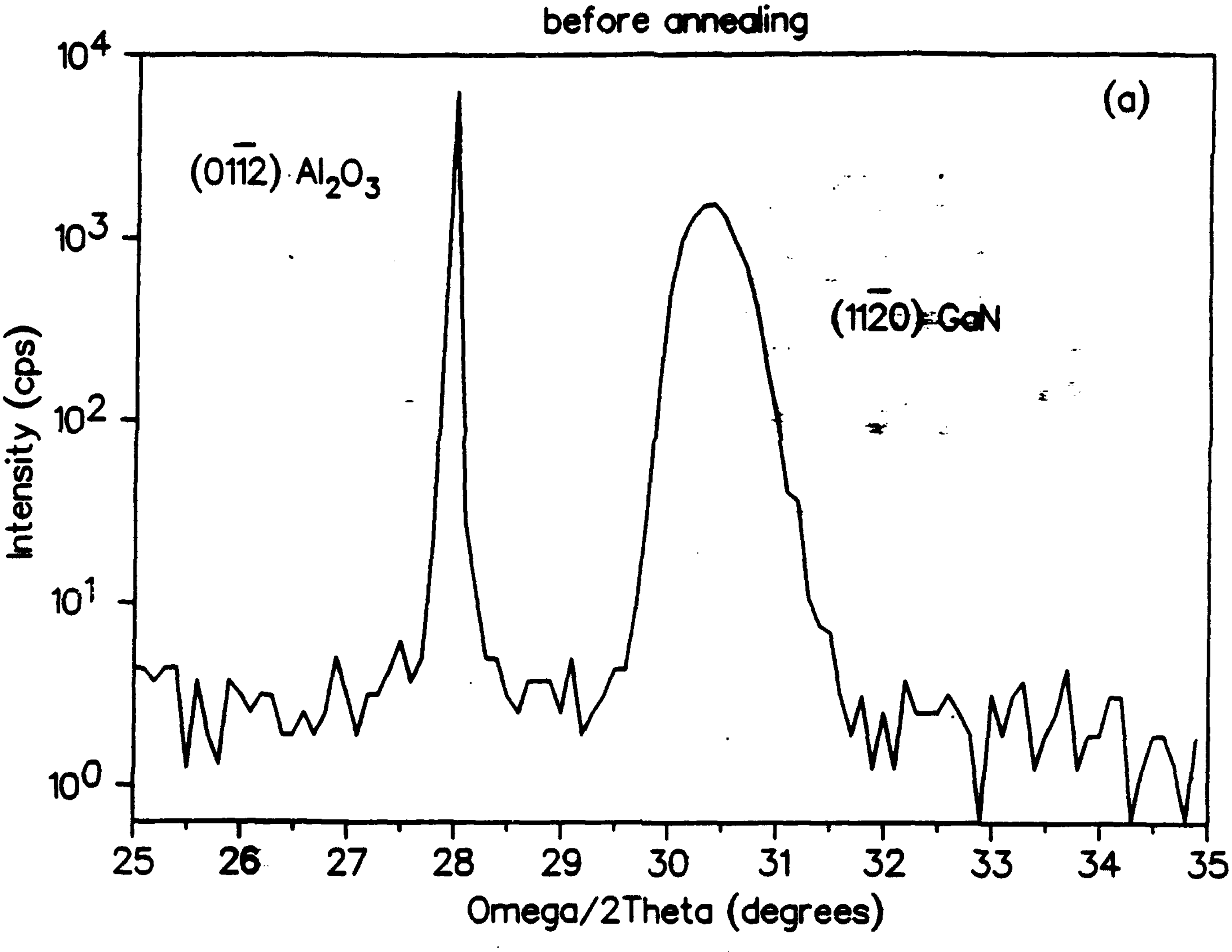

before annealing
(a)
(01̄12) $Al_2O_3$
(112̄0) GaN
Intensity (cps)
$10^4$
$10^3$
$10^2$
$10^1$
$10^0$
25
26
27
28
29
30
31
32
33
34
35
Omega/2Theta (degrees)

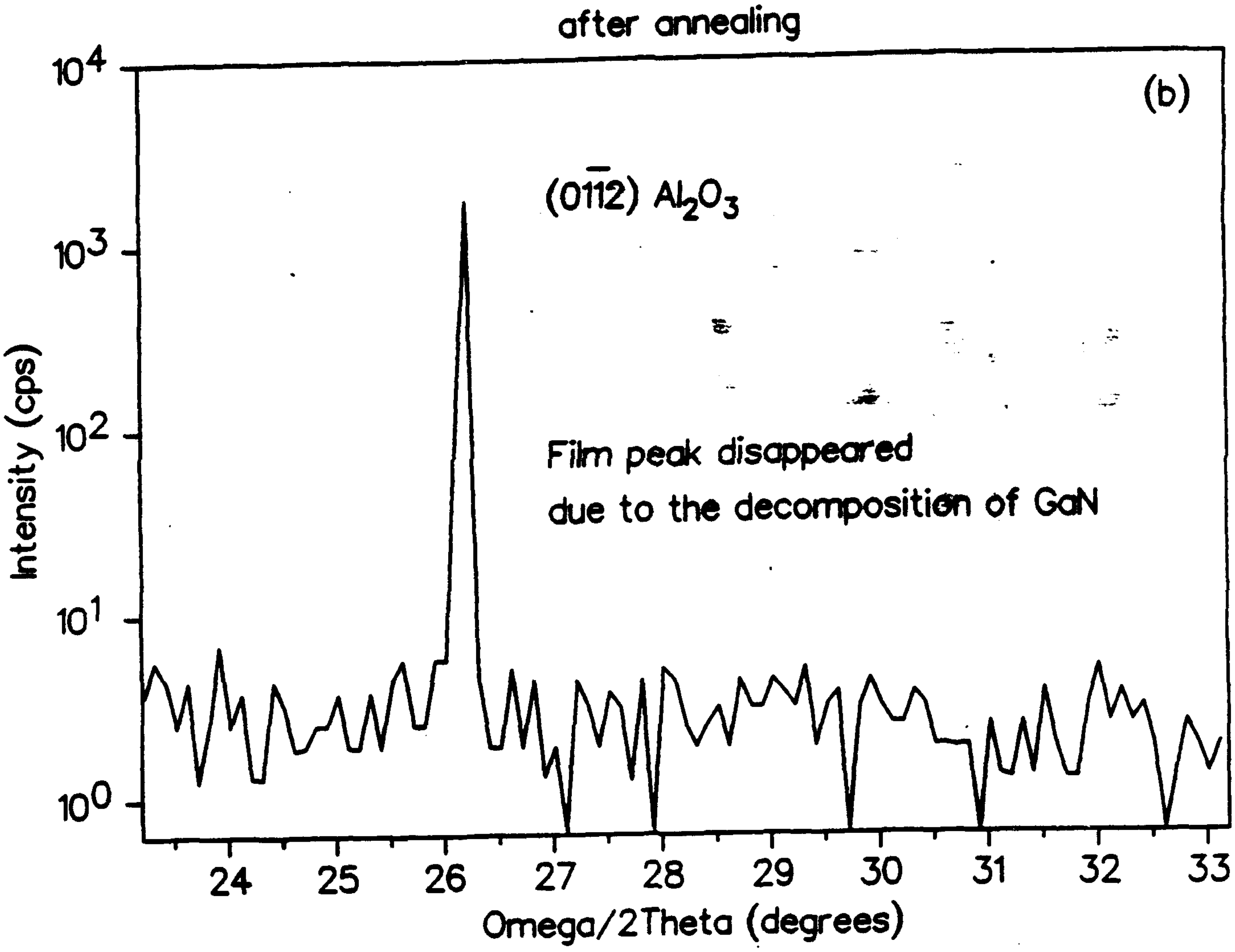

after annealing
(b)
(01̄12) $Al_2O_3$
Film peak disappeared
due to the decomposition of GaN
Intensity (cps)
$10^4$
$10^3$
$10^2$
$10^1$
$10^0$
24
25
26
27
28
29
30
31
32
33
Omega/2Theta (degrees)

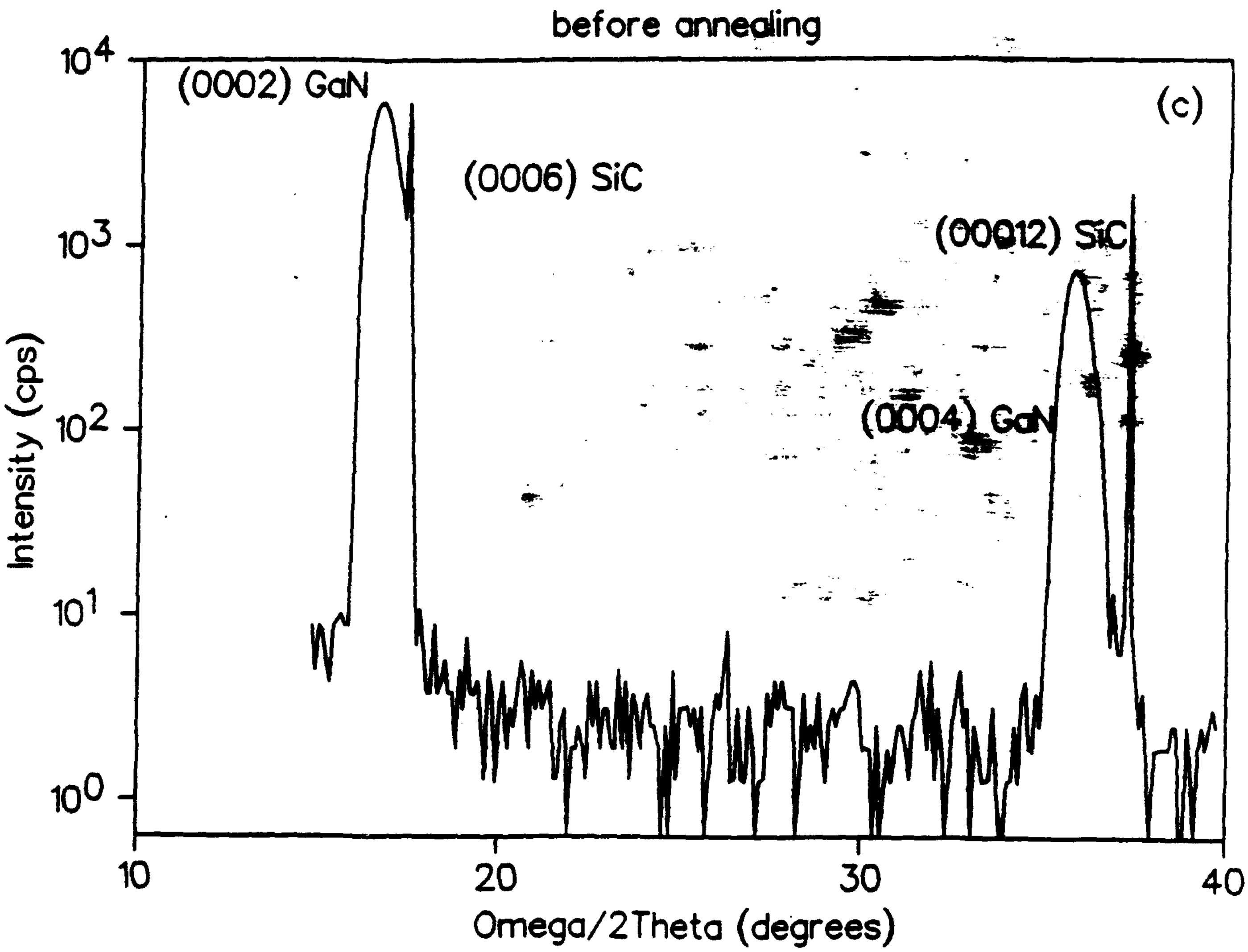

before annealing
(0002) GaN
(0006) SiC
(00012) SiC
(0004) GaN
(c)
Intensity (cps)
$10^4$
$10^3$
$10^2$
$10^1$
$10^0$
10
20
30
40
Omega/2Theta (degrees)

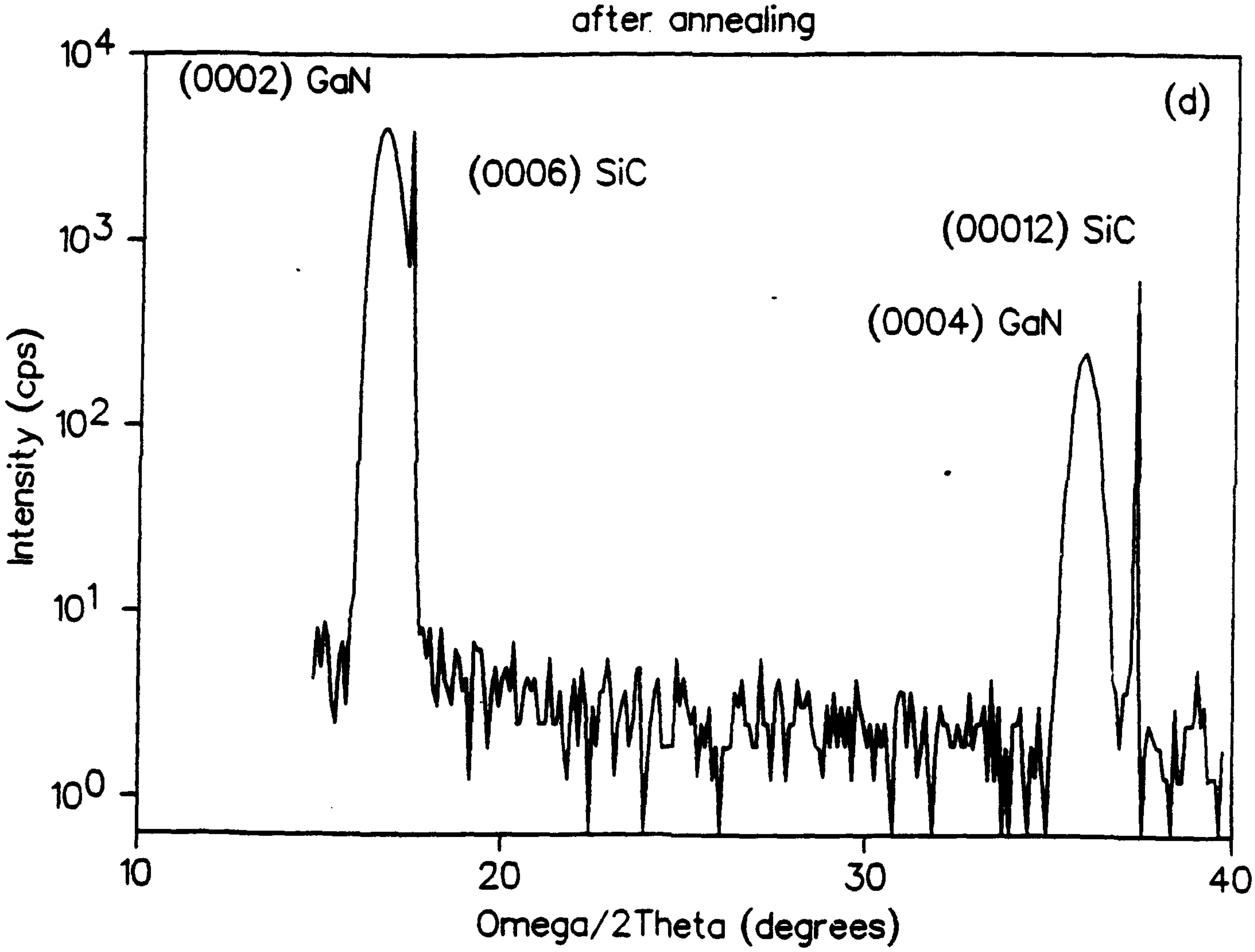

after annealing
(0002) GaN
(d)
(0006) SiC
(00012) SiC
(0004) GaN
Intensity (cps)
$10^4$
$10^3$
$10^2$
$10^1$
$10^0$
10
20
30
40
Omega/2Theta (degrees)


10 μm

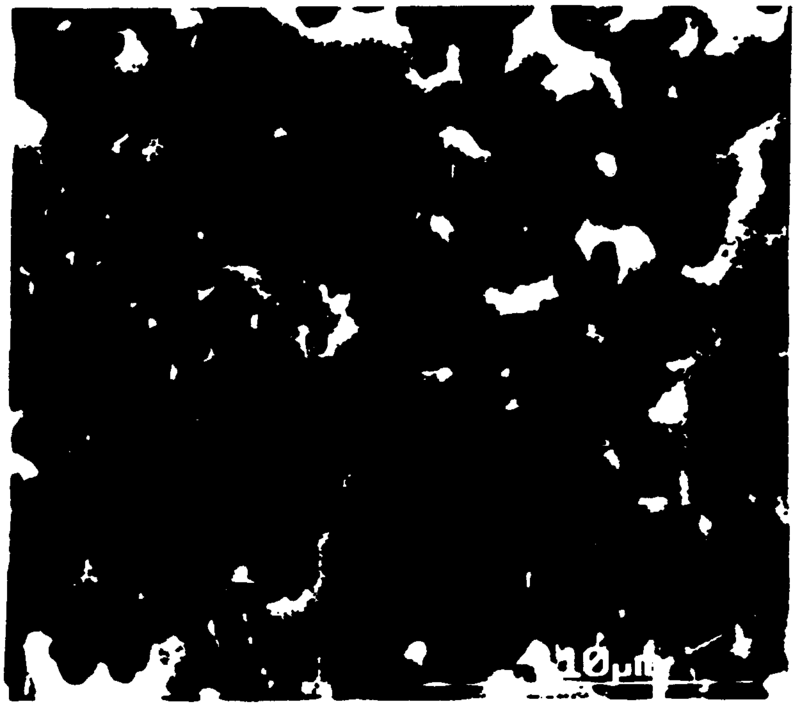
10µm

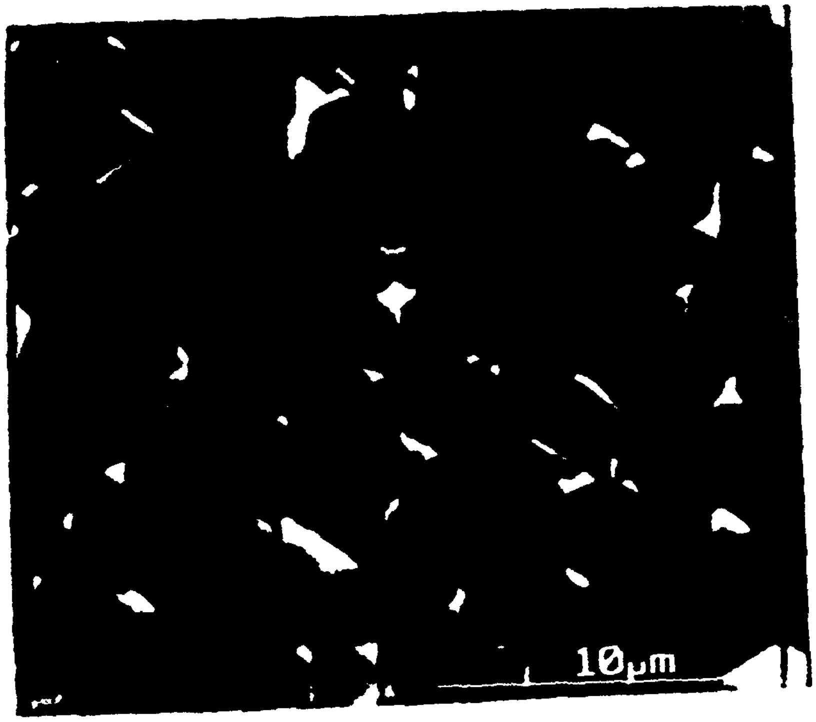
10μm

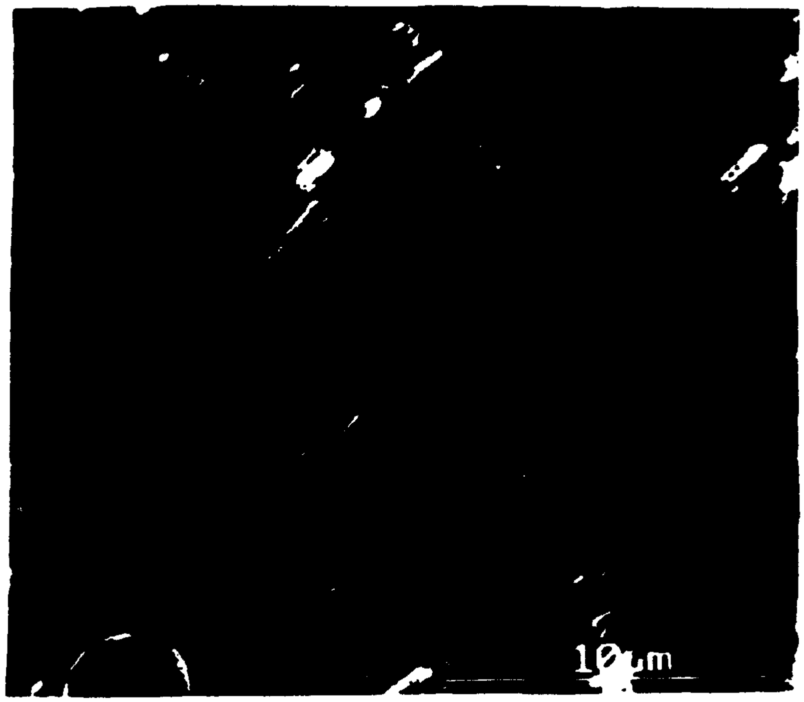
10 µm

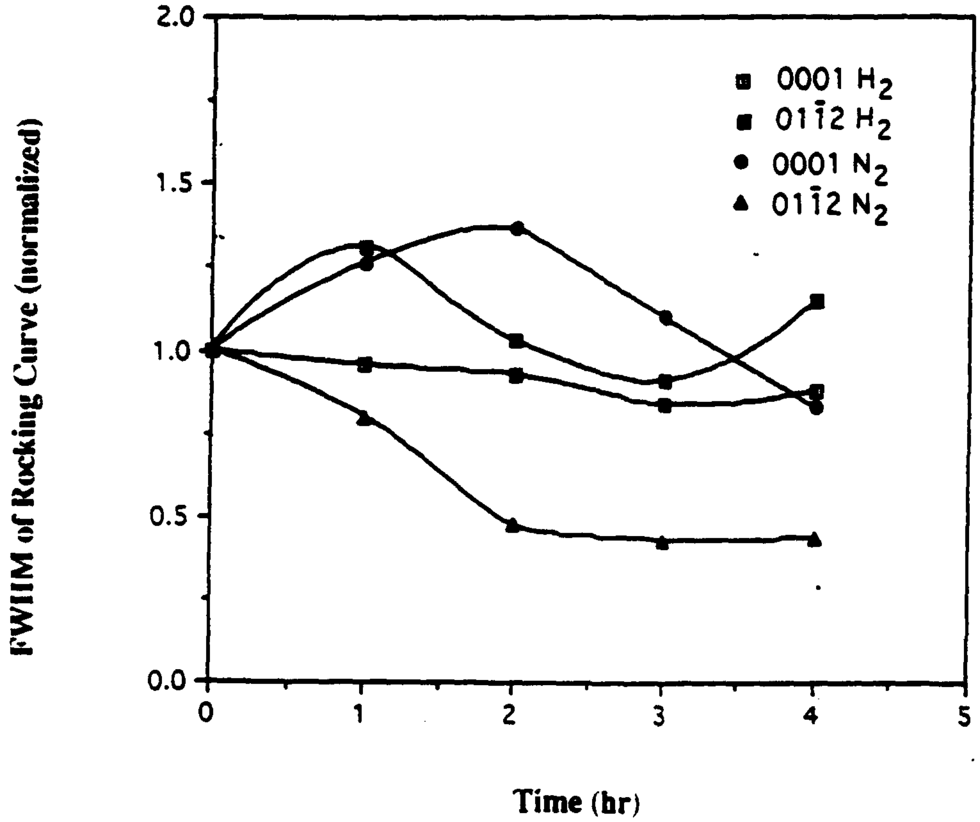
2.0
1.5
1.0
0.5
0.0
0
1
2
3
4
5
0001 H2
01Ī2 H2
0001 N2
01Ī2 N2
FWHM of Rocking Curve (normalized)
Time (hr)

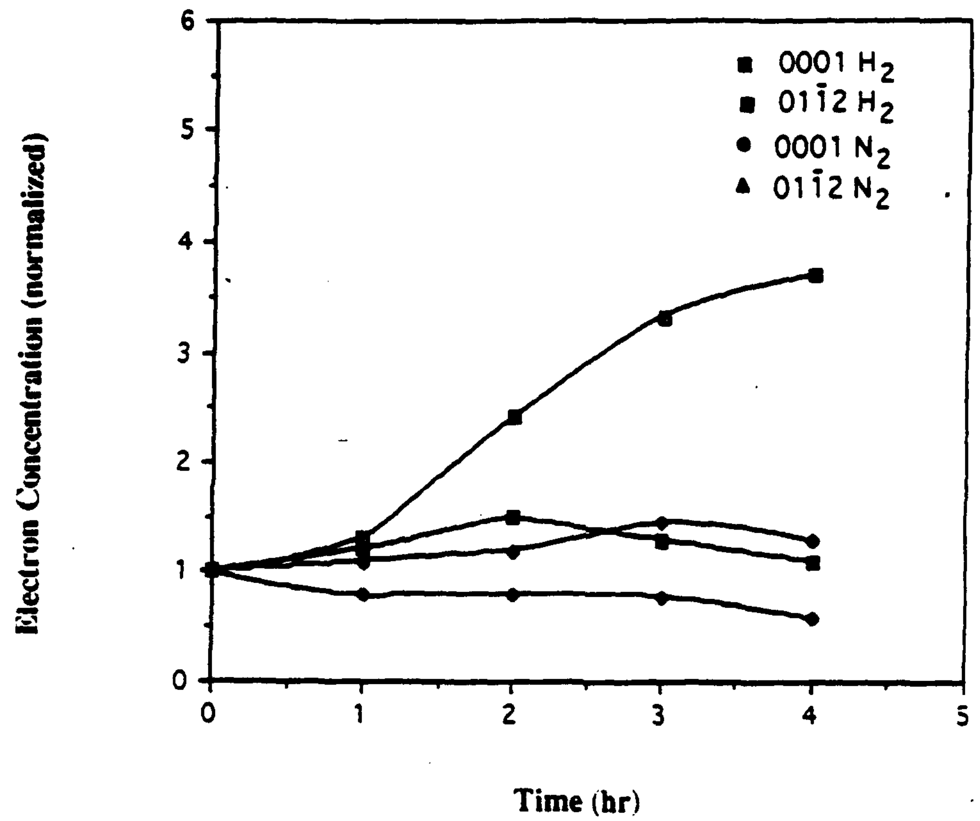

Electron Concentration (normalized)
Time (hr)
0001 H2
01$\bar{1}$2 H2
0001 N2
01$\bar{1}$2 N2

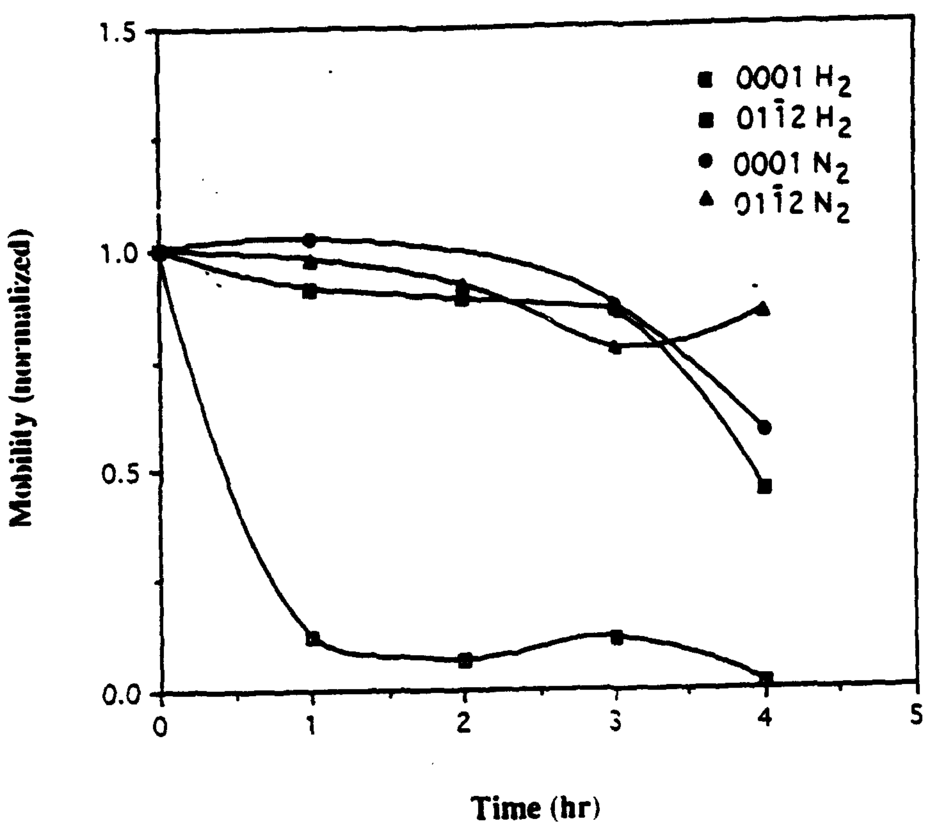

1.5
1.0
0.5
0.0
0
1
2
3
4
5
Mobility (normalized)
Time (hr)
0001 $H_2$
01$\bar{1}$2 $H_2$
0001 $N_2$
01$\bar{1}$2 $N_2$

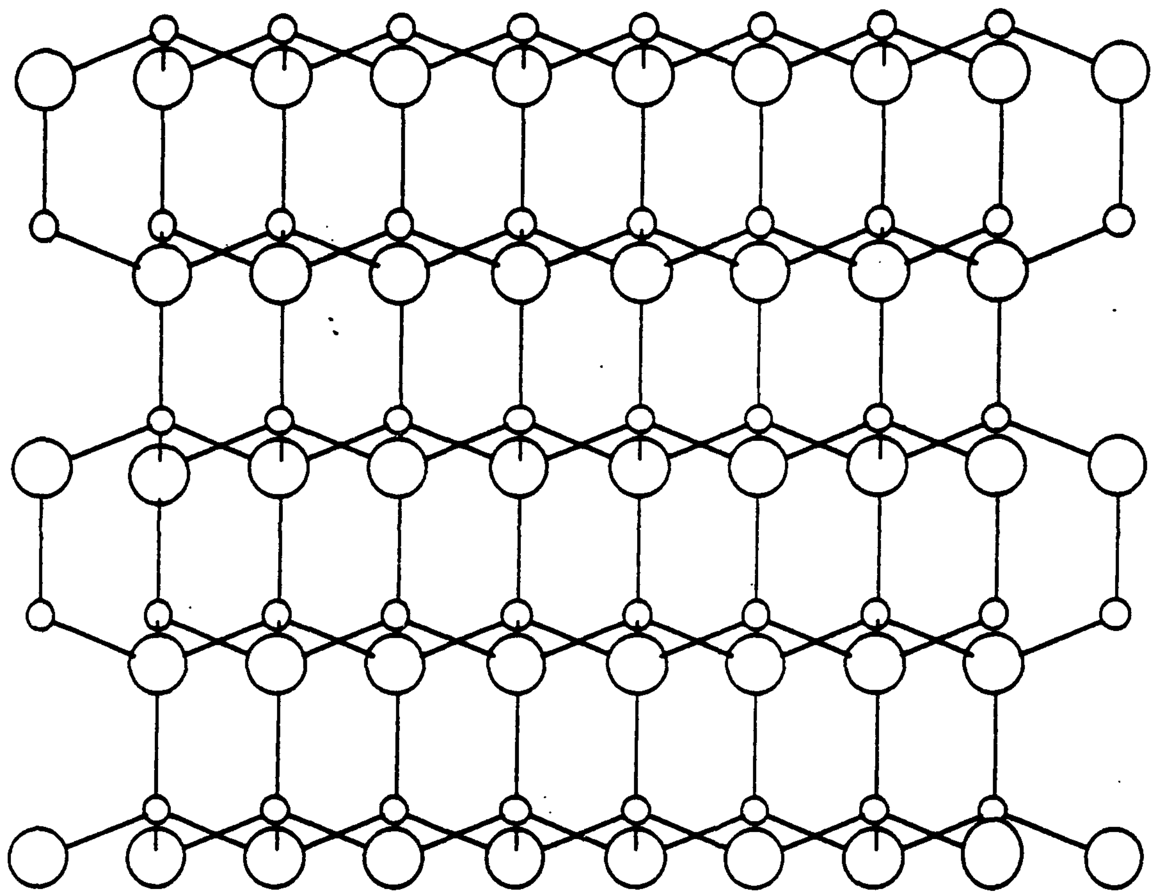

Nitrogen atom ○ Gallium atom

Gallium terminated (0001) GaN

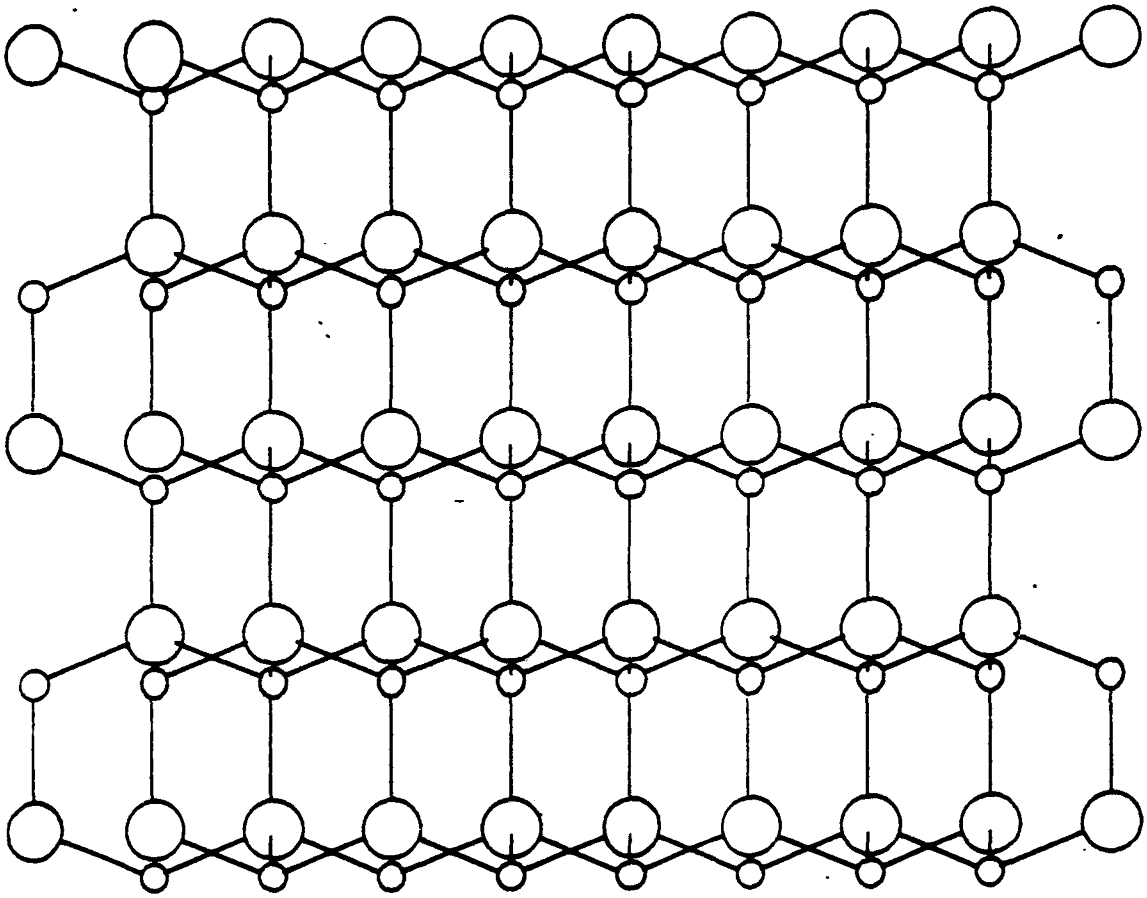

○ **Nitrogen atom** ○ **Gallium atom**

**Nitrogen terminated (0001) GaN**

BY: susan REV: bob@xy2/third/CLS_journals3/GRP_apl/JOB_17jan94/DIV_034403aplc ♦ 034403apl

THIS IS A LASER PROOF
Certain diacritic and other characters may appear inaccurate. They will be corrected on the final typeset output.

AUTHOR PLEASE NOTE: All Corrections ... On The Page Proof, ... The Manuscript

# High quality aluminum nitride epitaxial layers grown on sapphire substrates

A. Saxler, P. Kung, C. J. Sun, E. Bigan, and M. Razeghi
*Center for Quantum Devices, Electrical Engineering and Computer Science Department, Northwestern University, Evanston, Illinois 60208*

(Received 22 July 1993; accepted for publication 5 November 1993)

In this letter we report the growth of high quality AlN epitaxial layers on sapphire substrates. The AlN grown on (00·1) sapphire exhibited a better crystalline quality than that grown on (01·2) sapphire. An x-ray rocking curve of AlN on (00·1) $Al_2O_3$ yielded a full width at half-maximum of 97.2 arcsec, which is the narrowest value reported to our knowledge. The AlN peak on (01·2) $Al_2O_3$ was about 30 times wider. The absorption edge measured by ultraviolet transmission spectroscopy for AlN grown on (00·1) $Al_2O_3$ was about 197 nm.

Aluminum nitride with a direct band gap energy of 6.2 eV at room temperature is an ideal material for optoelectronic devices operating in the ultraviolet (UV) spectral region. AlN can form alloys of $Al_xGa_{1-x}N$ with GaN which can have a tunable direct band gap from 6.2 eV for $x=1$ to 3.39 eV for $x=0$. In its equilibrium phase AlN has a wurtzite type crystal structure belonging to the space group $P6_3mc$. Currently the predominant problem with the growth of AlN is to obtain high quality films and to be able to dope the films. In this letter, we report the growth and characterization of AlN epitaxial layers on (00·1)$Al_2O_3$, (01·2)$Al_2O_3$ and (100)Si substrates.

AlN thin films were grown in a horizontal, atmospheric pressure metal-organic chemical-vapor deposition (MOCVD) reactor. The sapphire and silicon substrates were first degreased with hot trichloroethylene, hot methanol, and acetone. Then, the $Al_2O_3$ substrates were etched in a hot $H_2SO_4:H_3PO_4=3:1$ solution, and the Si substrates were dipped into HF, before they were rinsed in de-ionized water and dried with filtered nitrogen. For each growth the (00·1)$Al_2O_3$, (01·2)$Al_2O_3$ and (100)Si substrates were placed side-by-side in the reactor. The Al and N sources were trimethylaluminum (TMAl) carried on at 25 °C and electronic grade (99.999%) ammonia ($NH_3$). The carrier gas was ultraplus (99.9995%) high purity nitrogen ($N_2$). The flow rates were 5, 400, and 1200 cc/min for TMAl, $NH_3$, and $N_2$, respectively. In order to reduce parasitic chemical reactions.

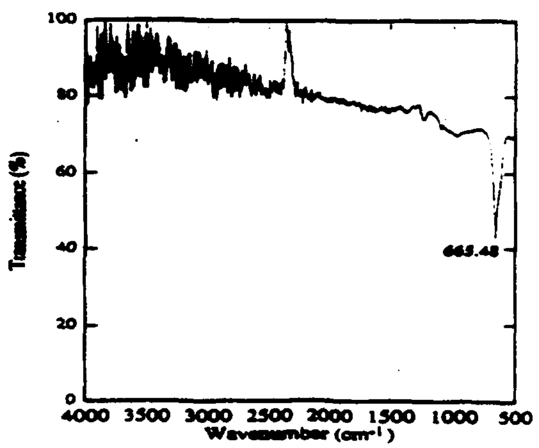


FIG. 1. FTIR spectrum of the AlN thin films deposited on Si substrates.

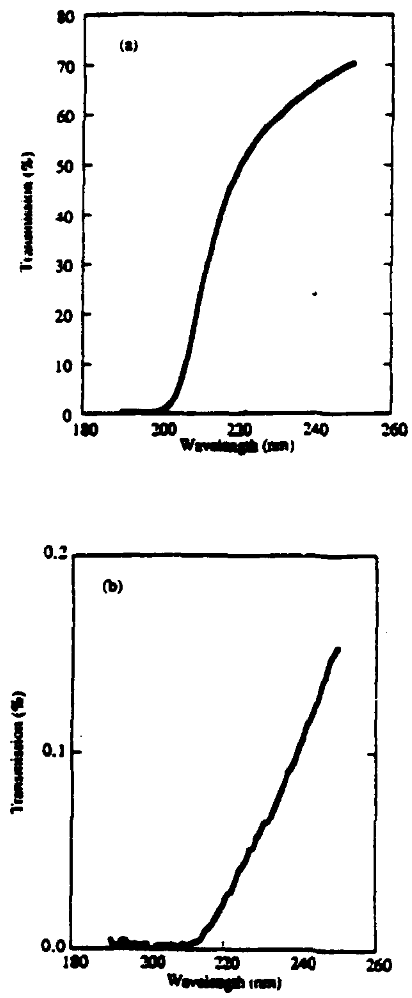


FIG. 2. (a) UV transmission spectrum for (00·1)AlN//(00·1)$Al_2O_3$. (b) UV transmission spectrum for (11·0)AlN//(01·2)$Al_2O_3$.

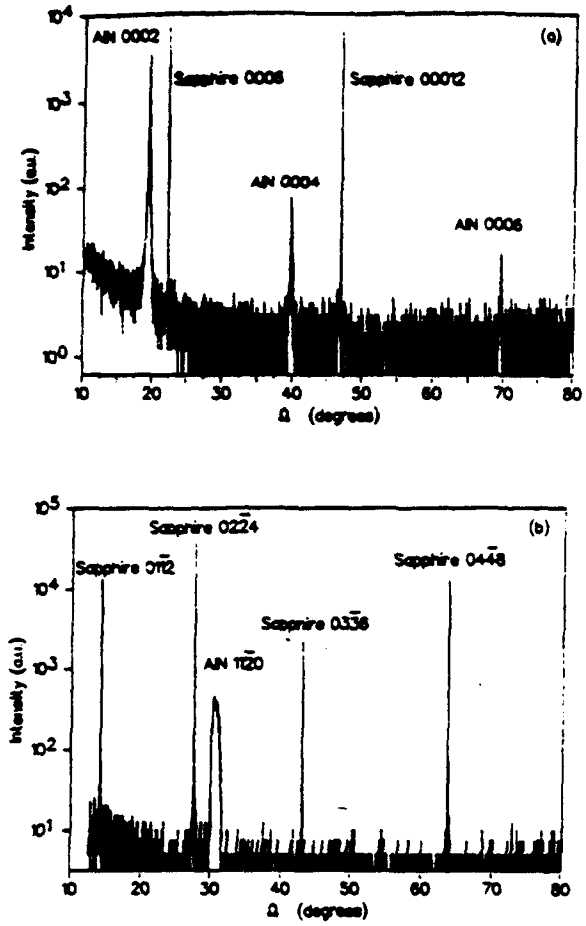


FIG. 3. (a) Ω-2Θ x-ray diffraction spectrum for (00·1)AlN//(00·1)$Al_2O_3$. (b) Ω-2Θ x-ray diffraction spectrum for (11·0)AlN//(01·2)$Al_2O_3$.

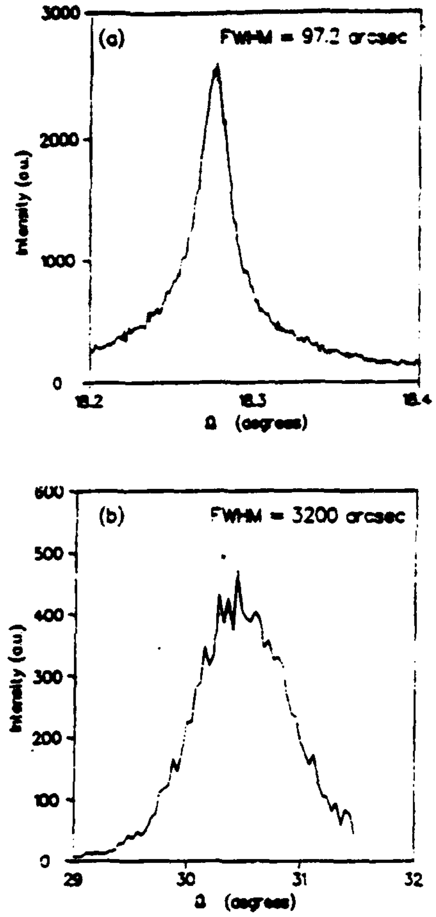


FIG. 4. (a) X-ray rocking curve of the (00·2) peak of AlN. (b) X-ray rocking curve of the (11·0) peak of AlN.

the TMAl and $NH_3$ were mixed at the entrance of the reactor chamber. The susceptor temperature was 1050 °C. During 2 h of growth, a film about 1 μm thick was deposited as determined by ball polishing thickness measurement. Fourier transform infrared spectroscopy (FTIR), UV transmission spectroscopy and a four-crystal monochromator x-ray diffractometer (MPD)1880/HP),[1] developed at Philips Research Laboratories were used to characterize the epitaxial layers.

Since sapphire crystals absorb radiation in the spectral region where we expect to find a phonon mode peak for AlN, FTIR spectroscopy was only performed on the films grown on silicon substrates. Figure 1 shows the transmittance as a function of wave number. A clear peak at 665 $cm^{-1}$ was present, which corresponds to the transverse optical (TO) =667 $cm^{-1}$ and to the $E_2$=665 $cm^{-1}$ phonon modes of AlN.[2] No other strong peaks were detected.

Using UV transmission spectroscopy, the absorption edge of the AlN films was measured. Figures 2(a) and 2(b) show the spectra for the epilayers grown on (00·1) and (01·2)$Al_2O_3$, respectively. The film grown on (00·1)$Al_2O_3$ had a sharp edge at about 197 nm, confirming the presence of high quality AlN. However, the film grown on (01·2)$Al_2O_3$ showed a much less sharp edge at about 213 nm.

Figures 3(a) and 3(b) represent the Omega/2Theta scans for the epilayers grown on (00·1) and (01·2)$Al_2O_3$, respectively. These spectra showed the (00·1) and (11·0) faces of AlN are parallel to the (00·1) and (01·2) faces of $Al_2O_3$, respectively, which is analogous to GaN epilayers grown on the same $Al_2O_3$ substrate orientations.[3,4]

Figure 4(a) shows the x-ray rocking curve of the (00·2) peak of AlN grown on (00·1)$Al_2O_3$. The full width at half-maximum (FWHM) was 97.2 arcsec, which is the narrowest value reported to our knowledge.[5] As shown in Fig. 4(b), the rocking curve of the (11·0) peak of AlN grown on (01·2)$Al_2O_3$ presented a FWHM of about 3200 arcsec.[6] We previously reported that GaN films grown on (01·2)$Al_2O_3$ exhibited a better crystalline quality than those grown on (00·1)$Al_2O_3$.[3]

A difference in the thermal mismatch for the two $Al_2O_3$ orientations may be responsible for these disparate results. Table I shows the thermal expansion coefficients[7,8] and lattice parameters[9] of AlN, GaN, and $Al_2O_3$. Using these values, we calculated the thermal and lattice mismatch values given in Table II. We estimated the thermal expansion coefficient in

TABLE I. Thermal expansion coefficients (TEC) and lattice constants for AlN, GaN, and $Al_2O_3$.

| | $a$ direction TEC ($\times 10^{-6}$/K) | $c$ direction TEC ($\times 10^{-6}$/K) | $a$ (Å) | $c$ (Å) |
|---|---|---|---|---|
| AlN | 5.27 | 4.15 | 3.112 | 4.982 |
| GaN | 5.59 | 7.75 (700–900 K) | 3.189 | 5.185 |
| $Al_2O_3$ | 7.28 | 8.11 | 4.758 | 12.991 |

the $[\bar{1}\bar{2}1]Al_2O_3$ direction to be about $8\times10^{-6}$/K in the range from 20 to 800 °C, using the data from Yim and Paff[7] and $c' = \sqrt{3a^2+c^2}$ for a translational period in the $(01\cdot2)Al_2O_3$ plane.[8] The thermal mismatch is higher for $(11\cdot0)$AlN grown on $(01\cdot2)Al_2O_3$ than for $(00\cdot1)$ AlN grown on $(00\cdot1)Al_2O_3$. The thermal mismatch for $(00\cdot1)$GaN grown on $(00\cdot1)Al_2O_3$ is larger than for $(11\cdot0)$ GaN grown on $(01\cdot2)Al_2O_3$.

There are also other factors that may contribute to poorer quality AlN films grown on $(01\cdot2)Al_2O_3$ substrates. The thermal and lattice mismatches are different for the two translational symmetry directions in the epilayer $(11\cdot0)$ plane. The mismatches in the $[\bar{1}10]$ direction of $(11\cdot0)$AlN are the same as the ones for the $(00\cdot1)$ epilayer grown on $(00\cdot1)Al_2O_3$ (−28% and 13.3%), while the mismatches in the $c$ direction of AlN are shown in Table II (−48% and −2.9%). In the $[\bar{1}10]$ direction of $(11\cdot0)$AlN, the lattice mismatch is compressive, while in the [001] direction it is expansive. Also, in the simple crystallographic model of Kung *et al.*,[10] the hexagonal closed packing of atoms is continued in the growth direction for the epitaxial layers on $(00\cdot1)Al_2PO_3$ whereas it is not for epilayers on $(01\cdot2)Al_2O_3$. This leads to intrinsic defects at the interface between $(11\cdot0)$AlN and $(01\cdot2)Al_2O_3$.

TABLE II. Thermal and lattice mismatches of AlN and GaN on $(00\cdot1)$ and $(01\cdot2)$ $Al_2O_3$.

| Epitaxial layer | Substrate | Thermal mismatch | Lattice mismatch |
|---|---|---|---|
| $(00\cdot1)$AlN | $(00\cdot1)Al_2O_3$ | −28% | 13.3% |
| $(11\cdot0)$AlN | $(01\cdot2)Al_2O_3$ | −48% | −2.9% |
| $(00\cdot1)$GaN | $(00\cdot1)Al_2O_3$ | −23% | 16.1% |
| $(11\cdot0)$GaN | $(01\cdot2)Al_2O_3$ | −3% | 1.1% |

In summary, we have reported the growth of aluminum nitride films on (100) silicon, $(00\cdot1)$ and $(01\cdot2)$ sapphire substrates. Those grown on $(00\cdot1)Al_2O_3$ had higher crystal quality than those grown on $(01\cdot2)Al_2O_3$. The x-ray rocking curves yielded a FWHM of about 97.2 arcsec for the AlN epilayers grown on $(00\cdot1)Al_2O_3$, the narrowest value ever reported to our knowledge. The absorption edge for these epilayers was at 197 nm, and it was sharper than for the AlN epilayers grown on $(01\cdot2)Al_2O_3$. It was shown that the better crystallinity of AlN films was due to the smaller thermal mismatch between $(00\cdot1)$AlN and $(00\cdot1)Al_2O_3$.

The authors would like to thank Max Yoder and Dean Jerry Cohen for their permanent support and encouragement. This work is supported by the Office of Naval Research under Grant No. N00014-93-1-0235.

[1] W. J. Bartels, J. Vac. Sci. Technol. B 1, 338 (1983).
[2] O. Brafman, G. Lengyel, S. S. Mitra, P. J. Gielisse, J. N. Plendl, and L. C. Mansur, Solid State Commun. 6, 523 (1968).
[3] C. J. Sun and M. Razeghi, Appl. Phys. Lett. 63, 973 (1993).
[4] T. Sasaki and S. Zembutsu, J. Appl. Phys. 61, 2533 (1986).
[5] M. A. Khan, J. N. Kuznia, R. A. Skogman, D. T. Olson, M. M. Millan, and W. J. Choyke, Appl. Phys. Lett. 61, 2539 (1992).
[6] S. Kaneko, M. Tanaka, K. Masu, K. Tsubouchi, and N. Mikoshiba, J. Crysta. Growth, 115, 643 (1991).
[7] W. M. Yim and R. J. Paff, J. Appl. Phys. 45, 1456 (1974).
[8] H. P. Maruska and J. J. Tietjen, Appl. Phys. Lett. 15, 327 (1969).
[9] S. Strite and H. Morkoc, J. VAc. Sci. Technol. B 10, 1237 (1992).
[10] P. Kung, C. J. Sun, A. Saxler, H. Ohsato, and M. Razeghi, (unpublished).

RTT #14

Presented at the [illegible]

[illegible] and [illegible]

# $Al_xGa_{1-x}N$ grown on (00·1) and (01·2) sapphire and (100) silicon


C. J. Sun, P. Kung, A. Saxler, H. Ohsato and M. Razeghi

Center for Quantum Devices

Department of Electrical Engineering and Computer Science

Northwestern University, Evanston, Illinois 60208



Ternary $Al_xGa_{1-x}N$ thin films have been successfully grown on (00•1) and (01•2) sapphire with prior growth of either AlN or GaN/AlN by atmospheric pressure metalorganic chemical vapor deposition. The composition x value of the thin films obtained varied from 0 to 0.6. The surface morphology, crystallinity and photoluminescence of the $Al_xGa_{1-x}N$ were investigated. The surface morphology of films grown on (00•1) sapphire showed a triangular structure and those grown on (01•2) sapphire showed a rectangular structure. The full width at half maximum or x-ray rocking curve of the $Al_{0.13}Ga_{0.87}N$ grown on (00•1) sapphire is about 10 min. The crystalline quality of $Al_xGa_{1-x}N$ became poor when the x value increased. The crystalline quality of films grown on (01•2) sapphire and (100) silicon substrate is much poorer compared with those grown on (00•1) sapphire, while the FWHM's of photoluminescence peak are as good as those grown on (00•1) sapphire.

The $Al_xGa_{1-x}N$[1,2] ternary thin films have attracted much attention with a direct band-gap in the visible to ultraviolet (uv) regions[3]. This makes it a good candidate for devices like blue light-emitting diodes[4], UV detectors[5], and high temperature and high power electron devices[6,7]. Recently, we reported the high quality AlN growth on sapphire with 92 arc seconds of the full width at half maximum (FWHM) of rocking curve[8]. In this paper we reported the high quality of $Al_xGa_{1-x}N$ growth on (00•1) and (01•2) sapphire ($\alpha-Al_2O_3$) and (100) silicon (Si) with prior growth of either AlN or GaN/AlN layer structures. The surface morphology, crystallinity and optical properties were investigated.

The $Al_xGa_{1-x}N$ was prepared by a atmospheric horizontal-type metalorganic chemical vapor phase (MOCVD) reactor[9]. (00•1) and (01•2) sapphire ($\alpha-Al_2O_3$) and (100) silicon (Si) were used as substrates. A dual infra-red lamp heating configuration was used to heat the graphite susceptor which was inclined at 15° with respect to horizontal. A thermocouple inserted into the susceptor monitored its temperature and provided feedback to the temperature controller. Trimethylgallium (TMGa), Trimethylaluminum (TMAl) and ammonia ($NH_3$) were used as Ga, Al and N source materials, respectively. Nitrogen ($N_2$) was used as the ambient gas. Metalorganics (MO) and nitrogen source were mixed just before entering the reactor, in order to reduce parasitic reactions of MO with nitrogen source.

Growth temperature varied from 900°C to 1050°C. The bubbler temperature were kept at -10°C for TMGa and 25°C for TMAl. The carrier gas bubbling flow rates were 0.5-5 cc/min for TMGa and 5-10cc/min for TMAl and $NH_3$ flow rate varied from 400 to 1100 cc/min, while the total gas flow remained constant at 1600 cc/min. Sapphire substrates were etched by a hot solution of $H_3PO_4 : H_2SO_4 = 1:3$ and then rinsed in deionized water and dried with filtered nitrogen. Si substrates were cleaned by dipping in hydrofluoric acid prior to the growth, rinsed and dried.

Before the growth, the substrates were kept at 1050°C for 15 min in a stream of $H_2$ gas to remove the oxide layer. After the substrate temperature was stabilized, $NH_3$ was fed into the reactor. A high quality AlN or a GaN/AlN layer structure was grown before the ternary $Al_xGa_{1-x}N$ growth.

The surface morphology of the $Al_xGa_{1-x}N$ thin films obtained were observed through a scanning electron microscope (SEM). The orientation relationship of thin films and substrate was determined by the precession camera using the $MoK_\alpha$ radiation[10]. A

high resolution 5-crystal x-ray diffractometer using the Cu $K_{\alpha 1}$ line was used to examine the crystalline quality of the $Al_xGa_{1-x}N$ thin films. Optical properties were characterized by photoluminescence (PL) measurement.

Fig. 1a shows a SEM photograph of $Al_{0.13}Ga_{0.87}N$ thin film grown on (00•1) sapphire with a prior growth of AlN. The surface morphology of the thin film is different from that of GaN which is usually hexagonal plate-like structure reported by Sasaki[11] and Akasaki et al.[12]. It consists of plate-like crystals which locate in three equivalent directions as a triangular structure shown in Fig. 1a . Those plates are pyramid surfaces which are parallel to a-axis as observed by SEM. Elwell et al[13] reported the morphology of GaN single crystal with {10•1} and {10•2} pyramid surfaces. So we believe the plates appeared on the (00•1) face are either {10•1} or {10•2}. These three equivalent plates make a triangle shape like a dendritic or hollowed crystals. Fig. 1b showed a much smooth surface of the AlGaN thin film grown on (00•1) sapphire. The (00•1) surface are formed by filling the hollowed portion among the plate-like crystals.

Fig. 2a and 2b show the SEM photographs of (11•0)$Al_{0.20}Ga_{0.80}N$ grown on (01•2) sapphire substrates with a prior growth of AlN. The surface morphology of the thin films is very smooth as shown in Fig. 2a. On some other samples, interesting figures are found, which also show plate-like crystals. Those crystals might be the same as those grown on (00•1) sapphire substrates. The pyramid surfaces are perpendicular to {11•0} surface. The face angles between the two pyramidal faces is 124.1 for {10•1} and 86.6 for {10•2}. The face angle observed by SEM between the two plate-like crystals is about 87°, so the plate-like surface should be (10•2) surface.

We believe the first step growth of AlGaN thin films is the plate-like crystal growth with {10•2} pyramid face in both (00•1) and (01•2) cases. A smooth surface will appear by filling the hollowed portion among the plate-like crystals.

Fig. 3a, 3b and 3c show the x-ray spectra of AlGaN grown on (00•1), (01•2)$Al_2O_3$ and (100)Si with a prior growth of GaN/AlN. The mole fraction of Al was determined by Vegard's law. The x value varied from 0 to 0.6 by changing the flow rate of TMGa. The $Al_xGa_{1-x}N$ thin films are single crystal for all the composition x and the FWHM of x-ray rocking curve of (00•1)$Al_{0.13}Ga_{0.87}N$ was as narrow as 10 min shown in Fig. 3a. The crystallinity of $Al_xGa_{1-x}N$ films became poor when the x value became larger. The crystalline quality of films grown on (100)Si is much poorer than those grown on sapphire as shown in Fig. 3a. 3b and 3c.

The PL experiments were performed using a LiCoNiX 200 Series continuous wave Helium-Cadmium (He-Cd) laser as the optical excitation source ( 325nm. maximum power 30mW). An optical chopper was used to avoid the low frequency noise. The samples were stuck on a copper plug on a liquid nitrogen (77K) cold finger kept in an evacuated chamber with quartz windows. The luminescence was focused at the slit of SpectraPro 275 spectrometer by a 10 cm lens. dispersed by a grating with a 1200 grooves/mm blazed at 300 nm. The signal was amplified by photomultiplier tube (PMT) and sent to the lock-in amplifier.

Fig. 4a, 4b and 4c show the low temperature PL spectra of AlGaN grown on (00•1), (01•2)$Al_2O_3$ and (100)Si with a prior growth of GaN/AlN. Fig. 4a shows an undecomposed peak of (00•1)GaN and (00•1)$Al_{0.13}Ga_{0.87}N$. Fig. 4b shows that the peak emissions from the (11•0)GaN and (11•0)$Al_{0.2}Ga_{0.8}N$ are at 355 nm and 341 nm, respectively. Fig. 4c shows that the peak emissions from the (00•1)GaN and (00•1)AlGaN are at 363 nm and 345 nm, respectively. The FWHM were about 95 meV for both GaN and AlGaN on all samples. There is an unknown luminescence peak observed at around 375 nm for all the samples. The luminescence efficiency was increased 10 times from room temperature to 77K for sapphire samples and 25 times for Si samples. Surprisingly, the luminescence from Si sample is as good as those from sapphire, though the crystalline quality of Si samples is much poorer.

In conclusion, we reported about the ternary $Al_xGa_{1-x}N$ thin films grown on (00•1). (01•2)$Al_2O_3$ and (100)Si with a prior growth of AlN or GaN/AlN. The surface morphology was different from those reported up to date. The plate-like crystals with (10•2) are grown on the sapphire substrate with a prior growth of AlN like the dendritic or hollow crystals, followed by forming a much smoother surface with filling the hollowed portion among the plate-like crystals. The x-ray spectra showed that the crystalline quality of ternary $Al_xGa_{1-x}N$ is as good as that of GaN. The FWHM's of PL peak of the ternary thin films are as narrow as that of GaN (95 meV).

The authors would like to thank Mr. Max Yoder for his interest and encouragement. This work is supported by the ONR through Grant No. N00014-93-1-0235. The authors would also like to thank Dean Jerome Cohen for his permanent support and encouragement.

## Reference


1. K. Ito, K. Hiramatsu, H. Amano and I. Akasaki. J. Cryst. Growth **104**, 533 (1990).
2. K. Hirosawa, K. Hiramatsu, N. Sawaki and I. Akasaki, Jpn. J. Appl. Phys. **32**, L1039 (1993).
3. S. Strite and H. Morkoc, J. Vac. Sci. Technol. B **10**(4), 12137 (1992).
4. B. Goldenberg, J. D. Zook and R. J. Ulmer, Appl. Phys. Lett. **62**(4), 381 (1993).
5. M. A. Khan, J. N. Kuznia, D. T. Olson, J. M. Van Hove, M. Blasingame and L. F. Reitz, Appl. Phys. Lett. **60**, 2917 (1992).
6. M. A. Khan, J. N. Kuznia, A. R. Bhattarai and D. T. Olson, Appl. Phys. Lett. **62**(15), 1786 (1993).
7. M. A. Khan, A. R. [illegible]tarai, J. N. Kuznia and D. T. Olson, Appl. Phys. Lett. **63**(9), 1214 (1993).
8. A. Saxler, P. Kung, C. J. Sun, F. Bigan and M. Razeghi, to be published in Appl. Phys. Lett.
9. M. Razeghi, The MOCVD Challenge (Adame Hilger, London. 1989).
10. M. J. Buerger, The Precession Method in X-ray Crystallography, Wiley, New York. 1964; Henry et al., The Interpretation of X-ray Diffraction Photographs. pp. 132-142: Jeffery, Methods in X-ray Crystallography, pp. 218-236.
11. T. Sasaki, J. Cryst. Growth, **129**, 81 (1993).
12. I. Akasaki, H. Amano, Y. K. Koide, K. Hiramatsu and N. Sawaki, J. Cryst. Growth, **98**, 209 (1989).
13. D. Elwell, R. S. Feigelson, M. M. Simkins and W. A. Tiller, J. Cryst. Growth. **66**, 45 (1984).

## List of Figure


Figure 1 SEM photograph of $Al_{0.13}Ga_{0.87}N$ thin film grown on (00•1) sapphire with a prior growth of AlN. (a) A triangular structure form by the plate-like crystals has been observed. (b) A smooth (00•1) surface has been formed by filling the hollowed portion among the plate-like crystals.

Figure 2 SEM photographs of (11•0)$Al_{0.20}Ga_{0.80}N$ grown on (01•2) sapphire substrates with a prior growth of AlN. (a) A smooth surface has been observed. (b) A rectangular structure form by the plate-like crystals has been observed.

Figure 3 The x-ray spectra of AlGaN grown on (a) (00•1)$Al_2O_3$. (b) (01•2)$Al_2O_3$ and (c) (100)Si . with a prior growth of GaN/AlN.

Figure 4 The low temperature PL spectra of AlGaN grown on (a) (00•1)$Al_2O_3$. (b) (01•2) and (c) (100)Si. with a prior growth of GaN/AlN.

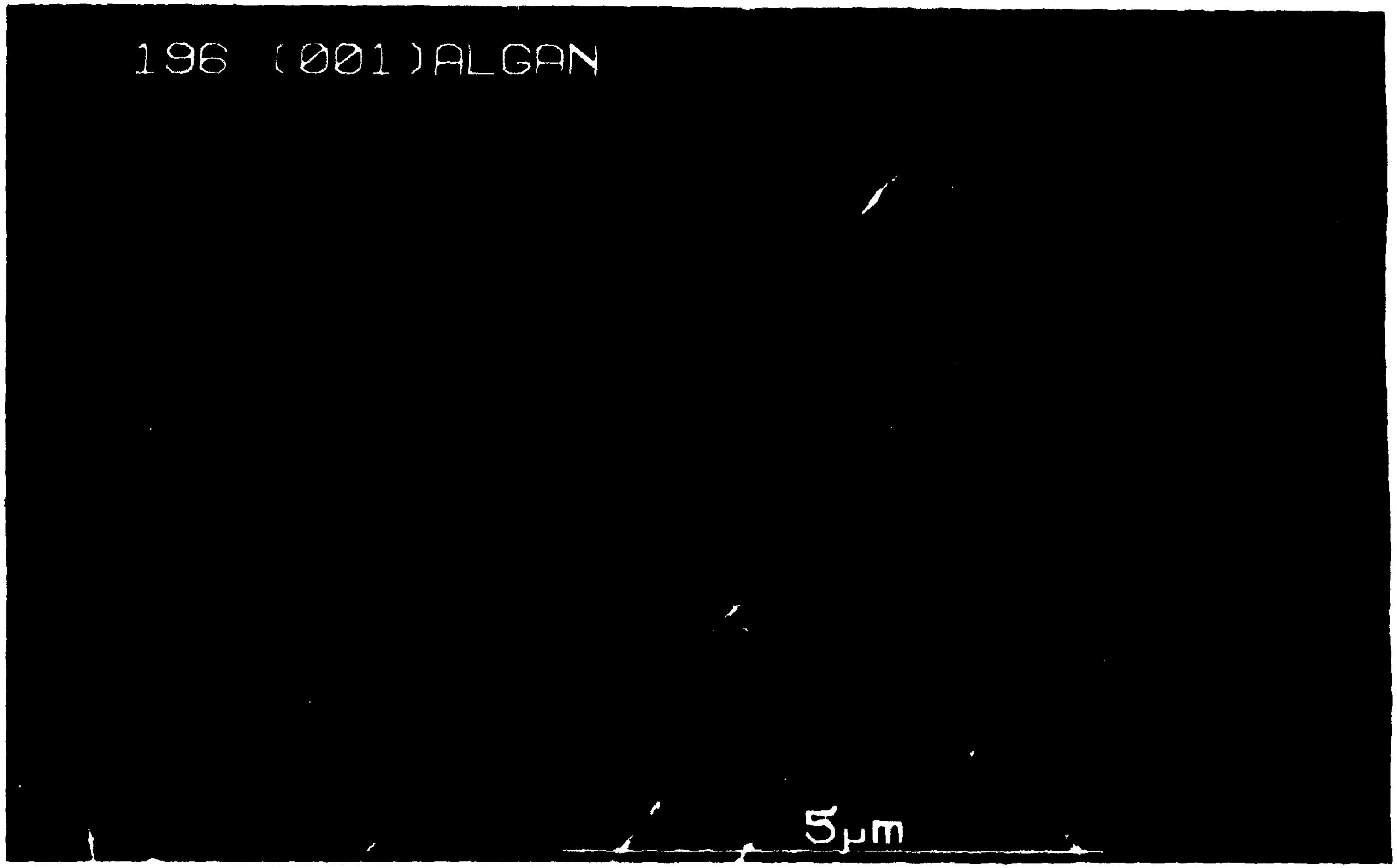
196 (001)ALGAN
5μm

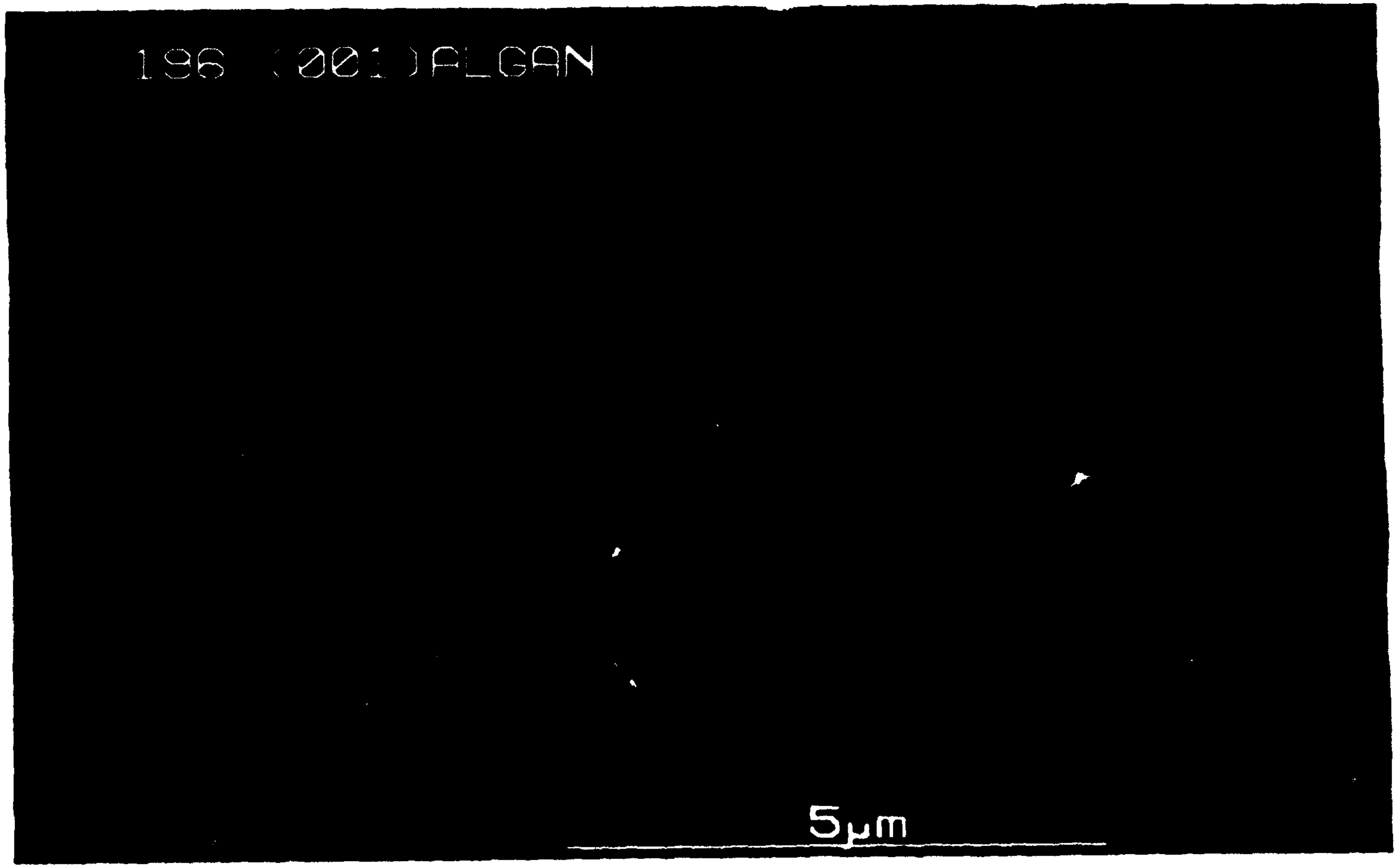
196 (001)ALGAN
5μm

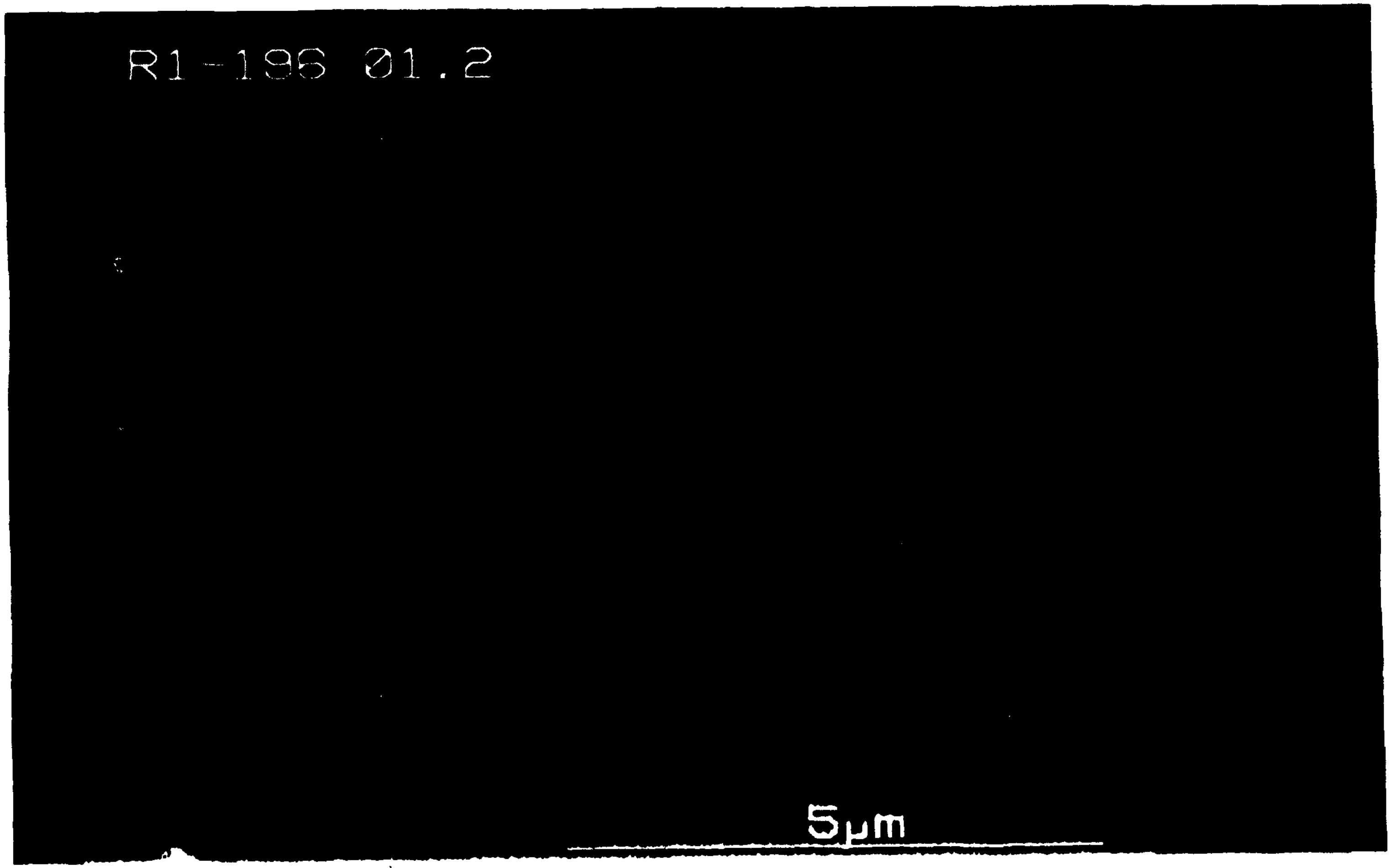
R1-196 01.2
5µm


R1-196 01.2F

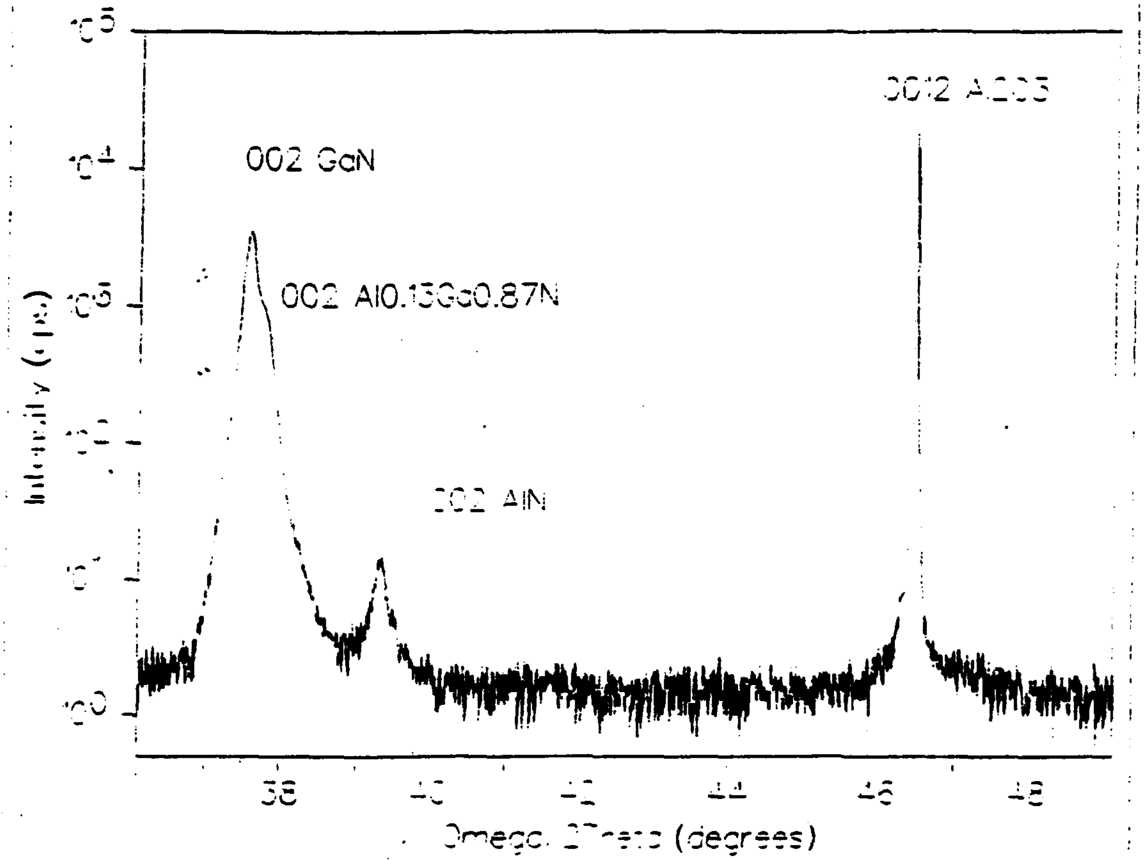

002 GaN
002 Al0.13Ga0.87N
002 AlN
0012 Al2O3
Intensity (cps)
38
40
42
44
46
48
Omega 2Theta (degrees)

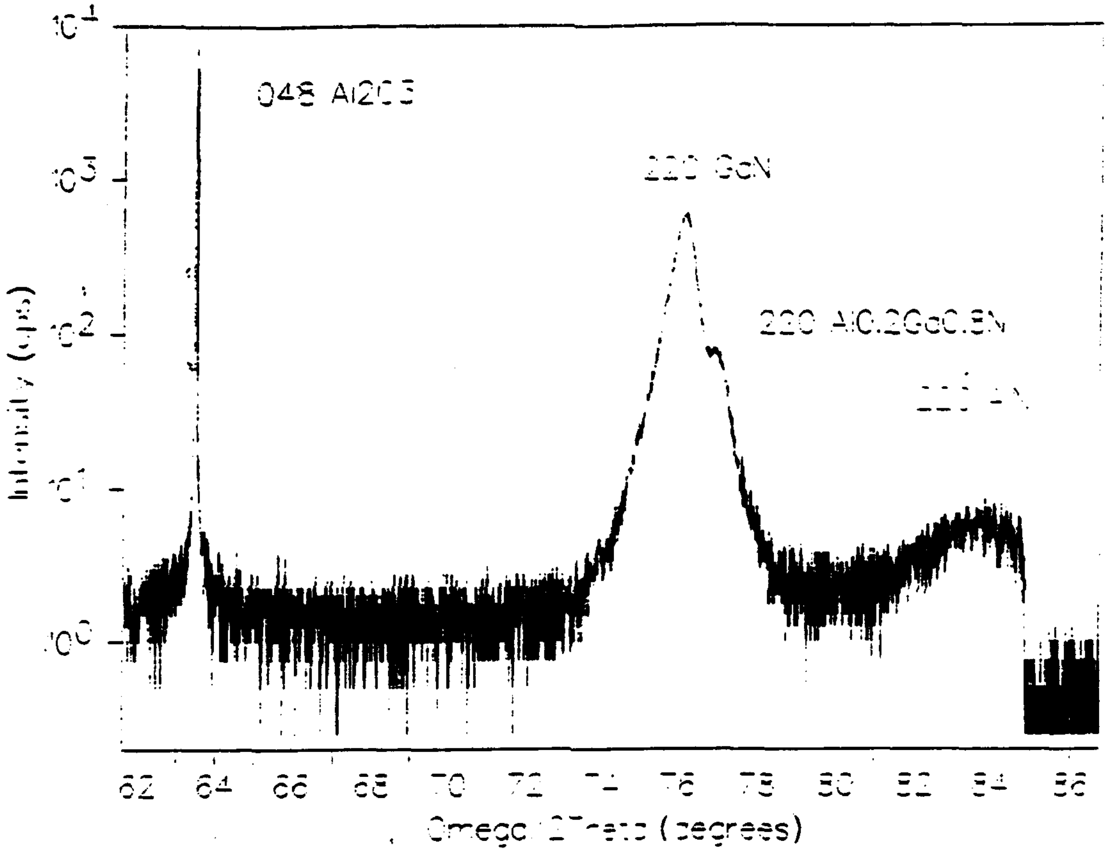

048 Al2O3
220 GaN
220 Al0.2Ga0.8N
Intensity (cps)
Omega/2Theta (degrees)
62
64
66
68
70
72
74
76
78
80
82
84
86

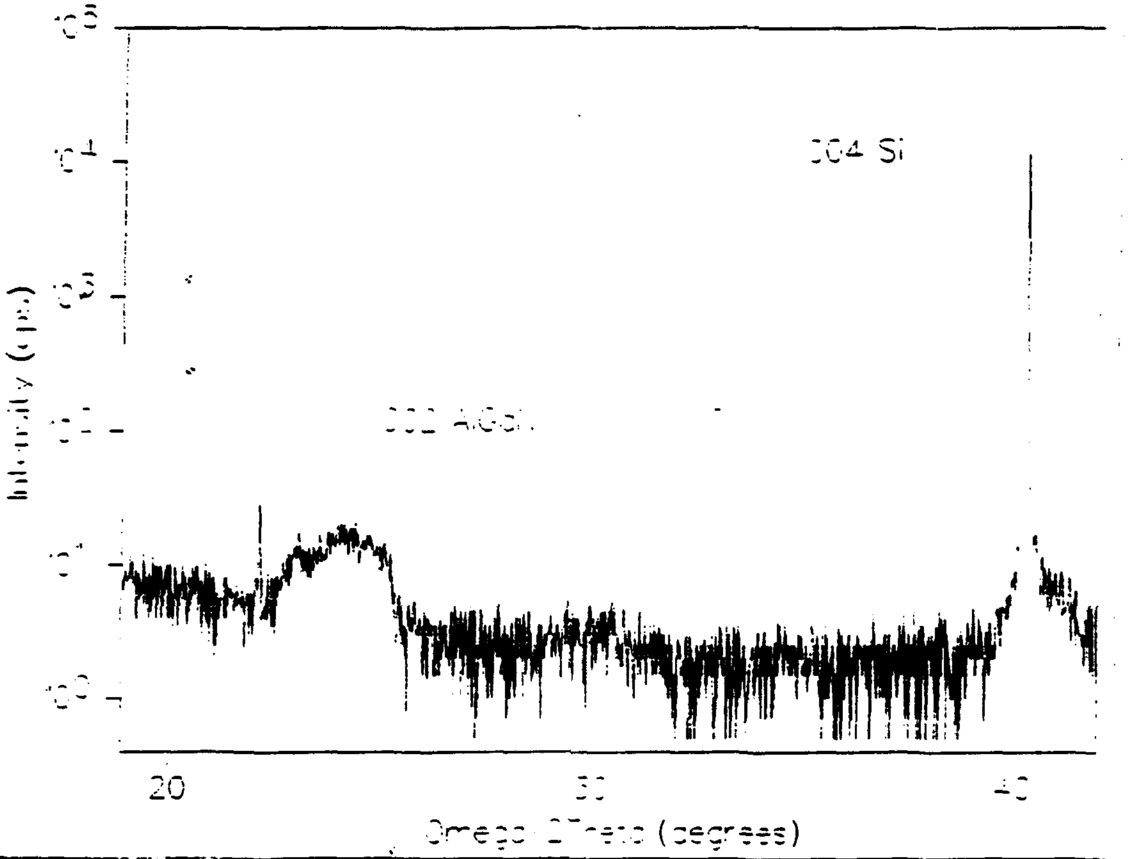
004 Si
002 AlGaN
Intensity (cps)
20
30
40
Omega-2Theta (degrees)